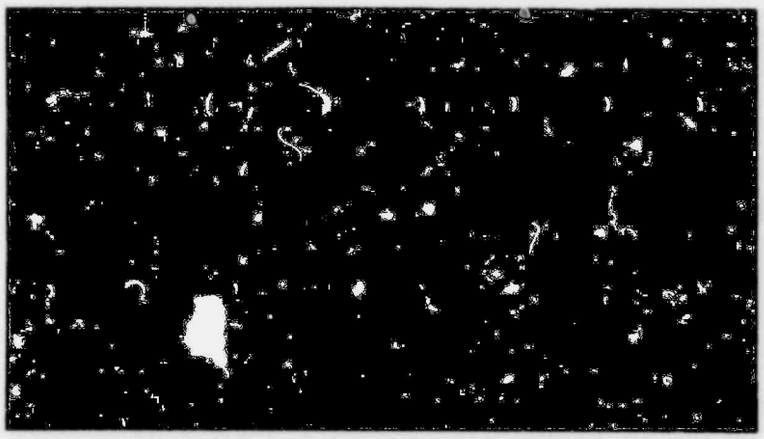

Yankee Atomic Electric Company

YAEC-1275

Vermont Yankee
Cycle 9
Core Performance Analysis

August 1981

Major Contributors:

A. A. F. Ansari
K. J. Burns
J. D. Candon
J. T. Cronin
R. Habert
M. J. Hebert
J. M. Holzer
D. M. Kapitz
E. E. Pilat
K. E. St.John
M. A. Sironen
D. M. VerPlanck
R. A. Woehlke

Approved by: R.J. Cacciapouti — 8/31/81
R. J. Cacciapouti, Manager (Date)
Reactor Physics Group

Approved by: Stephen P. Schultz — 8/31/81
S. P. Schultz, Manager (Date)
BWR Transient Analysis Group

Approved by: Liliane Schor for — 8/31/81
A. Husain, Manager (Date)
LOCA Group

Approved by: B.C. Slifer — 8/31/81
B. C. Slifer, Manager (Date)
Nuclear Engineering

DISCLAIMER OF RESPONSIBILITY

This document was prepared by Yankee Atomic Electric Company for its own use and on behalf of Vermont Yankee Nuclear Power Corporation. This document is believed to be completely true and accurate to the best of our knowledge and information. It is authorized for use specifically by Yankee Atomic Electric Company, Vermont Yankee Nuclear Power Corporation and/or the appropriate subdivisions within the Nuclear Regulatory Commission only.

With regard to any unauthorized use whatsoever, Yankee Atomic Electric Company, Vermont Yankee Nuclear Power Corporation and their officers, directors, agents and employees assume no liability nor make any warranty or representation with respect to the contents of this document or to its accuracy or completeness.

ABSTRACT

This report presents design information and calculational analysis results pertinent to the operation of Cycle 9 of the Vermont Yankee Nuclear Power Station. These include the fuel design and core loading pattern descriptions; calculated reactor power distributions, power peaking, shutdown capability and reactivity functions; and the results of the several safety analyses performed to justify plant operation throughout Cycle 9.

TABLE OF CONTENTS

TABLE OF CONTENTS
(Continued)

LIST OF FIGURES

LIST OF FIGURES

LIST OF TABLES

ACKNOWLEDGEMENTS

The authors and principal contributors would like to express their gratitude in the acknowledgement of contributions to this work by B. G. Baharynejad, K. G. Gavin, Q. A. Haque, J. Pappas, and R. K. Schmidt. Their assistance in performing the required calculations, documenting the results, and preparing figures and displays for this document is recognized and greatly appreciated. Special appreciation is expressed to S. M. Henchey and D. L. Nichols for preparation of the draft and final manuscript.

1.0 INTRODUCTION

This report provides justification to support the operation of the Vermont Yankee Nuclear Power Station through the forthcoming fuel reload cycle (Cycle 9). The refueling preceding Cycle 9 will involve the discharge of 120 irradiated fuel bundles and the insertion of 120 new fuel bundles. The resultant reload cycle will consist of 120 new fuel bundles of the pressurized retrofit 8X8 design (P8DPB289), 176 irradiated fuel bundles of the pressurized retrofit 8X8 design, 60 irradiated bundles of the retrofit 8X8 design (8DPB289), and 12 irradiated bundles of the earlier 8X8 design (8D274). All fuel bundles for Cycle 9 operation have been fabricated by General Electric (GE). The introduction of the new fuel is necesary in order to maintain sufficient reactivity for continued operation at full rated power.

This report contains descriptions and analyses results pertaining to the mechanical, thermal-hydraulic, physics, and safety analyses aspects of the Cycle 9 reload.

The cycle dependent parameters and operating limits to be incorporated into the Vermont Yankee Plant Technical Specifications for Cycle 9 are given in Appendix A.

2.0 RECENT RFACTOR OPERATING HISTORY

2.1 Operating History of the Current Cycle

The current operating cycle is Cycle 8. The reactor was started up for this cycle on December 24, 1980 and is projected to be shut down for refueling on October 17, 1981. During this period, control rod sequence exchanges were performed on the following schedule:

	SEQUENCE	
	from	to
March 14, 1981	A1	B2
May 11, 1981	B2	A2
August 1, 1981	A2	B1

During the week following the control rod sequence exchange in March, the reactor was operated at reduced power to allow special testing including a recirculation pump trip test and reactor stability testing [1]. To this time with these provisions, the reactor has been operated smoothly and uninterrupted at full power with the exception of a scram on May 11, 1981.

2.2 Operating History of Recent Applicable Cycles

Fuel to be re-irradiated in Cycle 9 includes fuel bundles which were initially inserted into the reactor in Cycle 6, Cycle 7, and Cycle 8. Cycle 7 reactor operation proceeded at full power with normal maintenance and

operational maneuvers with the exception of a 3 day outage in February 1980 to implement plant modifications required by the NRC (TMI fix). A total of six reactor scrams occurred during the cycle operations.

Cycle 6 operation was interrupted at about mid-cycle for an outage of approximately three weeks to identify and replace failed and suspect fuel rods in several assemblies (March 17 to April 3, 1979). The reactor operated at reduced power levels (~90% rated power) for two weeks prior to the outage. Operation prior to this outage has been designated Cycle 6. Subsequent to the return to power on April 3, coolant activity levels were at normally low levels and full power operation proceeded through the end-of-cycle. This period of operation has been designated Cycle 6A.

3.0 RELOAD CORE DESIGN DESCRIPTION

3.1 Core Fuel Loading

Reload 8 (Cycle 9) will discharge 120 spent fuel assemblies out of a core total of 368. Thus the Cycle 9 core will consist of 120 new assemblies and 248 irradiated assemblies. All assemblies have bypass flow holes in the lower tie plate. Table 3.1.1 characterizes the core by fuel type, batch size, and first cycle loaded. A description of each fuel type is found in Reference 2.

3.2 Design Reference Core Loading Pattern

The location of the assemblies in Cycle 9 is indicated by the map in Figure 3.2.1. For the sake of legibility only the northeast quadrant is shown. The other quadrants are mirror images with bundles of the same type having nearly identical exposure histories. The new bundles have been identified as R8XX. Similarly, irradiated bundles are designated by the reload number in which they were first introduced into the core. When the reloading is completed, specific bundle ID's will appear in these locations. Changes to the loading pattern at the time of refueling will be checked and verified acceptable under 10CFR50.59. The final loading pattern will be supplied with the Startup Test Report.

3.3 Assembly Exposure and Cycle 8 History

The exposure on the fuel bundles in the design reference loading pattern is given in Figure 3.2.1. To obtain this exposure distribution, previous cycles up to Cycle 8 were depleted in the SIMULATE model using actual plant

operating history [3,4]. For Cycle 8, plant operating history was used through 5/18/81, that is, a core average exposure of 13.641 GWD/ST. Beyond 5/18/81 the exposure was accumulated using a best-estimate rodded depletion analysis to the end of Cycle 8.

Table 3.3.1 gives the assumed minimum burnup on Cycle 8 and the BOC9 exposure that results from the shuffle. In this table, as in the rest of this report, the terms "End of Cycle (EOC)" and "End of Full Power Life (EOFPL)", as applied to Cycle 9, are used interchangeably.

TABLE 3.1.1

CYCLE 9 FUEL BUNDLE TYPES AND NUMBERS

	Fuel Designation	Cycle Loaded	Number	Span of Possible Bundle ID's
IRRADIATED	8DB274H	6	12	LJ7057-LJ7133
	8DPB289	6	60	LJB710-LJB769
	P8DPB289	7	70	LJG930-LJG999
	P8DPB289	7	24	LJH001-LJH024
	P8DPB289	7	2	LJL746 and LJL747
	P8DPB289	8	78	LJP191-L P268
	P8DPB289	8	2	LJU719 and LJU720
NEW	P8DPB289	9	120	Not yet specified

TABLE 3.3.1

DESIGN BASIS CYCLE 8 AND CYCLE 9 EXPOSURES

Assumed previous cycle core average exposure End of Cycle 8	16.67 GWD/ST
Assumed reload cycle core average exposure Beginning of Cycle 9	9.02 GWD/ST
Haling calculated core average exposure at End of Cycle 9 (Excluding Coastdown)	17.06 GWD/ST
Cycle 9 Capability to EOFPL9	8.04 GWD/ST

VERMONT YANKEE
CYCLE 9
BOC BUNDLE AVERAGE EXPOSURES

R5X2 19.57	R7XX 5.33	R5X2 20.01	R8XX 0.00	R5X2 20.21	R7XX 5.72	R5X2 20.57	R7XX 6.74	R6XX 14.23	R8XX 0.00	R7XX 7.40
R7XX 5.45	R5X1 15.58	R8XX 0.00	R6XX 12.62	R8XX 0.00	R8XX 13.20	R8XX 0.00	R8XX 13.41	R8XX 0.00	R7XX 7.39	R5X2 22.21
R5X2 20.12	R8XX 0.00	R6XX 12.66	R8XX 0.00	R6XX 12.52	R8XX 0.00	R6XX 13.03	R8XX 0.00	R6XX 14.35	R8XX 0.00	R5X1 21.87
R8XX 0.00	R6XX 12.70	R8XX 0.00	R6XX 12.64	R8XX 0.00	R6XX 12.93	R8XX 0.00	R7XX 6.68	R8XX 0.00	R5X2 20.61	
R5X2 20.27	R8XX 0.00	R6XX 12.60	R8XX 0.00	R6XX 12.36	R7XX 6.27	R6XX 13.82	R8XX 0.00	R7XX 7.64		
R7XX 5.78	R6XX 13.42	R8XX 0.00	R6XX 13.08	R7XX 6.39	R6XX 12.36	R8XX 0.00	R7XX 6.73	R5X2 20.26		
R5X2 20.67	R8XX 0.00	R6XX 13.32	R8XX 0.00	R6XX 13.98	R8XX 0.00	R6XX 14.55	R7XX 7.48	R5X2 22.85		
R7XX 6.92	R6XX 13.69	R8XX 0.00	R7XX 6.98	R8XX 0.00	R7XX 6.92	R7XX 7.64	R6XX 14.36			
R6XX 14.58	R8XX 0.00	R6XX 14.47	R8XX 0.00	R7XX 6.10	R5X2 20.54	R5X2 21.79				
R8XX 0.00	R7XX 7.63	R8XX 0.00	R5X2 20.89							
R7XX 7.61	R5X2 22.58	R5X1 21.97								

NORTH

FUEL TYPE ID
EXPOSURE (GWD/ST)

R5X1 - 8DB274H, RELOAD 5
R5X2 - 8DPB289, RELOAD 5
R6XX - P8DPB289, RELOAD 6
R7XX - P8DPB289, RELOAD 7
R8XX - P8DPB289, RELOAD 8

FIGURE 3.2.1

DESIGN REFERENCE CORE LOADING PATTERN, NORTHEAST QUADRANT

4.0 FUEL MECHANICAL AND THERMAL DESIGN

4.1 Mechanical Design

One hundred and twenty (120) fresh fuel bundles fabricated by General Electric Co. will be inserted into the Vermont Yankee reactor for Cycle 9 operation. The mechanical design parameters are identical to the General Electric fabricated bundles which were first inserted and irradiated during Cycles 7 and 8. Table 4.1.1 identifies the design parameters for all irradiated and fresh fuel bundle types in Cycle 9.

Further descriptions of the fuel rod mechanical design and mechanical design analyses are provided in Reference 2. These design analyses remain valid with respect to Cycle 9 reactor operation. Mechanical and chemical compatibility of the fuel assemblies with the in-service reactor environment is also addressed in Reference 2.

4.2 Thermal Design

The fuel thermal effects calculations were performed using the FROSSTEY computer code [5-7]. The FROSSTEY code calculates pellet-to-clad gap conductance and fuel temperatures from a combination of theoretical and empirical models which include fuel and cladding thermal expansion, fission gas release, pellet swelling, pellet densification, pellet cracking, and fuel and cladding thermal conductivity.

The thermal effects analysis included the calculation of fuel temperatures and fuel cladding gap conductance under nominal core steady state and peak linear heat generation rate conditions. Figures 4.2.1 and 4.2.2 provide the core-average response of gap conductance and fuel temperature, respectively. These calculations integrate the responses of individual fuel batch average operating histories over the core average exposure range of Cycle 9. The gap conductance values are weighted axially by power distributions and radially by volume. The core-wide gap conductance values for the RETRAN system simulations described in Section 7.1 are from this data set at the particular exposure point of interest. The fuel temperature values presented in Figure 4.2.2 are weighted axially and radially by volume.

The gap conductance value input to the RETRAN Hot-Channel/MAYU4 calculations was evaluated for the P8X8R fresh fuel bundle type at the peak assembly power to the cycle exposure point of peak bundle reactivity. Gap conductance calculated at this point was bounded by a value of 1000 BTU/hr-ft^2-^{o}F. With consideration for the hot channel transient response to bundle power level and gap conductance values calculated for all other fuel types in Cycle 9, a gap conductance value of 1000 BTU/hr-ft^2-^{o}F was utilized for all RETRAN Hot-Channel/MAYU4 calculations at all exposure points and for all fuel bundle types.

Fuel rod local linear heat generation rates at fuel centerline incipient melt were calculated as a function of local axial segment exposure for the gadolinia concentrations in Vermont Yankee fuel bundles and are displayed in

Table 4.2.1. Initial conditions assumed that fuel rods operate to the local segment power level of the maximum allowable linear heat generation rate (13.4 kw/ft) prior to a power increase.

4.3 Operating Experience

All fuel bundles scheduled to be reloaded in Cycle 9 have operated as expected in previous cycles of Vermont Yankee. Since the Cycle 6/6A outage, offgas measurements are at normally low levels indicating that no fuel failures are present.

TABLE 4.1.1

NOMINAL FUEL MECHANICAL DESIGN PARAMETERS

	FUEL TYPE		
	8X8	8X8R	P8X8R
Fuel Pellets			
Fuel Material (sintered Pellets)	UO_2	UO_2	UO_2
Initial Enrichment, w/o U-235	2.74	2.89	2.89
Pellet Density, % theoretical	95.0	95.0	95.0
Pellet Diameter, inches	0.416	0.410	0.410
Fuel Rod			
Active Length, inches	144.0	150.0	150.0
Plenum Length, inches	16.0	9.5	9.5
Fuel Rod Pitch, inches	0.640	0.640	0.640
Diametral Gap (cold), inches	0.009	0.009	0.009
Fill Gas	Helium	Helium	Helium
Fill Gas Pressure, psig	**	**	**
Cladding			
Material	Zr-2	Zr-2	Zr-2
Outside Diameter, inches	0.493	0.483	0.483
Thickness, inches	0.034	0.032	0.032
Inside Diameter, inches	0.425	0.419	0.419
Fuel Channel			
Material	Zr-4	Zr-4	Zr-4
Inside Dimension, inches	5.278	5.278	5.278
Wall Thickness, inches	0.080	0.080	0.080
Fuel Assembly			
Fuel Rod Array	8x8	8x8	8x8
Fuel Rods per Assembly	63	62	62
Spacer Grid Material	Zr-4	Zr-4	Zr-4

** GE Proprietary

TABLE 4.2.1

PEAK LINEAR HEAT GENERATION RATES CORRESPONDING TO INCIPIENT FUEL CENTERLINE MELTING AND 1% CLAD PLASTIC STRAIN(1)

Exposure (MWD/MT)	0.0 w/o Gd_2O_3 Melt (kw/ft)	0.0 w/o Gd_2O_3 1% ε_p (kw/ft)	3.0 w/o Gd_2O_3 Melt (kw/ft)	3.0 w/o Gd_2O_3 1% ε_p (kw/ft)
FUEL TYPE 8X8				
1000	21.5	21.5	21.5	21.5
25000	21.5	21.5	21.0	21.5
50000	21.0	17.5	19.5	17.5
FUEL TYPE 8X8R				
1000	21.5	21.5	21.5	21.5
25000	21.5	21.5	21.0	21.5
50000	21.5	19.0	20.0	18.5
FUEL TYPE P8X8R				
1000	21.5	21.5	21.5	21.5
25000	21.5	21.5	21.5	21.5
50000	21.5	18.5	20.5	18.5

Note (1): Peak linear heat generation rates shown are minimum bounding values to the occurrence of the given condition.

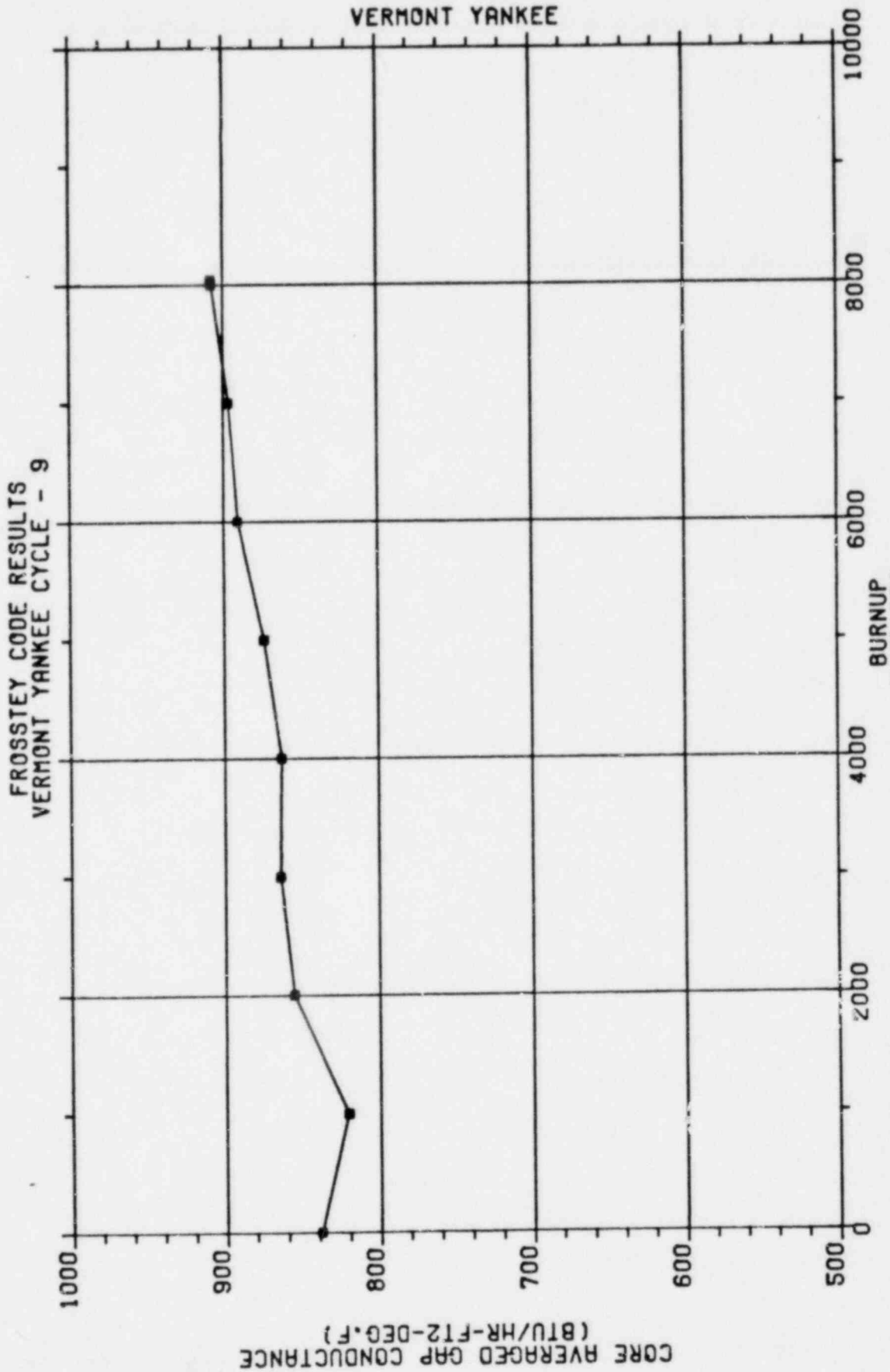

FIGURE 4.2.1

CORE AVERAGED GAP CONDUCTANCE VERSUS CYCLE BURNUP

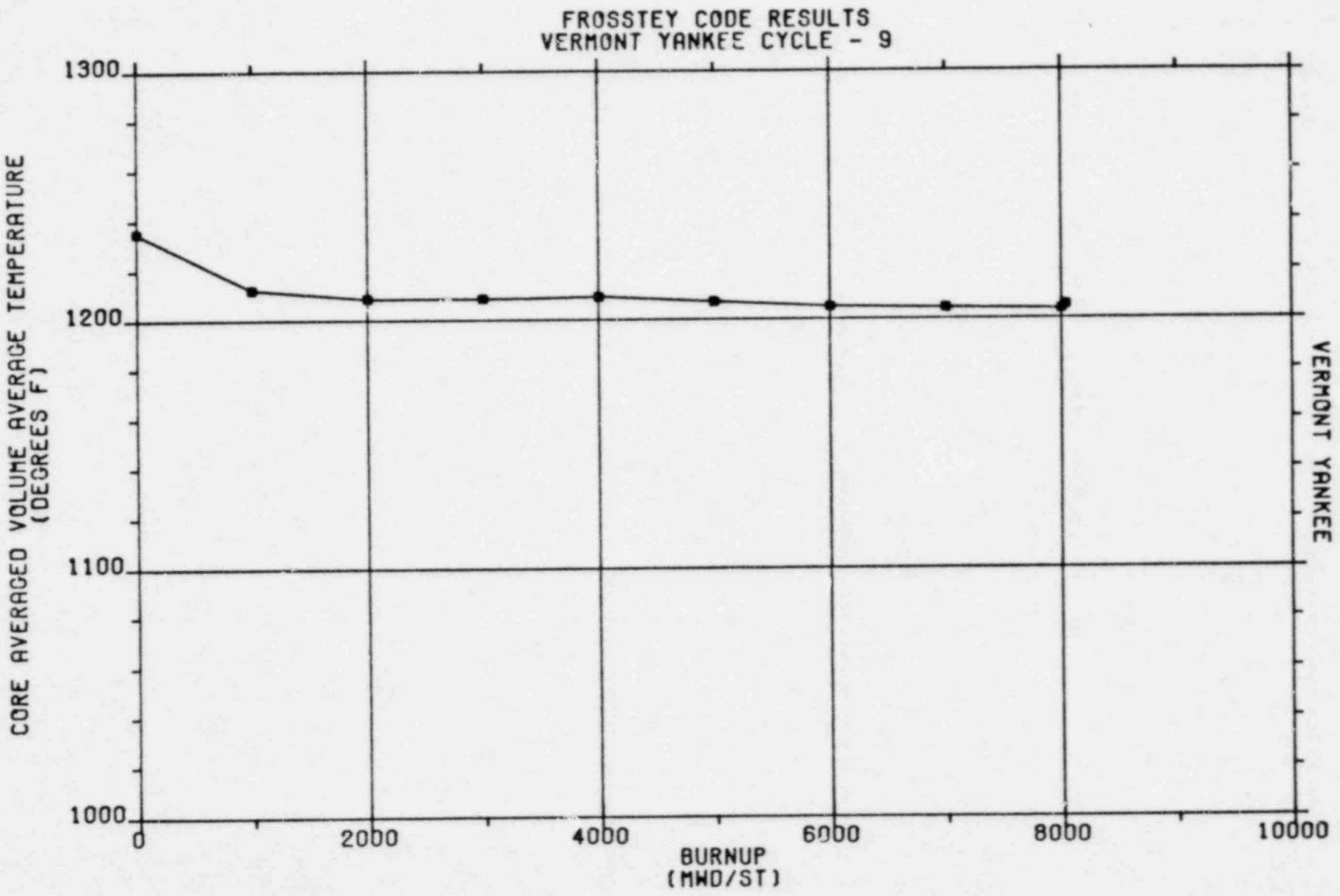

FIGURE 4.2.2

CORE AVERAGED VOLUME AVERAGE TEMPERATURE VERSUS CYCLE BURNUP

5.0 NUCLEAR DESIGN

5.1 Core Power Distributions

The cycle was depleted using SIMULATE [3] to give both a rodded depletion and an All-Rods-Out (ARO) Haling depletion. The Haling depletion serves as the basis for defining core reactivity characteristics for most transient and accident evaluations. This is due primarily to its flat power shape which has weak scram characteristics. Because of the more realistic prediction of initial CPR values, the rodded depletions were used to evaluate the misloaded bundle error and rod withdrawal error.

5.1.1 Haling Power Distribution

The Haling power distribution is calculated in the All-Rods-Out condition. The Haling iteration converges on a self-consistent power and exposure shape for the exposure step to end of cycle. In principle, this should provide the overall minimum peaking power shape for the cycle. This does not mean that during the actual cycle flatter power distributions cannot be achieved by shaping with control rods. However, such shaping would leave underburned regions in the core which would peak at another point in time. Figures 5.1.1 and 5.1.2 give the Haling radial and axial average power distributions.

5.1.2 Rodded Depletion Power Distribution

To generate the rodded depletion, control rod patterns were developed which gave critical eigenvalues at each point in the cycle and gave peaking similar to the Haling calculation. The resulting patterns were generally more

peaked than the Haling but were not in excess of the bundle and local power peaks seen in past cycles. However, as stated above, the underburned regions of the core can exhibit peaking in excess of the Haling when pulling ARO at End of Cycle. Figures 5.1.3 and 5.1.4 give the ARO, end of cycle power distributions for the rodded depletion. Note in Figure 5.1.4 that the average axial power is more bottom peaked, thus the better scram characteristics.

5.2 Core Exposure Distributions

Cycle 9 was calculated to be capable of a cycle exposure of 8037 MWD/ST at EOFPL (no coastdown). Table 3.3.1 summarizes the resultant core average exposures.

As stated, the Haling power shape produces a self-consistent change in exposure. The BOC radial exposure distribution is given in Figure 3.2.1. The Haling calculation produced the EOFPL radial exposure distribution given in Figure 5.2.1. Since the Haling power shape is constant, it can be held fixed by SIMULATE for smaller exposure steps to give the exposure distributions at various mid-cycle points. BOC, EOC-2000 MWD/ST, EOC-1000 MWD/ST, and EOC conditions were used to develop reactivity input for core wide transient analysis.

The rodded depletion may differ considerably from the Haling during the cycle due to the shaping of the power by the rods. However, rod sequences are swapped frequently and the overall exposure distribution at end of cycle is similar to the Haling. Figure 5.2.2 gives the EOFPL radial exposure distribution for the rodded depletion.

5.3 Cold Core Reactivity and Shutdown Margin

The cold K_{eff} with all rods withdrawn (ARO) and the cold K_{eff} with all rods inserted (ARI) at BOC were calculated using the SIMULATE code and are shown in Table 5.3.1. K_{eff} with ARO minus the cold critical K_{eff} [3] is the amount of excess core reactivity. K_{eff} with ARI minus the cold critical K_{eff} is the worth of all the control rods.

Technical Specifications [8] state that the core must be subcritical by at least 0.25% +R (defined below) with the strongest worth control rod withdrawn for sufficient shutdown margin. Again using SIMULATE, a search was made for the strongest worth control rod at various exposures in the cycle. This is necessary because rod worths change with exposure. Then the cold K_{eff} with the strongest rod out was calculated every 1000 MWD/ST through the cycle. Subtracting each cold K_{eff} with the strongest rod out from the cold critical K_{eff} defines the shutdown margin as a function of exposure. Figure 5.3.1 is the result. Because the core reactivity increases with exposure, the cold K_{eff}'s increase and therefore, the shutdown margin decreases. To account for this, the value R is calculated as the difference between the cold K_{eff} with the strongest rod out at BOC and the maximum cold K_{eff} with the strongest rod out in the cycle. The R for Cycle 9 is given in Table 5.3.1.

5.4 Standby Liquid Control System Shutdown Capability

The shutdown capability of the standby liquid control system (SLCS) is designed to bring the reactor from full power to cold, ARO, xenon free shutdown with at least 5% margin. Using the boron concentration search option

in SIMULATE, the ppm of boron was adjusted until the K_{eff} reached the cold critical K_{eff} minus .05 minus a 95% confidence level uncertainty. This case assumed cold, xenon-free conditions with All-Rods-Out at the most reactive time in the cycle. The criticality search found that the plant would be 5% subcritical at the worst point in time with 702 ppm of boron injected. VY Technical Specifications require that 800 ppm of boron be available for injection. Table 5.4.1 lists the amount of boron concentration and the shutdown margin.

TABLE 5.3.1

K_{eff} VALUES: SHUTDOWN MARGIN CALCULATION

BOC K_{eff} - Uncontrolled	1.1084
BOC K_{eff} - Controlled	.9605
Cold Critical K_{eff} - Search Eigenvalue	.9954
BOC K_{eff} - Controlled Strongest Worth Rod Withdrawn	.9810
BOC Minimum Shutdown Margin	1.44% Δ K
R, Maximum increase in Cold K_{eff} With Exposure	0.66% Δ K
Cycle Minimum Shutdown Margin at 5037 MWD/ST	0.78% Δ K

TABLE 5.4.1

STANDBY LIQUID CONTROL SYSTEM SHUTDOWN CAPABILITY

ppm of Boron	Shutdown Margin
702	.050
800	.068

VERMONT YANKEE
CYCLE 9 HALING DEPLETION
EOC BUNDLE AVERAGE RELATIVE POWERS

R5X2 0.969	R7XX 1.163	R5X2 1.029	R8XX 1.306	R5X2 1.036	R7XX 1.162	R5X2 0.972	R7XX 1.085	R6XX 0.936	R8XX 0.936	R7XX 0.606
R7XX 1.161	R5X1 1.051	R8XX 1.311	R8XX 1.171	R8XX 1.326	R6XX 1.131	R8XX 1.251	R8XX 1.034	R8XX 1.082	R7XX 0.841	R5X2 0.459
R5X2 1.028	R8XX 1.310	R6XX 1.181	R8XX 1.365	R8XX 1.184	R8XX 1.319	R6XX 1.107	R8XX 1.189	R6XX 0.901	R8XX 0.800	R5X1 0.391
R8XX 1.304	R6XX 1.169	R8XX 1.364	R6XX 1.197	R8XX 1.346	R6XX 1.137	R8XX 1.248	R7XX 1.080	R8XX 0.949	R5X2 0.563	
R5X2 1.033	R8XX 1.323	R6XX 1.182	R8XX 1.344	R6XX 1.149	R7XX 1.174	R6XX 1.028	R8XX 1.061	R7XX 0.771		
R7XX 1.178	R8XX 1.125	R8XX 1.316	R6XX 1.133	R7XX 1.171	R8XX 1.047	R8XX 1.104	R7XX 0.886	R5X2 0.529		
R5X2 0.968	R8XX 1.246	R8XX 1.100	R8XX 1.244	R8XX 1.023	R8XX 1.102	R8XX 0.844	R7XX 0.724	R5X2 0.404		
R7XX 1.078	R6XX 1.025	R8XX 1.184	R7XX 1.072	R8XX 1.057	R7XX 0.882	R7XX 0.723	R6XX 0.519			
R8XX 0.928	R8XX 1.077	R6XX 0.897	R8XX 0.944	R7XX 0.762	R5X2 0.525	R5X2 0.407				
R8XX 0.930	R7XX 0.835	R8XX 0.796	R5X2 0.548							
R7XX 0.801	R5X2 0.463	R5X1 0.388								

FUEL TYPE ID
RELATIVE POWER

NORTH

R5X1 - 8DB274H, RELOAD 5

R5X2 - 8DPB289, RELOAD 5

R8XX - P8DPB289, RELOAD 6

R7XX - P8DPB289, RELOAD 7

R8XX - P8DPB289, RELOAD 8

FIGURE 5.1.1

VY CYCLE 9 HALING DEPLETION EOC BUNDLE AVERAGE RELATIVE POWERS

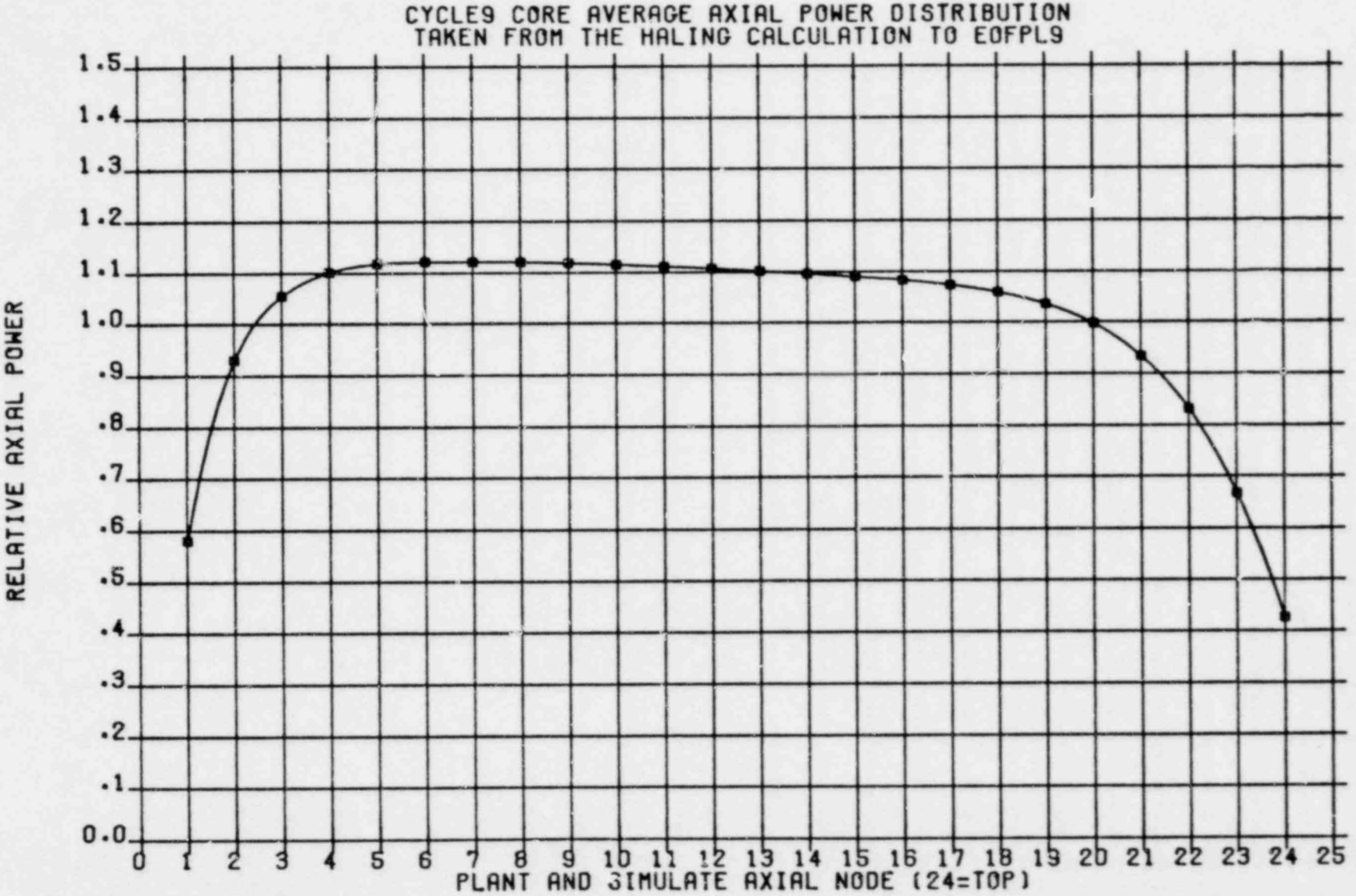

FIGURE 5.1.2

CYCLE 9 CORE AVERAGE AXIAL POWER DISTRIBUTION TAKEN FROM THE HALING CALCULATION TO EOFPL9

VERMONT YANKEE CYCLE 9
RODDED DEPLETION -- ALL RODS OUT AT EOFPL9
BUNDLE AVERAGE RELATIVE POWERS

R5X2 1.045	R7XX 1.255	R5X2 1.099	R8XX 1.389	R5X2 1.076	R7XX 1.207	R5X2 0.975	R7XX 1.070	R8XX 0.919	R8XX 0.918	R7XX 0.588
R7XX 1.260	R5X1 1.133	R8XX 1.410	R8XX 1.235	R8XX 1.384	R8XX 1.156	R8XX 1.285	R8XX 1.024	R8XX 1.067	R7XX 0.824	R5X2 0.446
R5X2 1.100	R8XX 1.405	R8XX 1.251	R8XX 1.429	R8XX 1.219	R8XX 1.345	R8XX 1.112	R8XX 1.179	R8XX 0.886	R8XX 0.785	R5X1 0.379
R8XX 1.374	R8XX 1.218	R8XX 1.414	R8XX 1.222	R8XX 1.367	R8XX 1.136	R8XX 1.242	R7XX 1.062	R8XX 0.933	R5X2 0.536	
R5X2 1.058	R8XX 1.352	R8XX 1.195	R8XX 1.348	R8XX 1.139	R7XX 1.153	R8XX 1.007	R8XX 1.039	R7XX 0.746		
R7XX 1.173	R8XX 1.120	R8XX 1.305	R8XX 1.113	R7XX 1.139	R8XX 1.017	R8XX 1.073	R7XX 0.859	R5X2 0.509		
R5X2 0.948	R8XX 1.222	R8XX 1.075	R8XX 1.210	R8XX 0.990	R8XX 1.085	R8XX 0.814	R7XX 0.895	R5X2 0.383		
R7XX 1.040	R8XX 0.993	R8XX 1.147	R7XX 1.034	R8XX 1.018	R7XX 0.846	R7XX 0.691	R8XX 0.488	→ NORTH		
R8XX 0.894	R8XX 1.039	R8XX 0.866	R8XX 0.910	R7XX 0.724	R5X2 0.498	R5X2 0.383				
R8XX 0.895	R7XX 0.803	R8XX 0.765	R6X2 0.520							
R7XX 0.571	R5X2 0.431	R5X1 0.388	FUEL TYPE ID RELATIVE POWERS							

R5X1 - 8DB274H, RELOAD 5

R5X2 - 8DPB289, RELOAD 5

R8XX - P8DPB289, RELOAD 8

R7XX - P8DPB289, RELOAD 7

R8XX - P8DPB289, RELOAD 8

FIGURE 5.1.3

VY CYCLE 9 RODDED DEPLETION - ARO AT EOFPL9,
BUNDLE AVERAGE RELATIVE POWERS

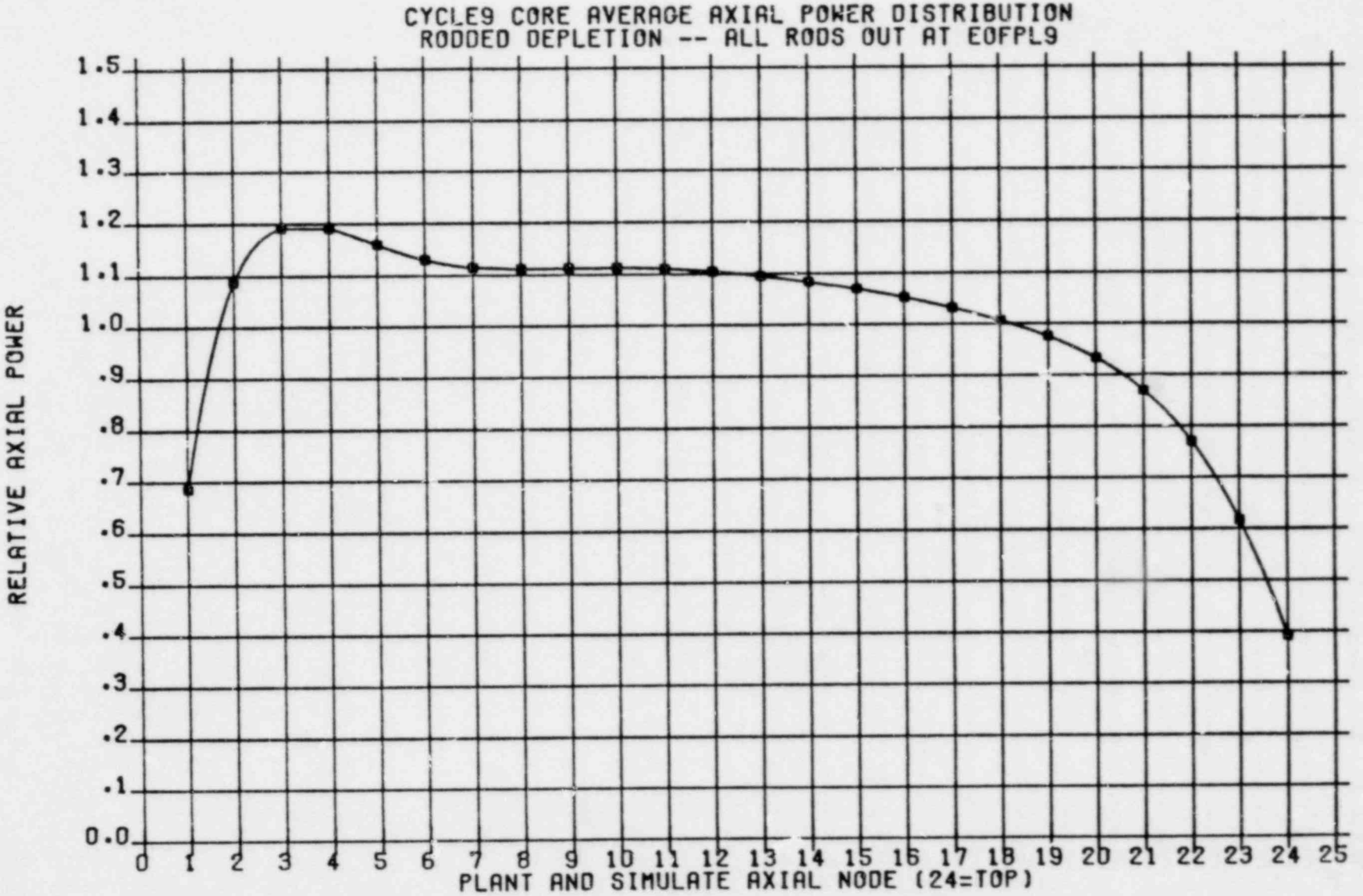

FIGURE 5.1.4

CYCLE 9 CORE AVERAGE AXIAL POWER DISTRIBUTION, RODDED DEPLETION - ARO AT EOFPL9

VERMONT YANKEE
CYCLE 9 HALING DEPLETION
EOC BUNDLE AVERAGE EXPOSURES

R5X2 27.64	R7XX 14.85	R5X2 28.39	R8XX 10.58	R5X2 28.54	R7XX 15.20	R5X2 28.36	R7XX 15.46	R6XX 21.76	R8XX 7.52	R7XX 12.26
R7XX 14.96	R5X1 24.10	R8XX 10.61	R6XX 22.04	R8XX 10.62	R6XX 22.24	R8XX 10.02	R6XX 21.71	R8XX 8.70	R7XX 14.15	R5X2 25.90
R5X2 28.49	R8XX 10.61	R6XX 22.15	R8XX 10.91	R6XX 21.95	R8XX 10.52	R6XX 21.88	R8XX 9.64	R6XX 21.80	R8XX 8.43	R5X1 24.99
R8XX 10.55	R6XX 22.10	R8XX 10.90	R6XX 22.17	R8XX 10.70	R6XX 22.00	R8XX 10.00	R7XX 15.36	R8XX 7.64	R5X2 25.06	
R5X2 28.58	R8XX 10.60	R6XX 22.02	R8XX 10.69	R6XX 21.51	R7XX 15.66	R6XX 22.07	R8XX 8.65	R7XX 13.87		
R7XX 15.23	R6XX 22.41	R8XX 10.50	R6XX 22.11	R7XX 15.76	R6XX 20.78	R8XX 8.92	R7XX 13.89	R5X2 24.53		
R5X2 28.43	R8XX 9.98	R6XX 22.12	R8XX 9.97	R6XX 22.19	R8XX 9.90	R6XX 21.38	R7XX 13.35	R5X2 26.12		
R7XX 15.58	R6XX 21.92	R8XX 9.50	R7XX 15.59	R8XX 8.52	R7XX 14.05	R7XX 13.49	R6XX 18.56			
R6XX 22.04	R8XX 8.86	R6XX 21.68	R8XX 7.80	R7XX 14.25	R5X2 24.78	R5X2 25.08				
R8XX 7.47	R7XX 14.34	R8XX 8.39	R5X2 25.31							
R7XX 12.33	R5X2 26.22	R5X1 25.07	FUEL TYPE ID EXPOSURE (GWD/ST)							

→ NORTH

R5X1 - BDB274H, RELOAD 5

R5X2 - BDP8289, RELOAD 5

R6XX - P8DPB289, RELOAD 6

R7XX - P8DPB289, RELOAD 7

R8XX - P8DPB289, RELOAD 8

FIGURE 5.2.1

VY CYCLE 9 HALING DEPLETION, EOC BUNDLE AVERAGE EXPOSURES

VERMONT YANKEE
CYCLE 9 RODDED DEPLETION
EOC BUNDLE AVERAGE EXPOSURES

R5X2 27.04	R7XX 14.20	R5X2 27.80	R8XX 9.44	R5X2 28.32	R7XX 15.25	R5X2 28.60	R7XX 15.98	R6XX 22.13	R8XX 7.30	R7XX 12.36
R7XX 14.03	R5X1 23.26	R8XX 9.11	R8XX 21.38	R8XX 9.64	R8XX 22.09	R8XX 9.63	R8XX 22.06	R8XX 8.62	R7XX 14.31	R5X2 25.99
R5X2 27.66	R8XX 9.10	R8XX 21.34	R8XX 9.82	R8XX 21.61	R8XX 9.90	R8XX 21.88	R8XX 9.43	R8XX 21.60	R8XX 8.15	R5X1 24.99
R8XX 9.46	R8XX 21.86	R8XX 10.06	R8XX 22.09	R8XX 10.36	R8XX 22.28	R8XX 9.86	R7XX 15.71	R8XX 7.49	R5X2 25.06	
R5X2 28.51	R8XX 10.05	R8XX 22.04	R8XX 10.51	R8XX 21.96	R7XX 16.24	R8XX 22.51	R8XX 8.62	R7XX 14.15		
R7XX 15.62	R8XX 22.76	R8XX 10.48	R8XX 22.69	R7XX 16.52	R8XX 21.50	R8XX 9.14	R7XX 14.42	R5X2 24.84		
R5X2 28.94	R8XX 10.08	R8XX 22.59	R8XX 10.21	R8XX 22.84	R8XX 9.20	R8XX 21.96	R7XX 13.93	R5X2 26.44		
R7XX 16.26	R8XX 22.48	R8XX 9.84	R7XX 16.16	R8XX 8.75	R7XX 14.65	R7XX 14.09	R8XX 19.05	→ NORTH		
R8XX 22.50	R8XX 8.70	R8XX 22.00	R8XX 7.60	R7XX 14.64	R5X2 25.14	R5X2 25.43				
R8XX 7.38	R7XX 14.81	R8XX 8.22	R5X2 25.39							
R7XX 12.61	R5X2 26.97	R5X1 25.13	FUEL TYPE ID EXPOSURE (GWD/ST)							

R5X1 - 8DB274H, RELOAD 5

R5X2 - 8DPB289, RELOAD 5

R8XX - P8DPB289, RELOAD 8

R7XX - P8DPB289, RELOAD 7

R8XX - P8DPB289, RELOAD 8

FIGURE 5.2.2

VY CYCLE 9 RODDED DEPLETION, EOC BUNDLE AVERAGE EXPOSURES

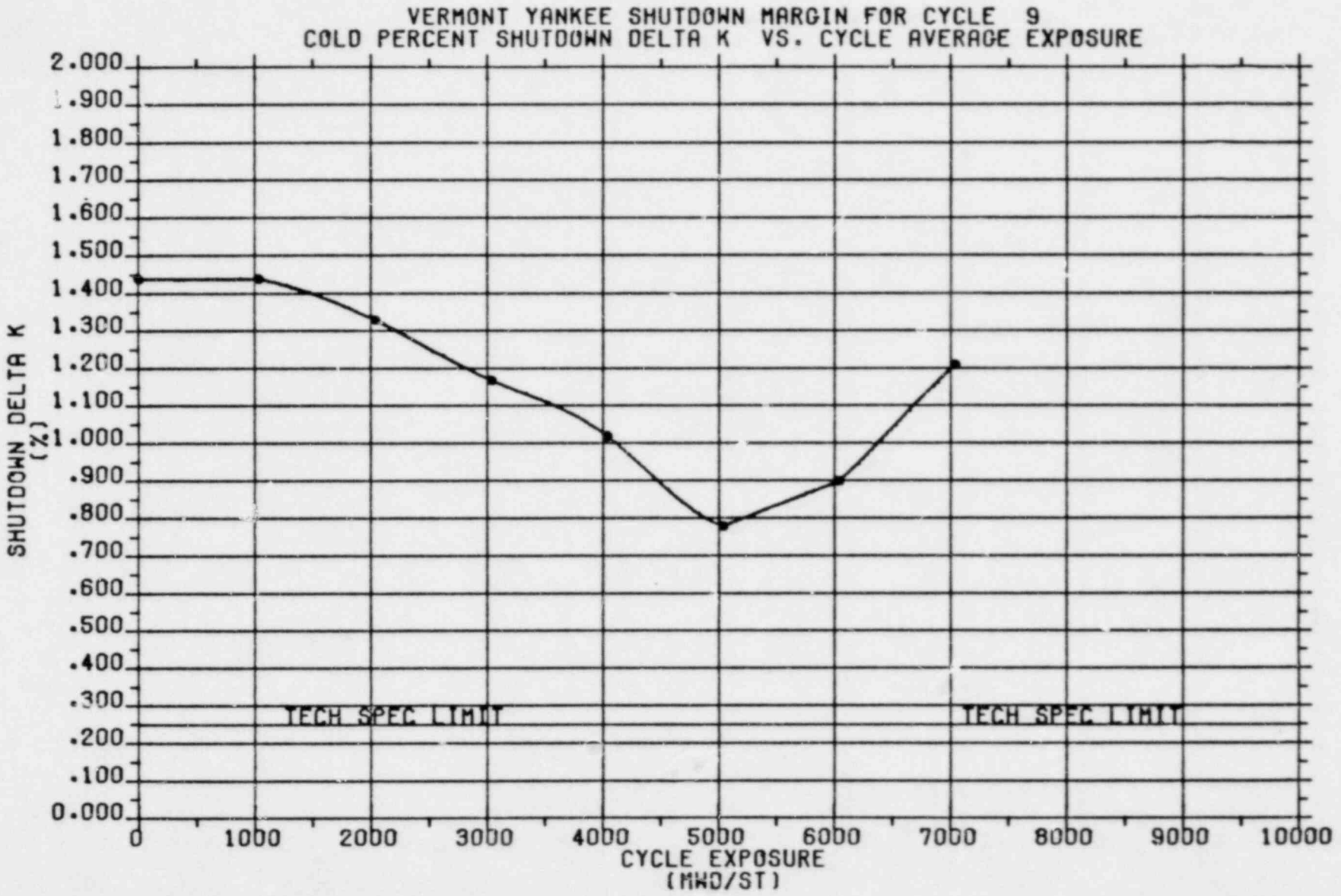

FIGURE 5.3.1

VY SHUTDOWN MARGIN FOR CYCLE 9, COLD PERCENT SHUTDOWN DELTA K VERSUS CYCLE AVERAGE EXPOSURE

6.0 THERMAL-HYDRAULIC DESIGN

The thermal hydraulic evaluation of the reload cycle was performed using the methods described in the following section.

6.1 Steady-State Thermal Hydraulics

Core steady state thermal-hydraulic analyses were performed using the FIBWR [9,10] computer code. The FIBWR code incorporates a detailed geometrical representation of the complex flow paths in a BWR core, and explicitly models the leakage flow to the bypass region. FIBWR calculates the core pressure drop and total bypass flow for a given total core flow. The power distribution, inlet enthalpy, and geometry are presumed known and are supplied to FIBWR. Power distribution is derived by the 3-D neutronic simulator SIMULATE [3]. Core pressure drop and total leakage flow predicted by the FIBWR code were used in setting the initial conditions for the system's transient analysis model. Further details are provided in Reference 9.

6.2 Reactor Limits Determination

The objective for normal operation and transient events is to maintain nucleate boiling and thus avoid a transition to film boiling, thereby protecting the fuel cladding integrity. Based on Reference 11, the fuel cladding integrity safety limit for Vermont Yankee is a lowest allowable minimum critical power ratio (LAMCPR) of 1.07 for 8X8R/P8X8R reload

cycles. Operating limits are specified to maintain adequate margin to the onset of the boiling transition. The figure of merit utilized for plant operation is the critical power ratio (CPR). This is defined as the ratio of the critical power (bundle power at which some point within the assembly experiences onset of boiling transition) to the operating bundle power. Thermal margin is stated in terms of the minimum value of the critical power ratio MCPR, which corresponds to the most limiting fuel assembly in the core. Both the transient (safety) and normal operating thermal limits in terms of MCPR are derived based on the GEXL correlation as described in Reference 11.

Vermont Yankee Technical Specification limits the operation of 8X8, 8X8R, and P8X8R fuel types to a maximum linear heat generation rate (MLHGR) of 13.4 KW/ft. The basis for a MLHGR of 13.4 KW/ft can be found in Reference 2.

7.0 ACCIDENT ANALYSIS

7.1 Core Wide Transient Analysis

Core wide transient simulations are performed to assess the impact of the particular transient on the heat transfer characteristics of the fuel. The figure of merit used is the critical power ratio [11].

More specifically, it is the purpose of the analysis to determine the minimum critical power ratio for each fuel type such that the safety limit critical power ratio is not exceeded for the transients considered.

7.1.1 Methodology

The analysis requires two types of simulations. A system level simulation is performed to determine the overall plant response. Transient core inlet and exit pressures and normalized power from the system level calculation are used to perform detailed thermal hydraulic simulations (referred to as "hot channel calculations") of each fuel type. The results of each of these latter simulations is the bundle transient ΔCPR (the initial bundle CPR minus the minimum CPR experienced during the transient).

The system level simulations are performed with the model documented in Reference 12.

The hot channel calculations are performed with the RETRAN [13] and MAYU4-YAEC [14] computer codes. The GEXL correlation [11] is used in MAYU4-YAEC to evaluate critical power ratio. The calculational procedure is outlined below.

The hot channel transient ΔCPR calculations are performed via a series of "inner" and "outer" iterations, as illustrated by the flow chart in Figure 7.1.1. The outer loop represents iterations on the hot channel initial power level. These iterations are necessary because the ΔCPR for a given transient varies with Initital Critical Power Ratio (ICPR), yet only the ΔCPR corresponding to a transient MCPR equal to the safety limit (i.e., 1.07 + ΔCPR = ICPR) is appropriate. The approximate constancy of the ΔCPR/ICPR ratio is useful in these iterations. Each outer iteration requires a RETRAN hot channel run to establish the transient boundary conditions of inlet flow, inlet enthalpy, channel pressure and power level required for input to the MAYU4-YAEC code. MAYU4-YAEC is then used to calculate a CPR at each time-step during the transient, from which a transient ΔCPR is derived. The hot channel is modeled using a chopped cosine axial power shape with a peak/average ratio of 1.4.

The inner loop represents iterations on the hot channel inlet flow. These iterations are necessary because the RETRAN hot channel model calculates an exit loss coefficent when given the inital power level, flow, and pressure drop as input. The pressure drop is assumed equal to the core average pressure drop, and the flow is varied for a given power level until the exit loss coefficient is correct. FIBWR [9] is utilized to estimate the correct inlet flow for a particular power level and pressure drop.

7.1.2 Initial Conditions and Assumptions

The initial conditions for the system simulations are based on 105% rated steam flow (maximum turbine capacity) and 100% core flow. The core axial power distribution for each of the exposure points is based on Haling-mode 3-D SIMULATE predictions associated with the generation of the reactivity data (Section 7.1.3). The core inlet enthalpy is set so that the amount of carryunder from the steam separators and the quality in the liquid region outside the separators is as close to zero as possible. For fast pressurization transients, this maximizes the initial pressurization rate and predicts a more severe neutron power spike. A summary of the initial operating state used for the system simulations is provided in Table 7.1.1.

Assumptions specific to a particular transient are discussed in the section describing the transient. In general, the following assumptions are made for all transients.

1. Scram setpoints are at Technical Specification limits.

2. Protective system logic delays are at equipment specification limits.

3. Safety/Relief Valve and Safety Valve capacities are based on Technical Specification rated values.

4. Safety/Relief Valve and Safety Valve setpoints are modeled as being 1% above the Technical Specification upper limit. Valve responses are based on slowest specified response values.

5. Control rod drive scram speed is based on the proposed Technical Specification limits. The analysis addresses a dual set of scram speeds as given in the proposed Technical Specifications. These are referred to as the "measured" and "67B" scram time sets.

7.1.3 Reactivity Functions

The methods used to generate the fuel temperature, moderator density, and scram reactivity functions are described in Reference 15 and are specifically as outlined in Figures 2.1 through 2.5 of that document. A complete set of reactivity functions, the axial power distribution, and kinetics parameters are generated from "defined" base states established for EOC, EOC-1000 MWD/ST, EOC-2000 MWD/ST, and BOC cycle exposure conditions. These states are characterized by exposure and void history distributions, control rod pattern, and core thermal-hydraulic conditions.

The Cycle 9 BOC hot, full power core state is established from the pre-defined Cycle 8 endpoint, the Cycle 9 reload pattern, and an estimate of the BOC control rod pattern. The EOC and intermediate core exposure and void history distributions were calculated via a Haling depletion as described in Section 5.2. The EOC state is unrodded and, as such, is defined sufficiently. However, EOC-1000 MWD/ST and EOC-2000 MWD/ST exposure points require a control rod pattern and such was developed using the following

algorithm. Beginning with the rodded depletion control configuration, all control rods which are more than half-inserted are fully inserted and all control rods which are less than half-inserted are fully withdrawn. If the SIMULATE-calculated parameters are less than or close to limits, then this configuration becomes the base case. If the limits are greatly exceeded in this SIMULATE calculation, a minimum number of control rods are adjusted a minimum number of notches until the parameters are less than or close to limits. Using this methodology, the control rod patterns and resultant power distributions are established so as to minimize the scram reactivity function and to maximize the core average moderator density reactivity coefficient. For the turbine trip without bypass, generator load rejection without bypass, and loss of feedwater heating transient analyses, these configurations maximize the power response.

In generating the fuel reactivity function data for RETRAN, 12 unique volume-specific table sets are produced which are analagous to that shown in Figure 3.7 of Reference 15. The moderator and relative moderator density functions also are 12 unique volume-specific tables, analagous to Figures 3.10 and 3.11 in Reference 15. A moderator density set is generated specifically for each transient type. The density reactivity functions for the subcooling transient are generated by quasi-statically varying the inlet subcooling only. The moderator enthalpy source distribution is in equilibrium with the calculated nuclear power. The density reactivity functions of the pressurization transients are generated by quasi-statically varying the core pressure. A series of the calculations are performed for various inlet moderator temperatures. The moderator enthalpy source distribution is that of the base state case.

In order to qualitatively compare the core reactivity characteristics between different base configurations, core average reactivity coefficients are calculated and provided in Table 7.1.2. Calculated kinetics parameters for RETRAN are also provided in the Table.

The reactivities versus scram insertion is calculated at constant, pre-transient moderator conditions. These calculated data are fit and evaluated to yield the highly detailed scram reactivity curves. These are then combined with the rod position versus time curves to establish the final RETRAN scram reactivity function. Figures 7.1.2 through 7.1.4 display the inserted rod worths and rod positions as functions of scram time for the "measured" scram time analysis. Figure 7.1.5 through 7.1.7 display similar curves for the "67B" scram time analysis.

7.1.4 Transients Analyzed

Past licensing experience has shown that the core wide transients most likely to result in the minimum core thermal margins are:

1. Generator load rejection with complete failure of the turbine bypass system.

2. Turbine trip with complete failure of the turbine bypass system.

3. Loss of feedwater heating.

The "feedwater controller failure (maximum demand)" transient is not a severe transient for Vermont Yankee, because of the plant's 110% steam flow bypass system. Past analyses have shown this transient to be considerably less severe than any of the above for all exposure points. Brief descriptions and the results of the core wide transients analyzed are provided in the following section.

7.2 Core Wide Transient Analysis Results

The transients selected for consideration were analyzed at exposure points of end of cycle (EOC), EOC-1000 MWD/ST, and EOC-2000 MWD/ST; the loss of feedwater heating was also evaluated at beginning of cycle conditions. A summary of the results of the analyses is provided in Table 7.2.1. The turbine trip without bypass transient is the most severe transient for the EOC condition; and the loss of feedwater heating transient is the most severe for the EOC-1000 MWD/ST and EOC-2000 MWD/ST conditions.

7.2.1 Turbine Trip Without Bypass Transient (TTWOB)

The transient is initiated by a rapid closure (0.1 sec. closing time) of the turbine stop valves. It is assumed that the steam bypass valves, which normally open to relieve pressure, remain closed. A reactor protection system signal is generated by the turbine stop valve closure switches. Control rod drive motion is conservatively assumed to occur 0.27 seconds after the start of turbine stop valve motion. The ATWS recirculation pump trip is assumed to occur at a setpoint of 1150 psig dome pressure. A pump trip time delay of 1.0 second is assumed to account for logic delay and M-G set generator field

collapse. In simulating the transient, the bypass piping volume up to the valve chest is lumped into the control volume upstream of the turbine stop valves. Predictions of the system parameters of main interest are shown in Figures 7.2.1 through 7.2.3 for the three exposure points for the "measured" scram time analysis.

7.2.2 Generator Load Rejection Without Bypass Transient (GLRWOB)

The transient is initiated by a rapid closure (0.3 seconds closing time) of the turbine control valves. As in the case of the turbine trip transient, the bypass valves are assumed to fail. A reactor protection system signal is generated by the hydraulic fluid pressure switches in the acceleration relay of the turbine control system. Control rod drive motion is conservatively assumed to occur 0.28 seconds after the start of turbine control valve motion. The same modeling regarding the ATWS pump trip and bypass piping are used in the simulation as in the turbine trip simulation. The influence of the accelerating main turbine-generator on the recirculation system is simulated by specifying the main turbine generator electrical frequency as a function of time for the M-G set drive motors. The main turbine generator frequency curve is based on a 100% power plant startup test and is considered representative for the simulation. The system model predictions for the three exposure points are shown in Figures 7.2.4 through 7.2.6 for the "measured" scram time analysis.

7.2.3 Loss of Feedwater Heating Transient (LOFWH)

A feedwater heater can be lost in such a way that the steam extraction line to the heater is shut off or the feedwater flow bypasses one of the heaters. In either case, the reactor will receive cooler feedwater, which will produce an increase in the core inlet subcooling, resulting in a reactor power increase.

The response of the system due to the loss of 100°F of the feedwater heating capability was analyzed. This represents the current licensing assumption for the maximum expected single heater or group of heaters that can be tripped or bypassed by a single event. The reactor is assumed to be on manual recirculation flow control when the heater is lost.

The transient response of the system was evaluated at several exposures during Cycle 9. Transient evaluation at EOC-2000 MWD/ST was found to be the limiting case between BOC to EOC.

Vermont Yankee has a scram set point (120% of NBR) as part of the reactor protection system (RPS) on high neutron flux. In this analysis, no credit was taken for scram on high neutron flux, thereby allowing the reactor power to reach its peak without scram. This approach was selected to provide a bounding and conservative analysis.

The results of the system response to a loss of 100°F feedwater heating capability evaluated at EOC-2000 MWD/ST as predicted by the RETRAN code are presented in Figure 7.2.7.

7.3 Overpressurization Analysis Results

Compliance with ASME vessel code limits is demonstrated by an analysis of the main steam isolation valves (MSIV) closing with failure of the MSIV position switch scram. End of cycle conditions were analyzed. The system model used is the same as that used for the core wide transient analysis (Section 7.1.1). The initial conditions and modeling assumptions discussed in Section 7.1.2 are applicable to this simulation. The maximum pressure at the bottom of the reactor vessel is calculated to be 1280 psig for the "measured" scram time analysis and 1310 psig for the "67" scram time analysis. This result is within the allowable code limit of 1375 psig, 10% above vessel design pressure for upset conditions.

The transient is initiated by a simultaneous closure of all four MSIV's. A 3.0 second closing time, which is the Tech Spec. minimum, is assumed. A reactor scram signal is generated on APRM high flux. Control rod drive motion is conservatively assumed to occur 0.28 seconds after reaching the high flux setpoint. The system response is shown in Figure 7.3.1 for the "measured" scram time analysis.

7.4 Rod Withdrawal Error Transient Results

The rod withdrawal error is a local core transient caused by an operator erroneously withdrawing a control rod in the continuous withdrawal mode. If the core is operating at its operating limits for MCPR and LHGR at the time of the error, then withdrawal of a control rod could increase both local and core power levels with the potential for overheating the fuel.

There is a broad spectrum of core conditions and control rod patterns which could be present at the time of such an error. For many situations it would be possible to fully withdraw a control rod without violating either fuel cladding integrity safety limit.

To bound the most severe of postulated rod withdrawal error events, a portion of the core MCPR operating limit envelope is specifically defined such that the cladding limits are not violated. The consequences of the error depend on the local power increase, the initial MCPR of the neighboring locations and the ability of the Rod Block Monitor System to stop the withdrawing rod before MCPR reaches 1.07.

The most severe postulated transient begins with the core operating according to normal procedures and within normal operating limits. The operator makes a procedural error and attempts to fully withdraw the maximum worth control rod at maximum withdrawal speed. The core limiting locations are close to the error rod and therefore experience the spatial power shape transient as well as the overall core power increase.

The core conditions and control rod pattern for the bounding case are specified using the following set of concurrent worst case assumptions:

1. The rod should have high reactivity worth. This is provided for by analysis of the core at the exposure corresponding to maximum control inventory with the xenon-free condition superimposed. The xenon-free condition and the additional control rod inventory needed to maintain

criticality exaggerates the worth of control rods substantially when compared to normal operation with normal xenon levels. A fully inserted high worth rod is selected as the error rod.

2. The core is initially at rated power and flow.

3. The core power distribution is adjusted with the available control rods to place the locations within the four by four array of bundles around the error rod as nearly on the operating limits as practical.

The Rod Block Monitor System's ability to terminate the bounding case is evaluated on the following bases:

1. Technical Specifications allow each of the separate RBM channels to remain operable if at least half of the LPRM inputs at every level are operable. For the interior RBM channels tested in this analysis, there are a maximum of four LPRM inputs per level. One RBM channel averages the inputs from the A and C levels; the other channel averages the inputs from the B and D levels. Considering the inputs for a single channel, there are eleven failure combinations of none, one and two failed LPRM strings. The RBM channel responses are evaluated separately at these eleven input failure conditions. Then, for each channel taken separately, the lowest response as a function of error rod position is chosen for comparison to the RBM setpoint.

2. The event is analyzed separately in each of the four quadrants of the core due to the differing LPRM string physical locations relative to the error rod.

Technical Specifications require that both RBM channels be operable during normal operation. Thus, the first channel calculated to intercept the RBM setpoint is assumed to stop the rod. To allow for control system delay times, the rod is assumed to move two inches after the intercept and stop at the following notch.

The analysis is performed using the three dimensional steady state SIMULATE core model demonstrated in Reference 3. Necessary properties of that model for use in this analysis are:

1. Accurate bundle power calculation as shown by the PDQ and gamma scan comparisons.

2. Accurate LPRM signal calculation as shown by the detailed TIP trace comparisons.

3. Accurate control rod worths and core power coefficient as shown by the consistent core eigenvalues.

Two separate cases are presented from explicit SIMULATE analyses. The reactor conditions and case descriptions are shown in Figures 7.4.1 and 7.4.2. Case 1 analyzes the bounding event with the concurrent abnormal xenon condition and rod pattern configuration provided to increase the worth of the error rod. The initial conditions for Case 2 approximate the expected full power conditions at the most reactive point in the cycle; the control rod density is at its maximum at the normal equilibrium xenon condition. The ΔCPR and MLHGR values for both cases are shown in Table 7.4.1. The ΔCPR values are

evaluated such that the implied operating limit MCPR equals 1.07 + ΔCPR, conserving the Figure of Merit (ΔCPR/Initial CPR) shown by the SIMULATE calculations. The use of this method provides valid ΔCPR values in the analysis of normal operating states where locations near the assumed error rod are not initially near the MCPR operating limit. Case 2 is the worst of three rod withdrawal transients analyzed from the same initial full power, full flow and rod pattern conditions. Cases using the rod at coordinates (22,27) and at (22,35) were found to be less severe than Case 2 and all were bounded by Case 1 with substantial MCPR margin.

As an example for Case 1, Figures 7.4.3 and 7.4.4 show the determinations of the end of transient control rod position at the point where the weakest RBM channel response first intercepts the RBM setpoint.

The operating limit ΔCPR envelope component versus Rod Block Monitor setpoint is taken from the Table 7.4.1 values for the bounding Case 1. The same table demonstrates margin to the 1% plastic strain limit including the 2.2% power spiking penalty.

7.5 Misloaded Bundle Error Analysis

7.5.1 Rotated Bundle Error

The primary result of an assembly rotation is a large increase in local pin peaking and R-factor as higher enrichment pins are placed adjacent to the surrounding wide water gaps. In addition, there may be a small increase in reactivity, depending on the exposure and void fraction states. The R-factor

increase results in a CPR reduction, while the local pin peaking factor increase results in a higher pin linear heat generation rate. The objective of the analysis is to insure that in the worst possible rotation, the safety limit linear heat generation rate and CPR are not violated with the most limiting monitored bundles on their operating limits.

To analyze the CPR response, rotated bundle R-factors as a function of exposure are developed by adding the largest possible ΔR-factor increase resulting from a rotation to the exposure dependent R-factors of the properly oriented bundles [11]. Using these rotated bundle R-factors, the minimum CPR values resulting from a bundle rotation are determined using the SIMULATE code, for each control rod sequence throughout the cycle. These minimum CPR values are in addition modified slightly to account for the change in reactivity resulting from the rotation. For each sequence, the MCPR for the properly oriented assemblies is ratioed by a factor necessary to place the minimum rotated CPR on its 1.07 safety limit. The maximum of these adjusted MCPR's is the rotated bundle operating limit.

To determine the maximum linear heat generation rate (MLHGR) resulting from a rotation, the ratios of the maximum rotated local peaking factor to the maximum unrotated local peaking are determined for the expected range of exposure and void conditions. The maximum of this ratio is applied to the operating limit LHGR. This maximum rotated bundle LHGR is in addition modified to account for (1) the possible reactivity increase resulting from the rotation and (2) a 2.2% power spiking penalty.

The results of the rotated bundle analysis are as given in Table 7.5.1.

7.5.2 Mislocated Bundle

Misloading a high reactivity assembly into a region of high neutron importance results in a location of high relative assembly average power. Since the assembly is assumed to be properly oriented (not rotated), R-factors used for the misloaded bundle are the standard values for the misloaded fuel type.

The analysis for Cycle 9 consists of an iterative procedure which successively eliminates potential misloading locations from any MCPR safety limit violations. The first step is to use SIMULATE to determine the largest possible ΔCPR which could result at any location as the result of misloading a high reactivity assembly into the location. This maximum ΔCPR is then applied to all core CPR's for various cycle exposure states. Even with this maximum ΔCPR applied, some locations will never exceed the MCPR safety limit of 1.07.

The next iteration consists of applying the same procedure to the locations which did not result in CPR's above the safety limit when the maximum ΔCPR from the first iteration was applied. Since these locations are of higher reactivity than those eliminated in the first iteration, they will result in a lower ΔCPR from a misloading. Using this new maximum ΔCPR, some of the remaining locations will be eliminated from potential CPR safety limit violations. This procedure is continued until all locations are shown to be above the MCPR safety limit due to a misloading, or until a limiting location is identified.

Using the above procedure, it has been demonstrated that for Cycle 9 all possible mislocations resulted in calculated MCPR's above the 1.07 safety limit, assuming an initial operating CPR limit of 1.24.

7.6 Control Rod Drop Accident Results

The control rod sequences are a series of rod withdrawal and banked withdrawal instructions specifically designed to minimize the worths of individual control rods. The sequences are examined so that, in the event of the uncoupling and subsequent free fall of the rod, the incremental rod worth is acceptable. Incremental worth refers to the fact that rods beyond Group 2 are banked out of the core and can only fall the increment from all-in to the rod drive withdrawal position. Acceptable worth is one which produces a maximum fuel enthalpy less than 280 calories/gram. This provides considerable margin to the sudden fuel pin rupture threshold of 425 calories/gram [16].

Some out-of-sequence control rods could accrue potential high worths. However, the Rod Worth Minimizer (RWM) will prevent withdrawing an out-of-sequence rod if accidentally selected. The RWM is functionally tested before each startup.

The sequence entered into the RWM will take the plant from All-Rods-In (ARI) to well above 20% CTP. Above 20% power even multiple operator errors will not create a potential rod drop situation above 280 calories per gram [17]. Below 20% CTP, however, the sequences must be examined for incremental rod worth. This is done using the full core, xenon free SIMULATE model at the projected most reactive point in the cycle. This assures that the maximum amount of reactivity is held in the rods.

Both the A and B sequences were examined. It was found that the highest worth occurred in the first rod pull of the second group. Any of the first four rod arrays shown in Figures 7.6.1 and 7.6.2 may be designated as the first group pulled. But, then a specific second group must follow as Table 7.6.1 illustrates. For added conservatism, the highest worth rod in the second group was deliberately assigned to be the first rod pulled. This assures that in any sequence followed at the plant, the worths will always be less than those calculated here.

Beyond Group 2, banking procedures [18] apply which severely limit the rod incremental worths. This is why the xenon free, hot standby worth is much less than the cold xenon free worth. The results of the calculations are presented in Table 7.6.2.

7.7 Stability Analysis Results

The analysis of reactor stability has been performed by General Electric as described in Section 5.4 of Reference 2. The 105% rod line was analyzed and the resultant decay ratio as a function of reactor power level is provided in Figure 7.7.1.

The reactor core stability decay ratio, x_2/x_0, is calculated to be 0.83. The channel hydrodynamic performance decay ratios, x_2/x_0, are calculated to be 0.38 and 0.30 for the 8X8 channel and the 8X8R/P8X8R channel, respectively.

TABLE 7.1.1

SUMMARY OF SYSTEM TRANSIENT MODEL
INITIAL CONDITONS FOR CORE WIDE TRANSIENT ANALYSES

Core Thermal Power (MWth)	1664.0
Turbine Steam Flow (% NBR)	105
Total Core Flow (10^6 lbm/hr)	48.0
Core Bypass Flow (10^6 lbm/hr)	5.3
Core Inlet Enthalpy (BTU/lbm)	520.5
Steam Dome Pressure (psia)	1034.7
Turbine Inlet Pressure (psia)	991.6
Total Recirculation Flow (10^6 lbm/hr)	23.5
Core Plate Differential Pressure (psi)	18.6
Average Fuel Gap Conductance (BTU/hr-ft^2-F)	
EOC	900.0
EOC-1000 MWD/ST	890.0
EOC-2000 MWD/ST	885.0
Narrow Range Water Level (in.)	35

Table 7.1.2

TRANSIENT ANALYSIS REACTIVITY COEFFICIENTS
VERMONT YANKEE CYCLE 9

Calculated Parameter	Cycle Exposure Point (MWD/ST) EOC	(EOC-1000)	(EOC-2000)	BOC
Axial Shape Index(1)	-0.0490	-0.2057	-0.2498	-0.1220
Moderator Density Coefficient (Subcooling), ¢/Δu(2) Pressure = 1050 psia Subcooling = 30 BTU/lbm	21.0	24.1	25.3	20.4
Moderator Density Coefficient (Pressurization), ¢/Δu Pressure = 1050 psia Inlet Enthalpy = 520 BTU/lbm	22.9	24.7	25.9	-
Fuel Temperature Coefficient at 1130°F, ¢/°F	-0.272	-0.267	-0.275	-0.249
Effective Delayed Neutron Fraction	0.005383	0.005471	0.005533	0.005999
Prompt Neutron Generation Time, microseconds	42.74	43.13	42.57	39.69

Notes: (1) Axial Shape Index (ASI) = $\frac{P_T - P_B}{P_T + P_B}$

(2) Δu = change in density, lbm/ft^3

TABLE 7.2.1

CORE WIDE TRANSIENT ANALYSIS RESULTS

Transient	Exposure	Peak Prompt Power (Fraction of Initial Value)	Peak Avg. Heat Flux (Fraction of Initial Value)	ΔCPR 8X8	ΔCPR 8X8R/P8X8R
Turbine Trip Without Bypass, "Measured" Scram Time	EOC	3.50	1.23	0.20	0.20
	EOC-1000	2.86	1.18	0.15	0.16
	EOC-2000	2.20	1.10	0.07	0.07
Turbine Trip Without Bypass, "67B" Scram Time	EOC	3.97	1.28	0.25	0.24
	EOC-1000	3.38	1.24	0.21	0.20
	EOC-2000	2.79	1.21	0.13	0.13
Generator Load Rejection Without Bypass, "Measured" Scram Time	EOC	3.35	1.22	0.20	0.19
	EOC-1000	2.78	1.17	0.16	0.15
	EOC-2000	2.08	1.08	0.06	0.06
Generator Load Rejection Without Bypass, "67B" Scram Time	EOC	3.93	1.27	0.26	0.25
	EOC-1000	3.40	1.23	0.23	0.23
	EOC-2000	2.78	1.14	0.15	0.13
Loss of 100°F Feedwater Heating	EOC	1.21	-	0.15	0.15
	EOC-1000	1.22	-	0.17	0.16
	EOC-2000	1.23	1.22	0.17	0.17
	BOC	1.21	-	0.15	0.15

TABLE 7.4.1

ROD WITHDRAWAL ERROR TRANSIENT SUMMARY
(WITH LIMITING INSTRUMENT FAILURE)

Case 1
Conditions in Figure 7.4.1

RBM Setpoint	Rod Position	ΔCPR 8X8/8X8R/P8X8R	MLHGR (kw/ft) 8X8/8X8R/P8X8R
104	08	.08	13.8
105	10	.11	14.5
106	12	.14	15.2
107	14	.18	15.8
108	18	.22	16.9

Case 2
Conditions in Figure 7.4.2

RBM Setpoint	Rod Position	ΔCPR 8X8/8X8R/P8X8R	MLHGR (kw/ft)* 8X8/8X8R/P8X8R
104	16	.06	11.8
105	18	.08	12.1
106	18	.08	12.1
107	24	.12	12.6
108	26	.14	12.6

* Not initially on limits

TABLE 7.5.1

ROTATED BUNDLE ANALYSIS RESULTS

Initial MCPR	Resulting MCPR	Resulting LHGR (kw/ft)
1.24	1.07	17.47

TABLE 7.6.1

CONTROL ROD DROP ANALYSIS - ROD ARRAY PULL ORDER

The order in which rod arrays are pulled is specific once the choice of first group is made.

First Group Pulled is:	Second Group Pulled Must Be:	Third Group Is Banked Out
Array 1	Array 2	Array 3 or 4
Array 2	Array 1	Array 3 or 4
Array 3	Array 4	Array 1 or 2
Array 4	Array 3	Array 1 or 2

TABLE 7.6.2

CONTROL ROD DROP ANALYSIS RESULTS

Maximum Incremental Rod Worth:

Cold Xenon Free	.86% ΔK
Hot Standby, Xenon Free	.28% ΔK

Bounding Analysis Worth for Enthalpy less than 280 Calories per Gram (References 17 and 19) 1.30% ΔK

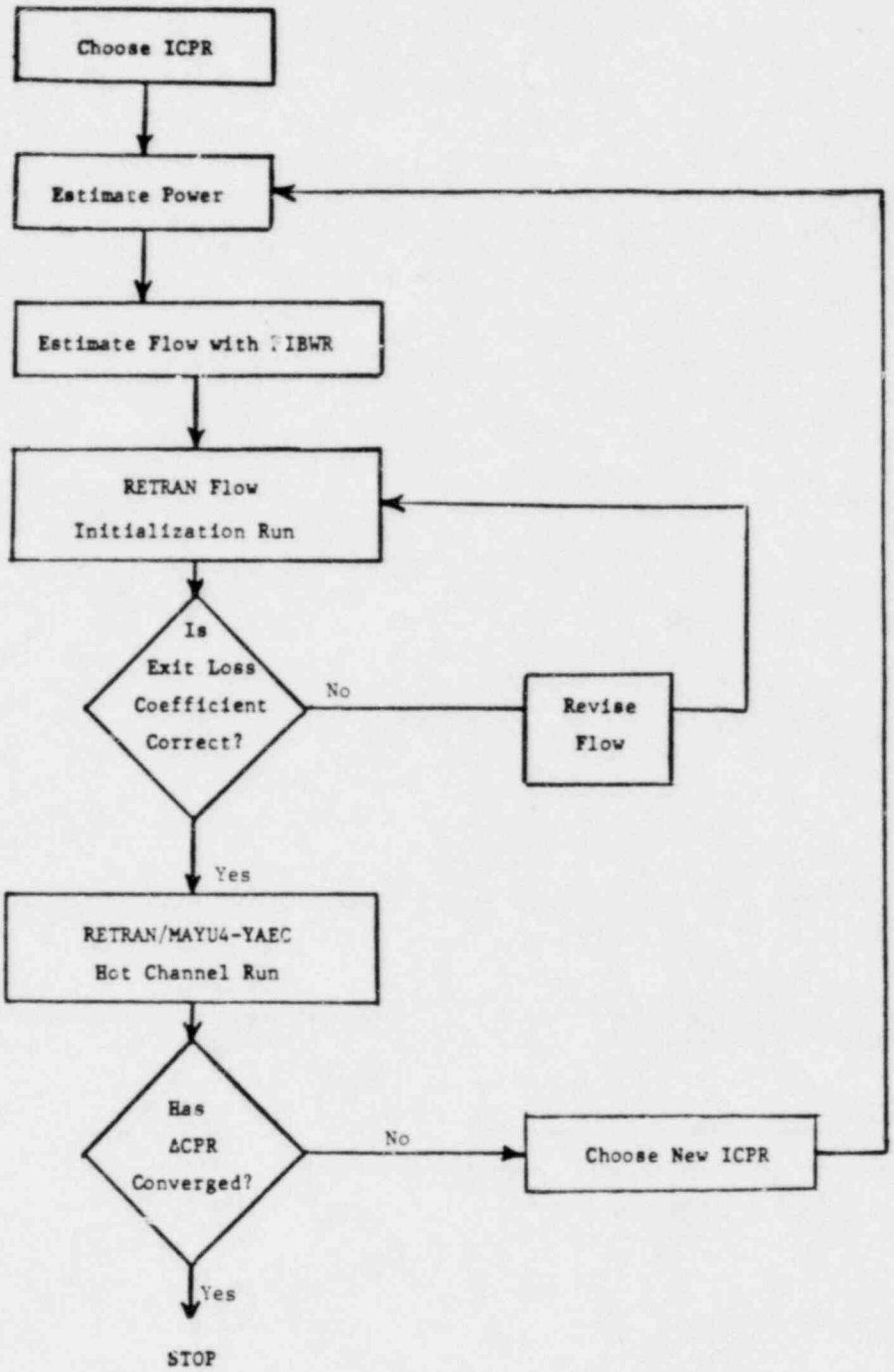

FIGURE 7.1.1

FLOW CHART FOR THE CALCULATION OF ΔCPR USING RETRAN/MAYU4 CODES

"MEASURED" SCRAM TIME

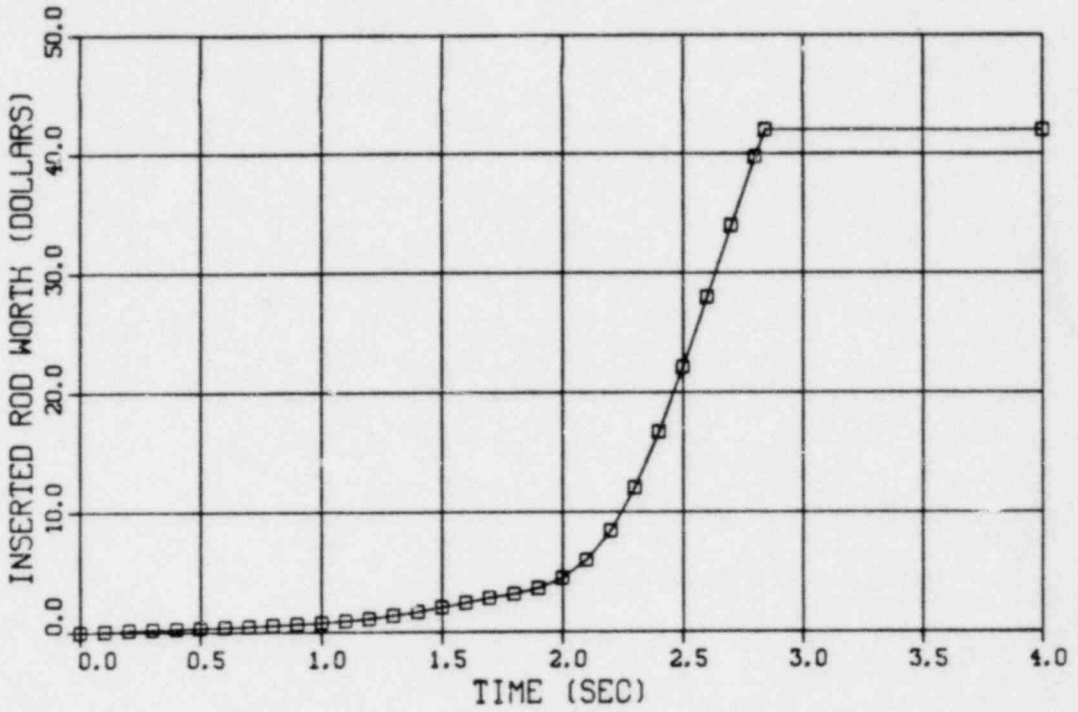

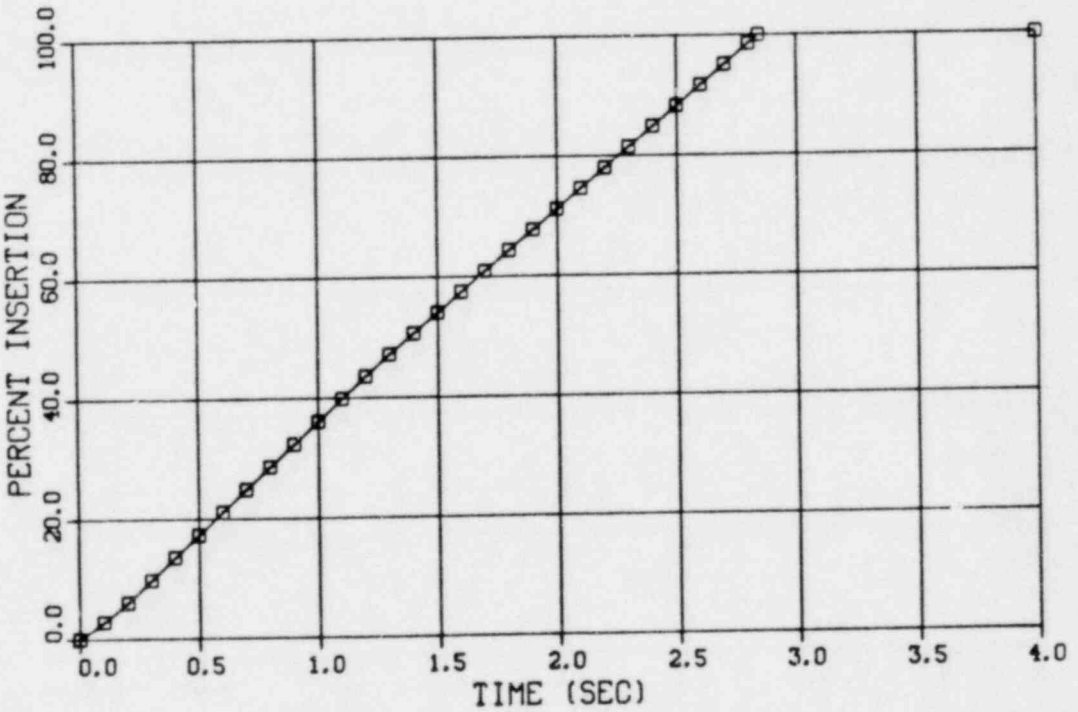

FIGURE 7.1.2

INSERTED ROD WORTH AND ROD POSITION VERSUS SCRAM TIME AT EOC

"MEASURED" SCRAM TIME

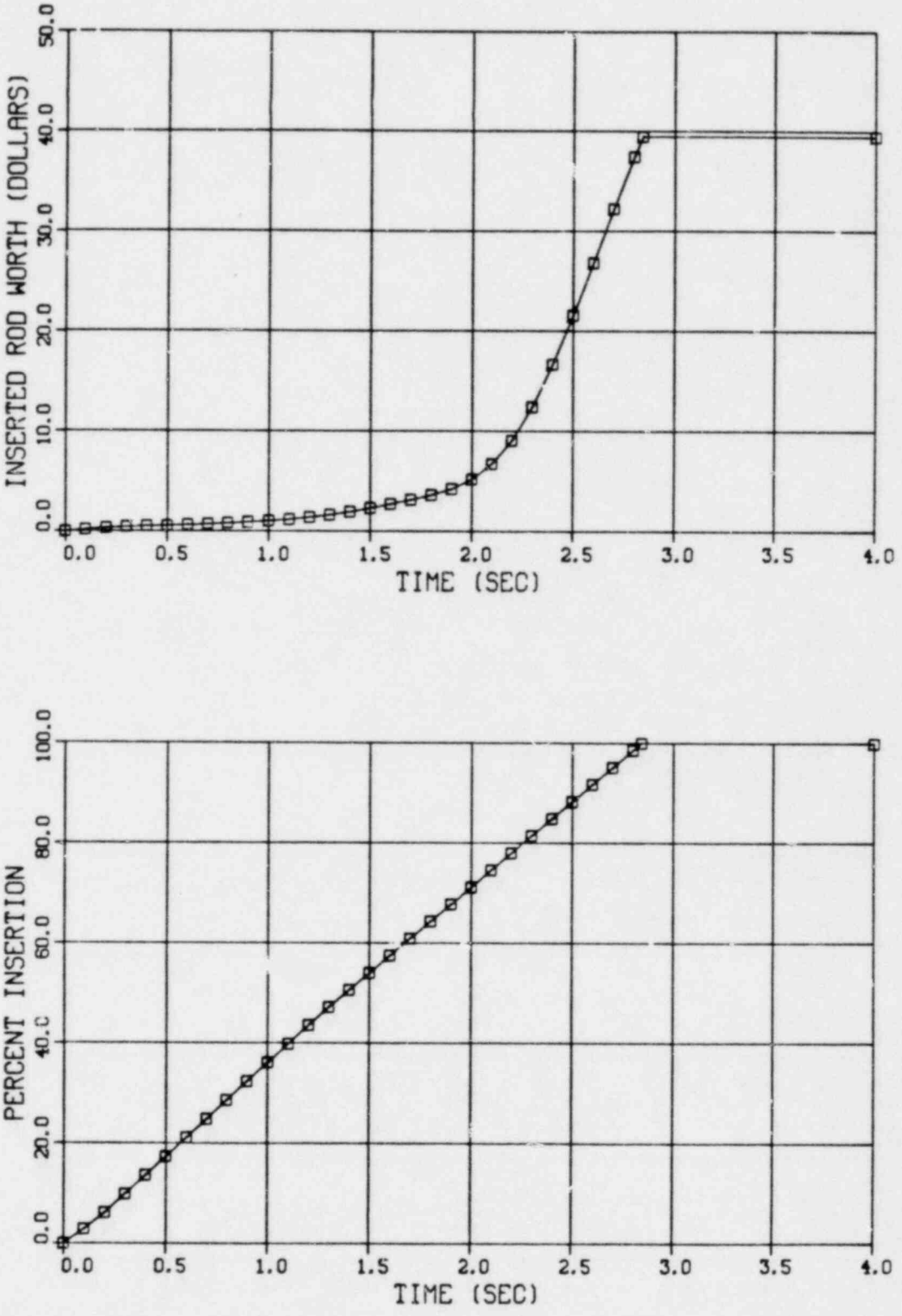

FIGURE 7.1.3

INSERTED ROD WORTH AND ROD POSITION VERSUS SCRAM TIME AT EOC-1000 MWD/ST

"MEASURED" SCRAM TIME

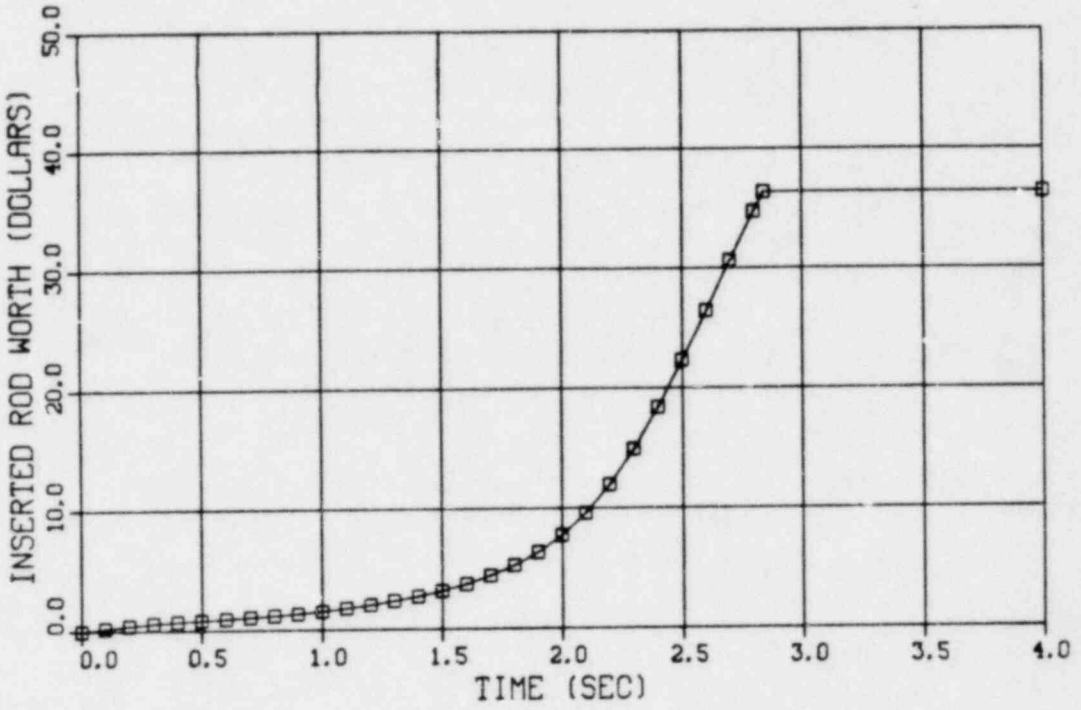

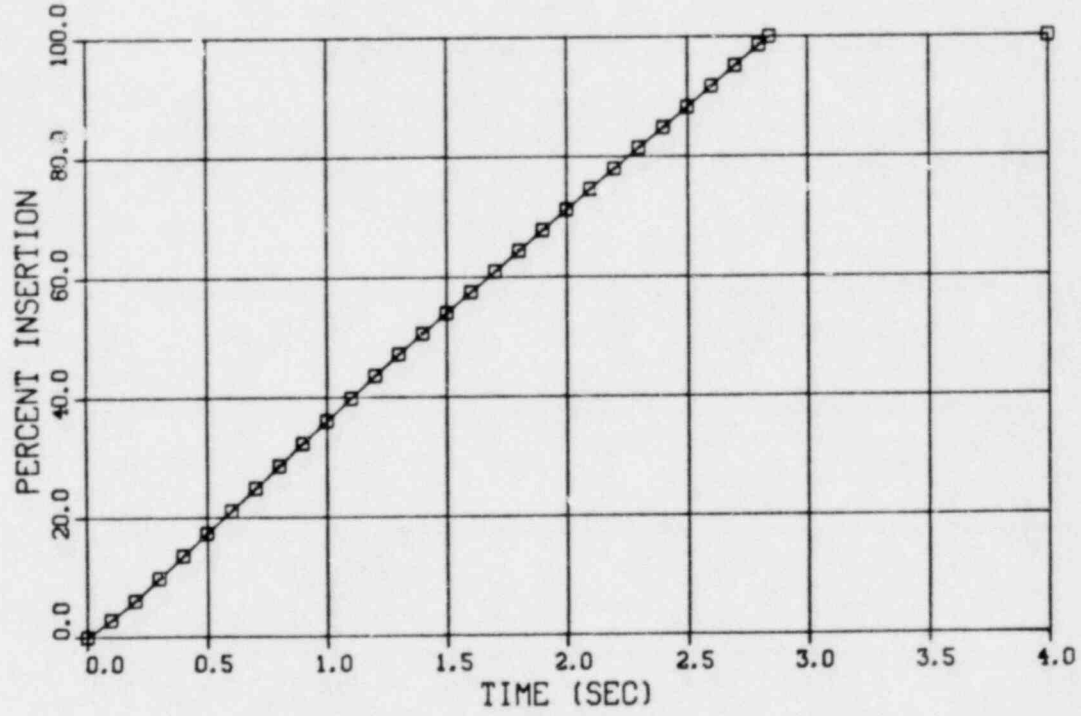

FIGURE 7.1.4

INSERTED ROD WORTH AND POSITION VEPSUS SCRAM TIME AT EOC-2000 MWD/ST

"67B" Scram Time

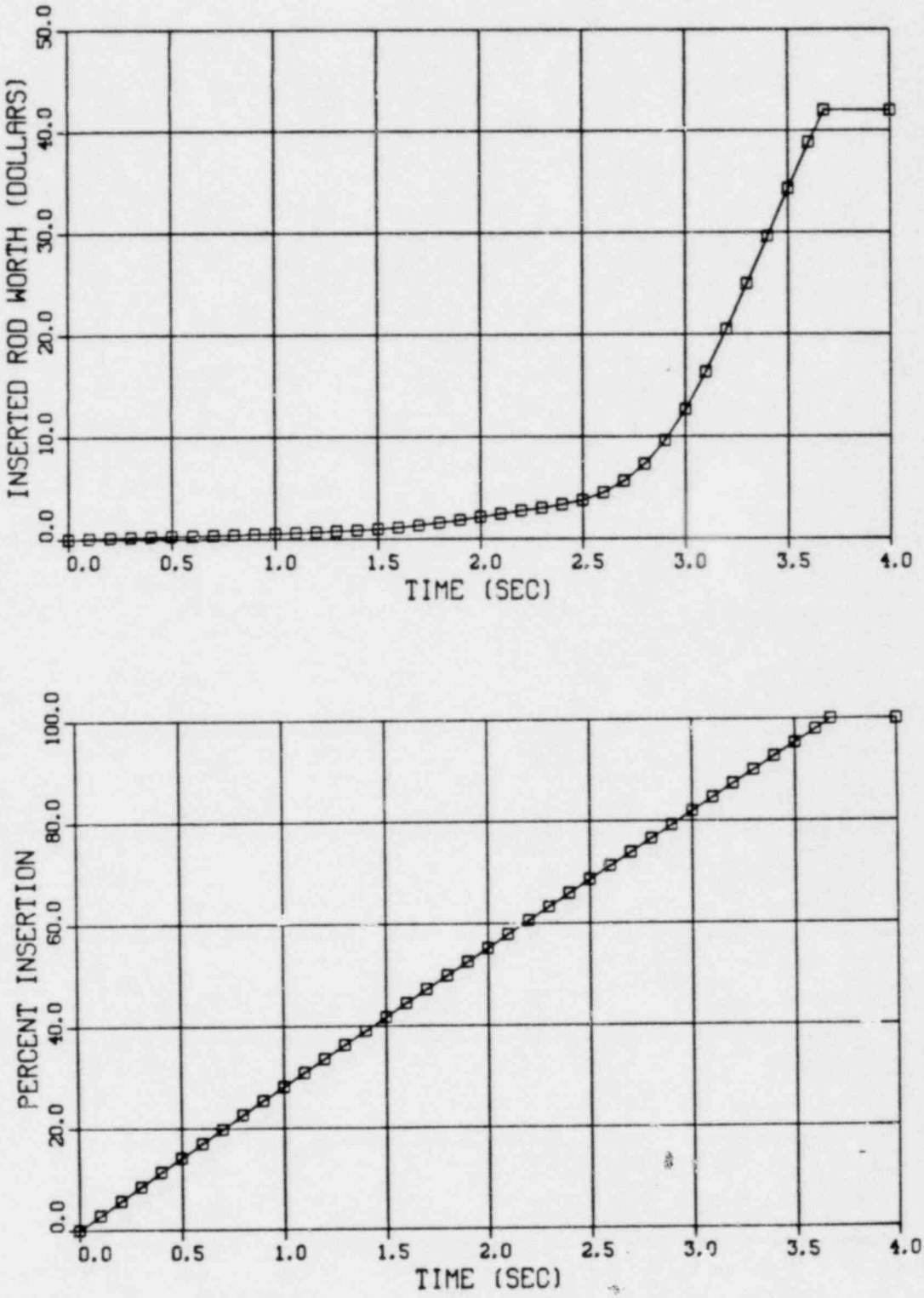

Figure 7.1.5

Inserted Rod Worth and Rod Position Versus Scram Time at EOC

"67B" Scram Time

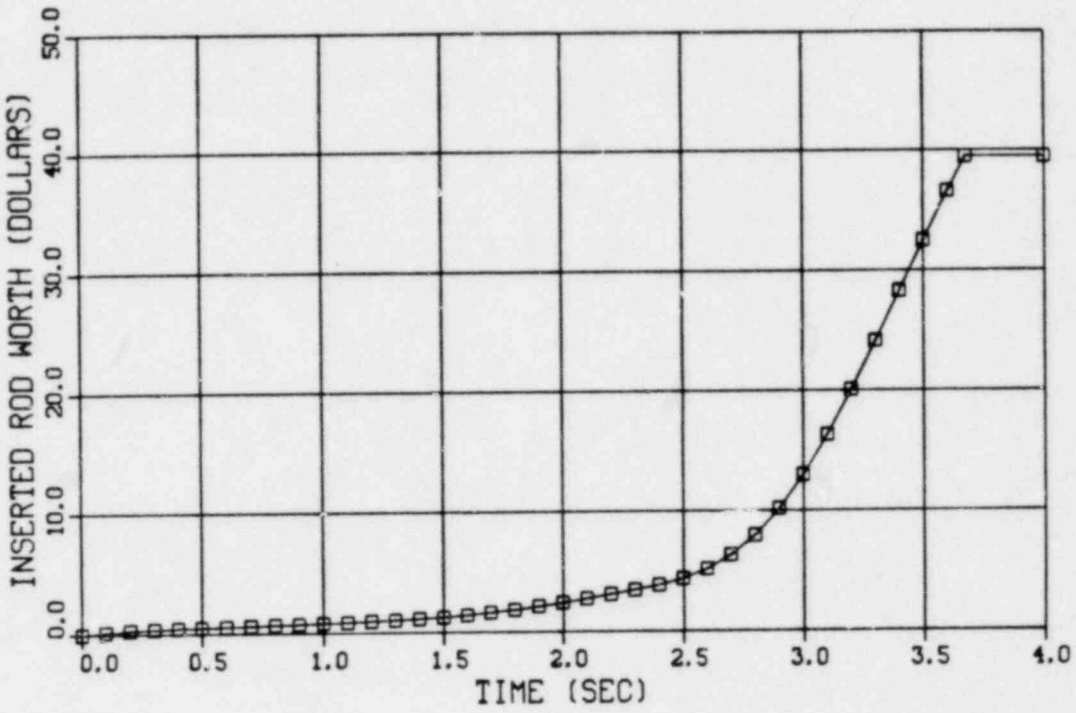

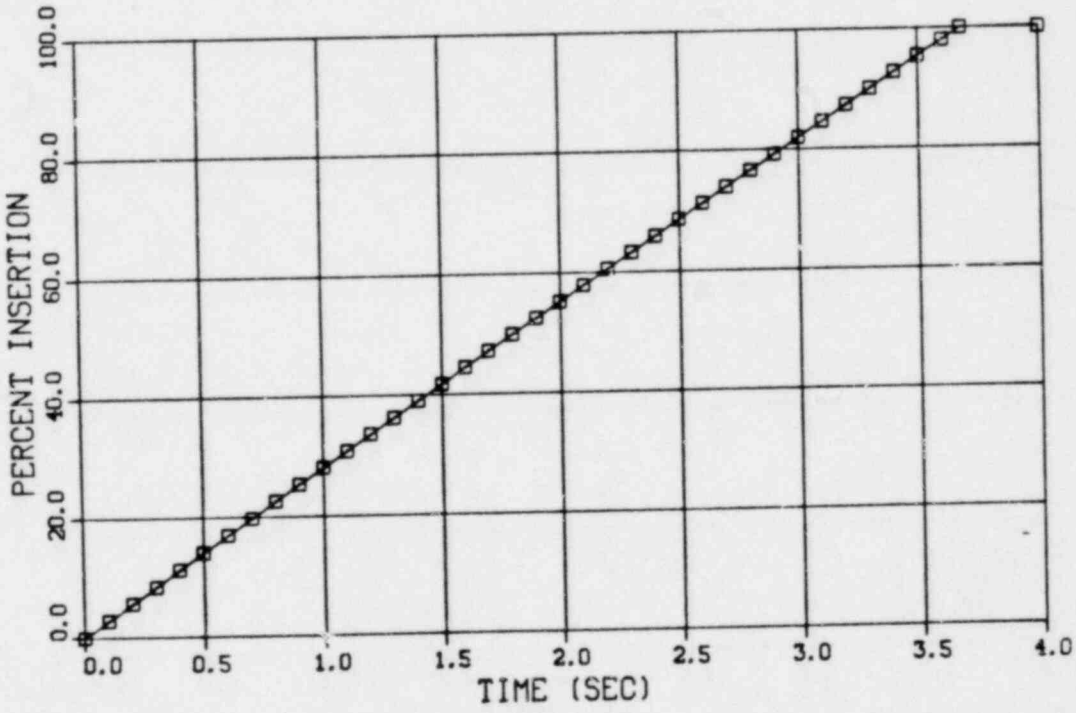

Figure 7.1.6

Inserted Rod Worth and Rod Position Versus Scram Time At EOC-1000 MWD/ST

"67B" Scram Time

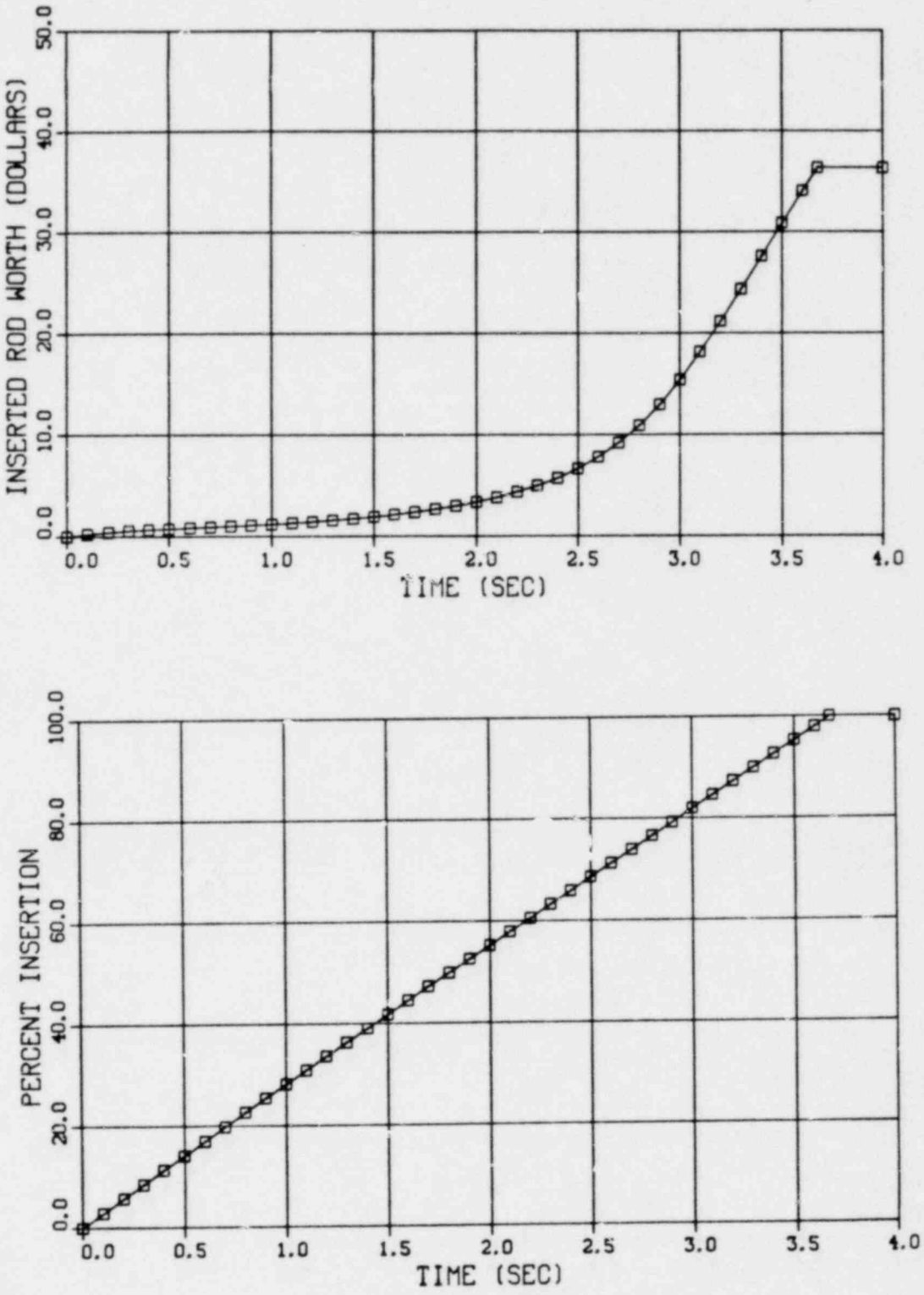

Figure 7.1.7

Inserted Rod Worth and Rod Position Versus Scram Time At EOC-2000 MWD/ST

"MEASURED" SCRAM TIME

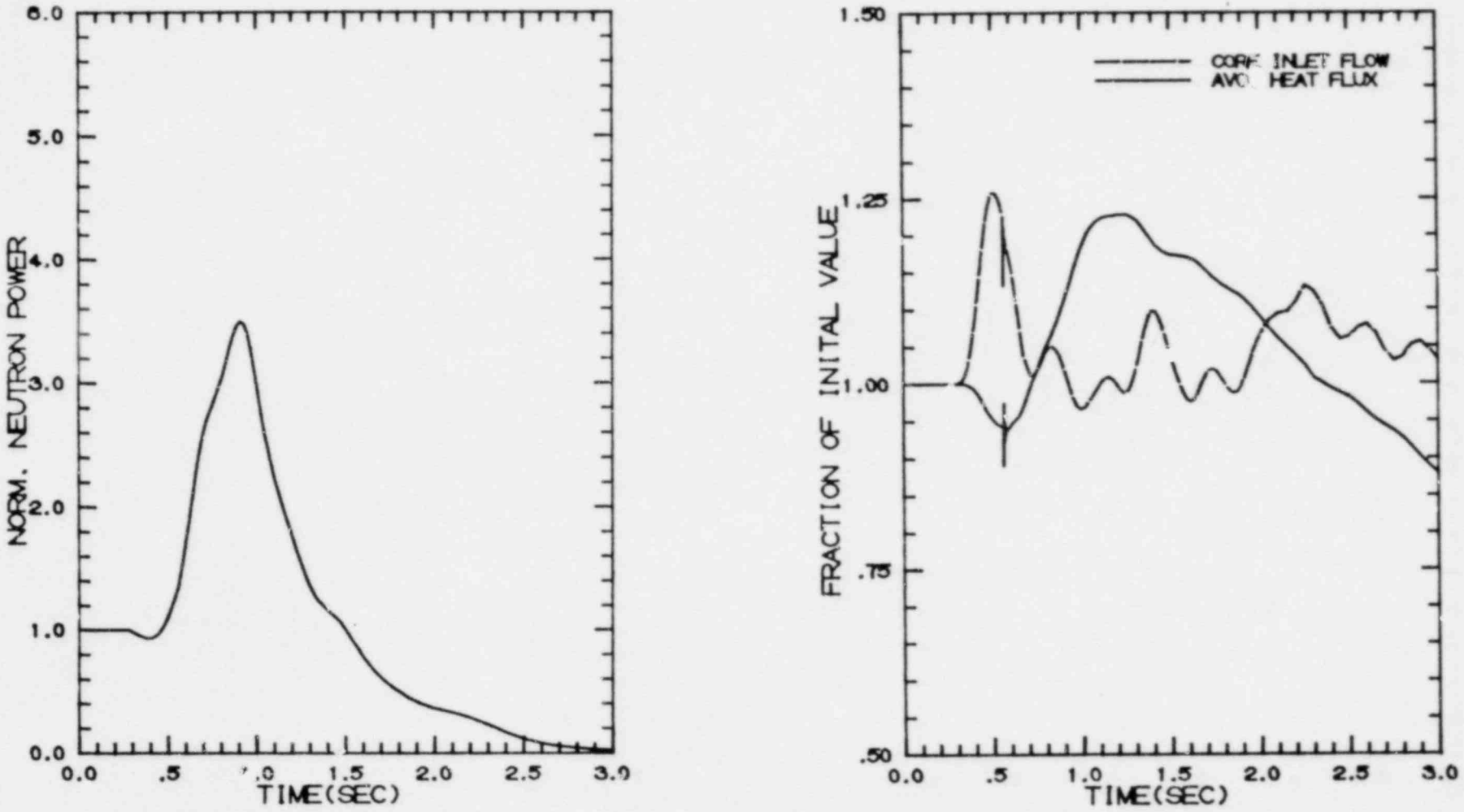

FIGURE 7.2.1-1

TURBINE TRIP WITHOUT BYPASS, EOC9

"MEASURED" SCRAM TIME

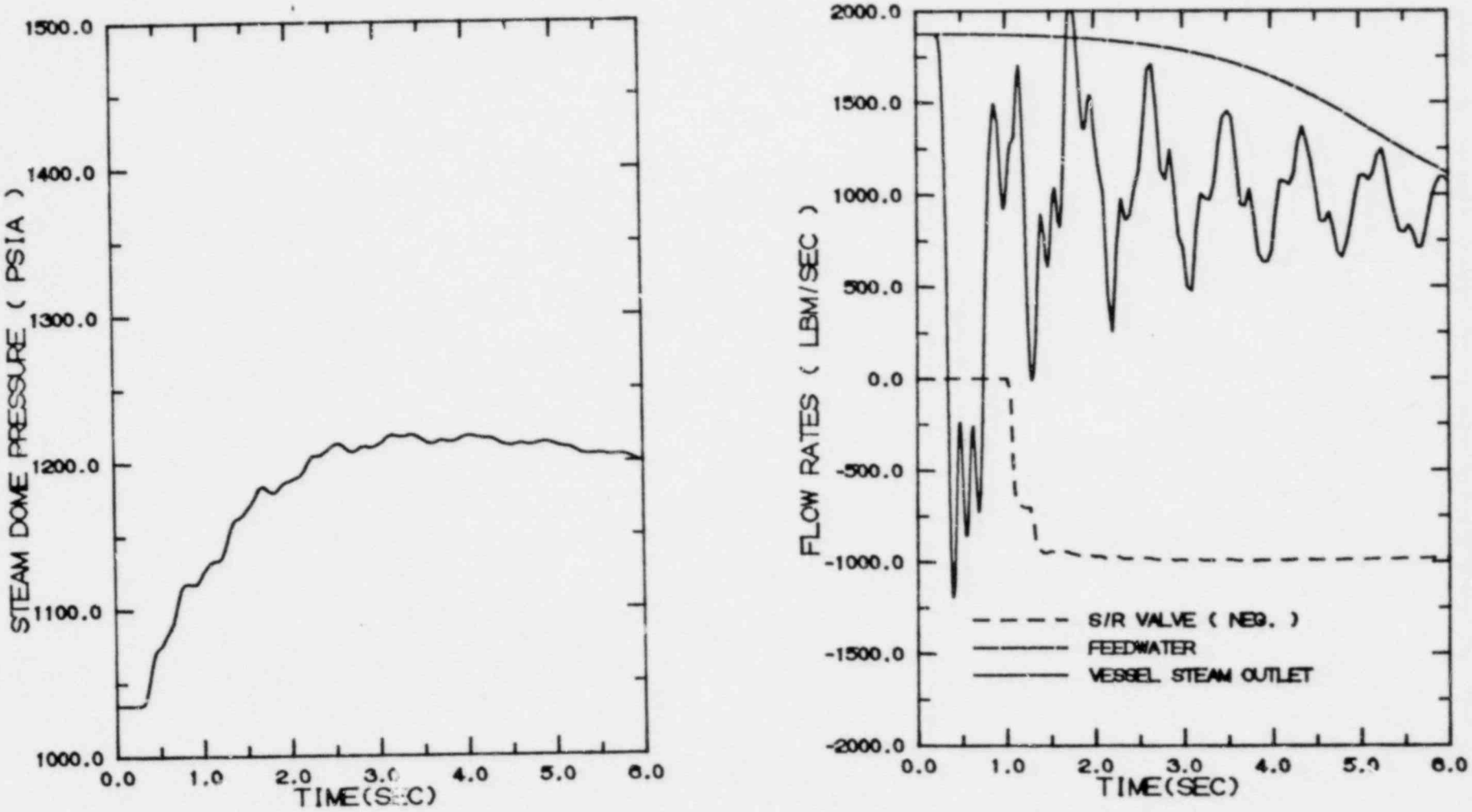

FIGURE 7.2.1-2

TURBINE TRIP WITHOUT BYPASS, EOC9

"MEASURED" SCRAM TIME

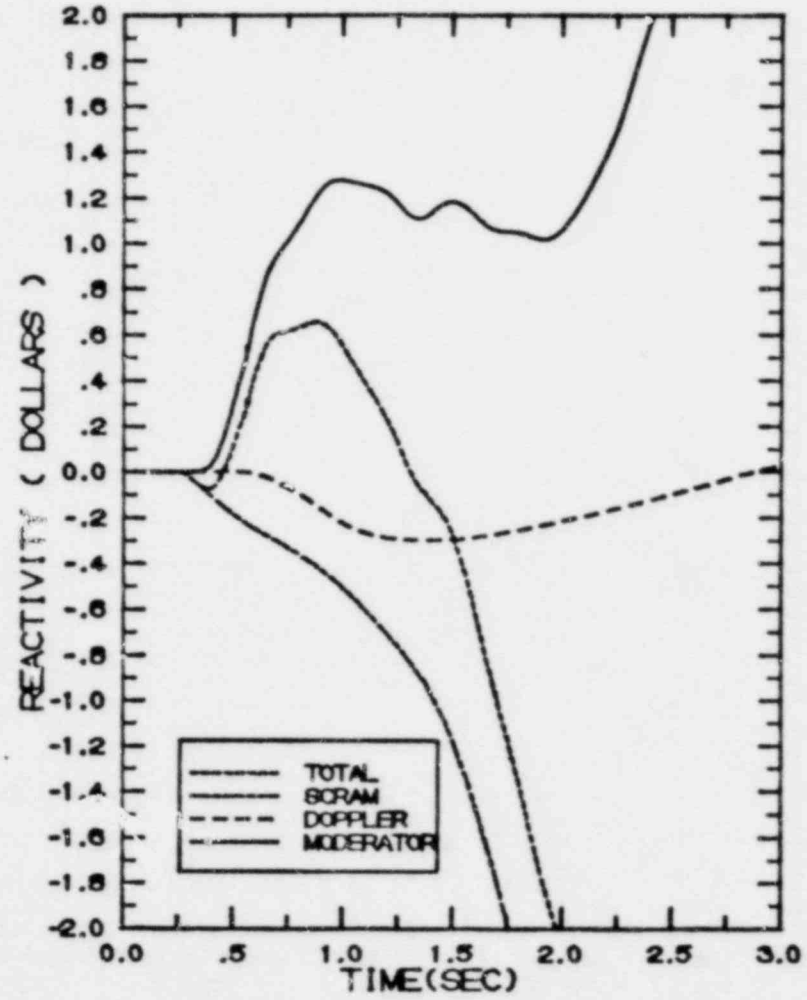

FIGURE 7.2.1-3

TURBINE TRIP WITHOUT BYPASS, EOC9

"MEASURED" SCRAM TIME

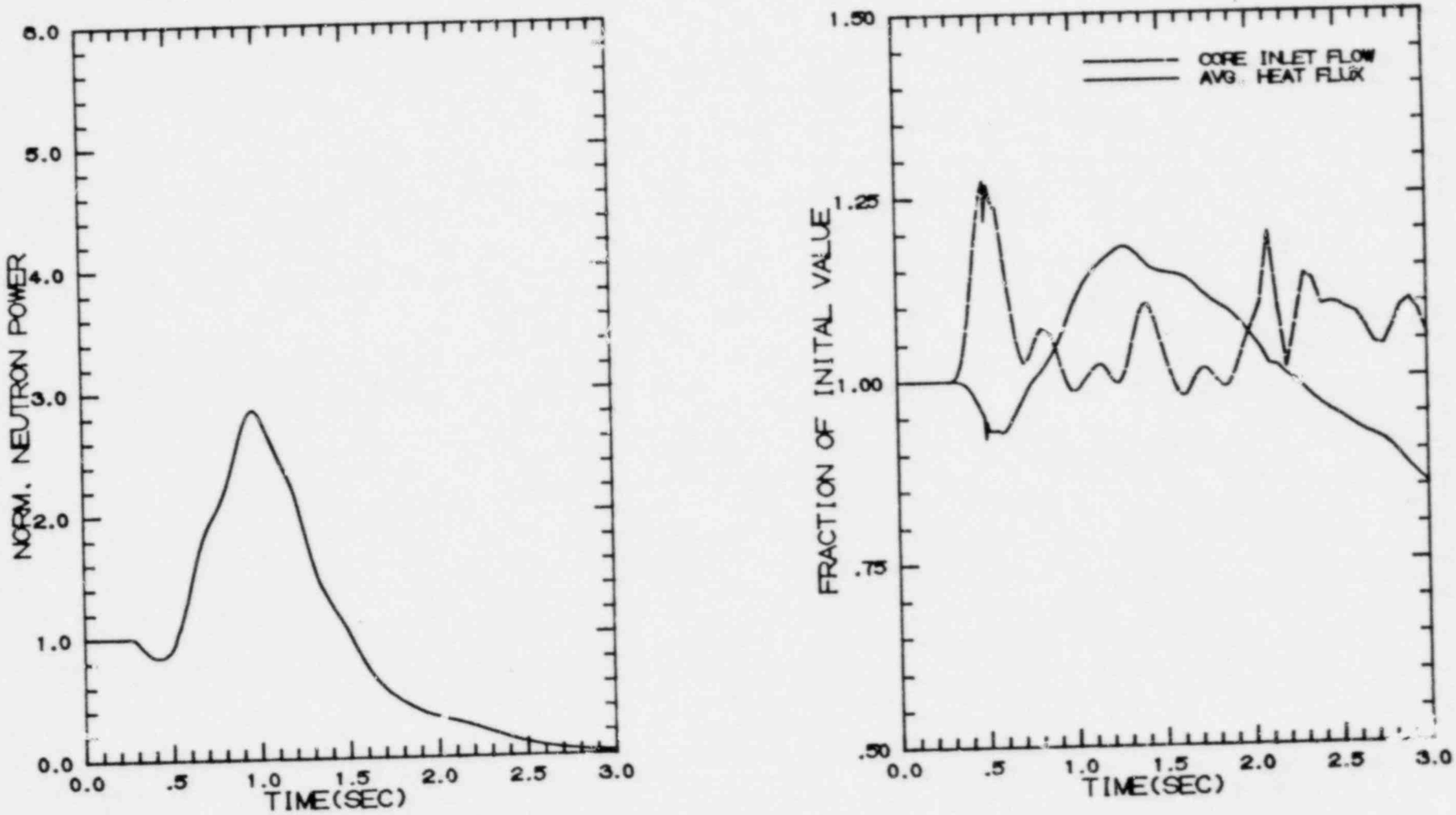

FIGURE 7.2.2-1

TURBINE TRIP WITHOUT BYPASS, EOC9-1000 MWD/ST

"MEASURED" SCRAM TIME

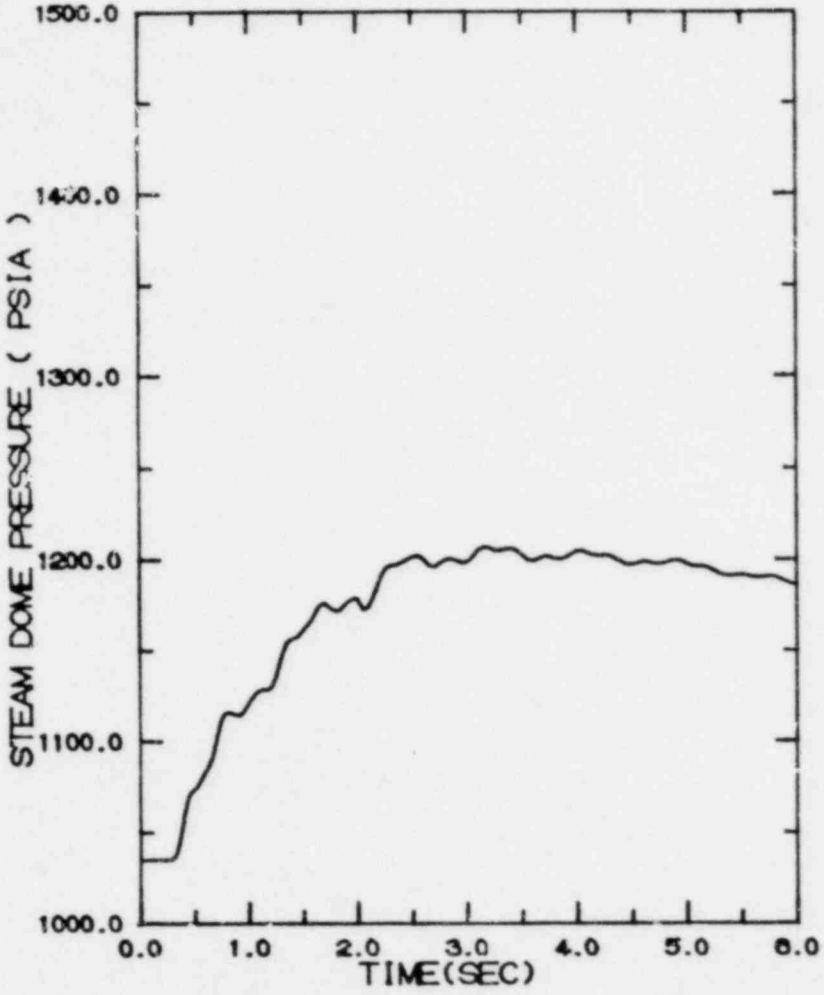

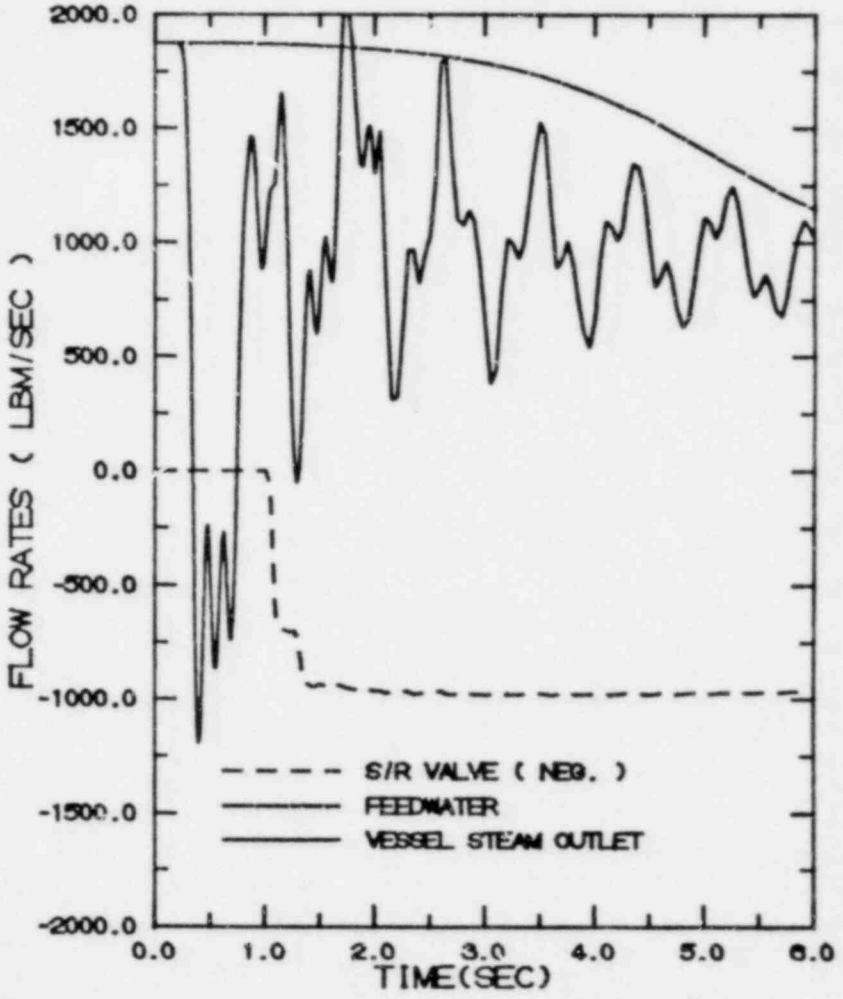

FIGURE 7.2.2-2

TURBINE TRIP WITHOUT BYPASS, EOC9-1000 MWD/ST

"MEASURED" SCRAM TIME

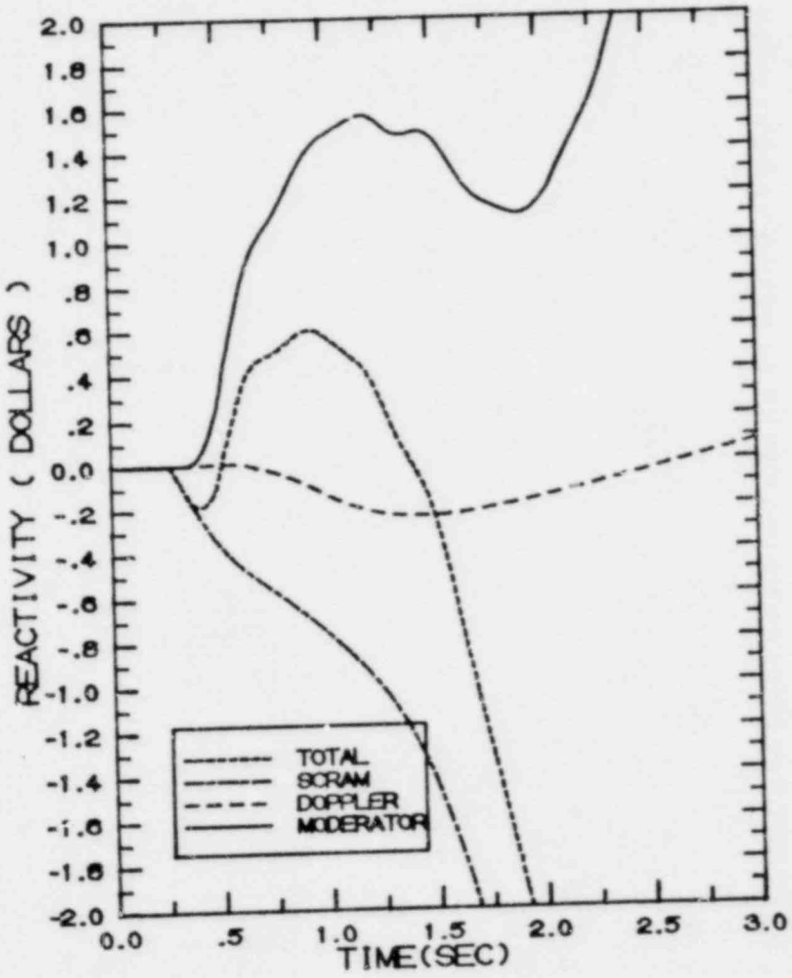

FIGURE 7.2.2-3

TURBINE TRIP WITHOUT BYPASS, EOC9-1000 MWD/ST

"MEASURED" SCRAM TIME

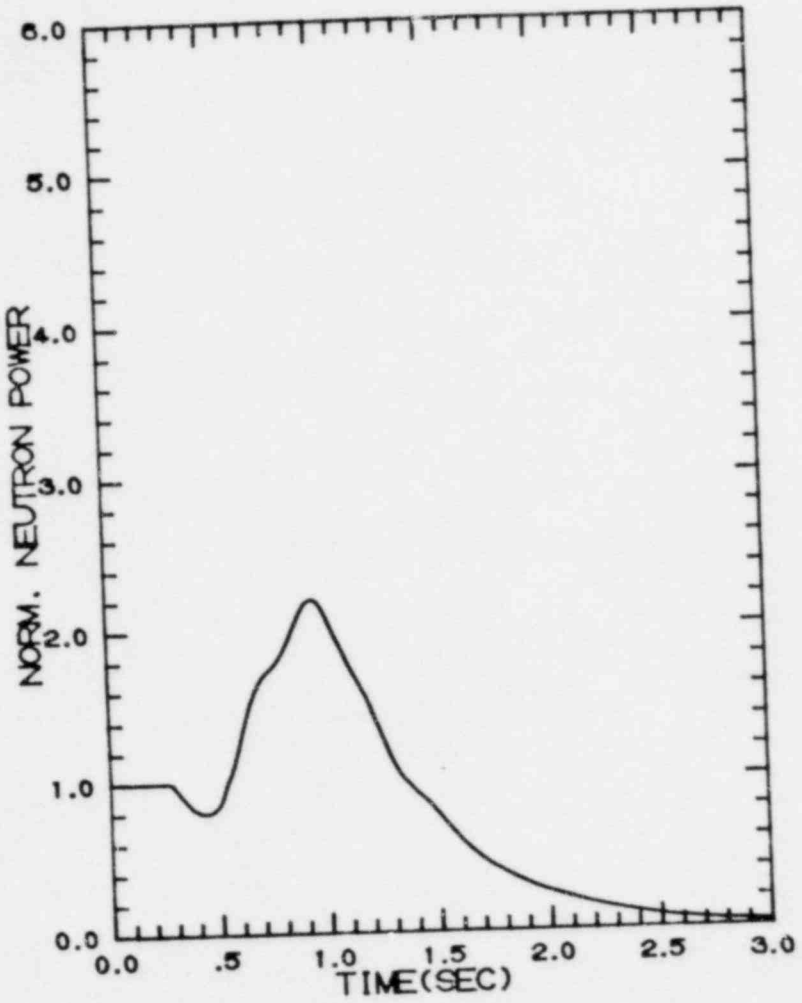

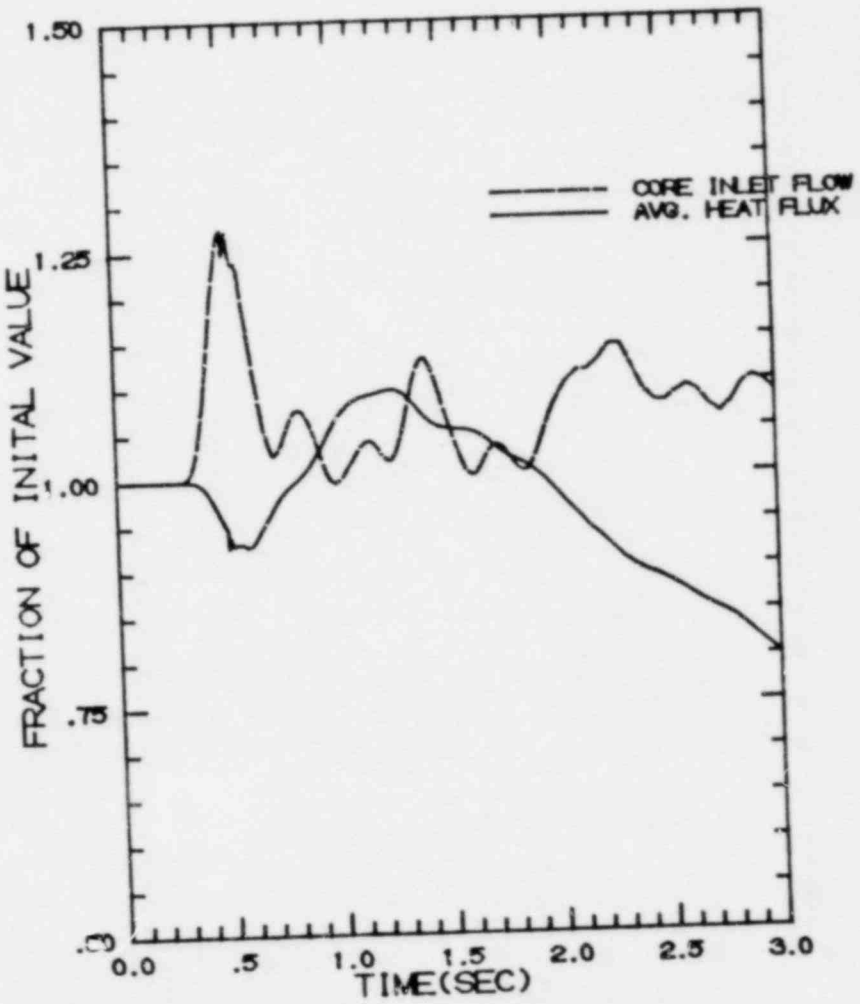

FIGURE 7.2.3-1

TURBINE TRIP WITHOUT BYPASS, EOC9-2000 MWD/ST

"MEASURED" SCRAM TIME

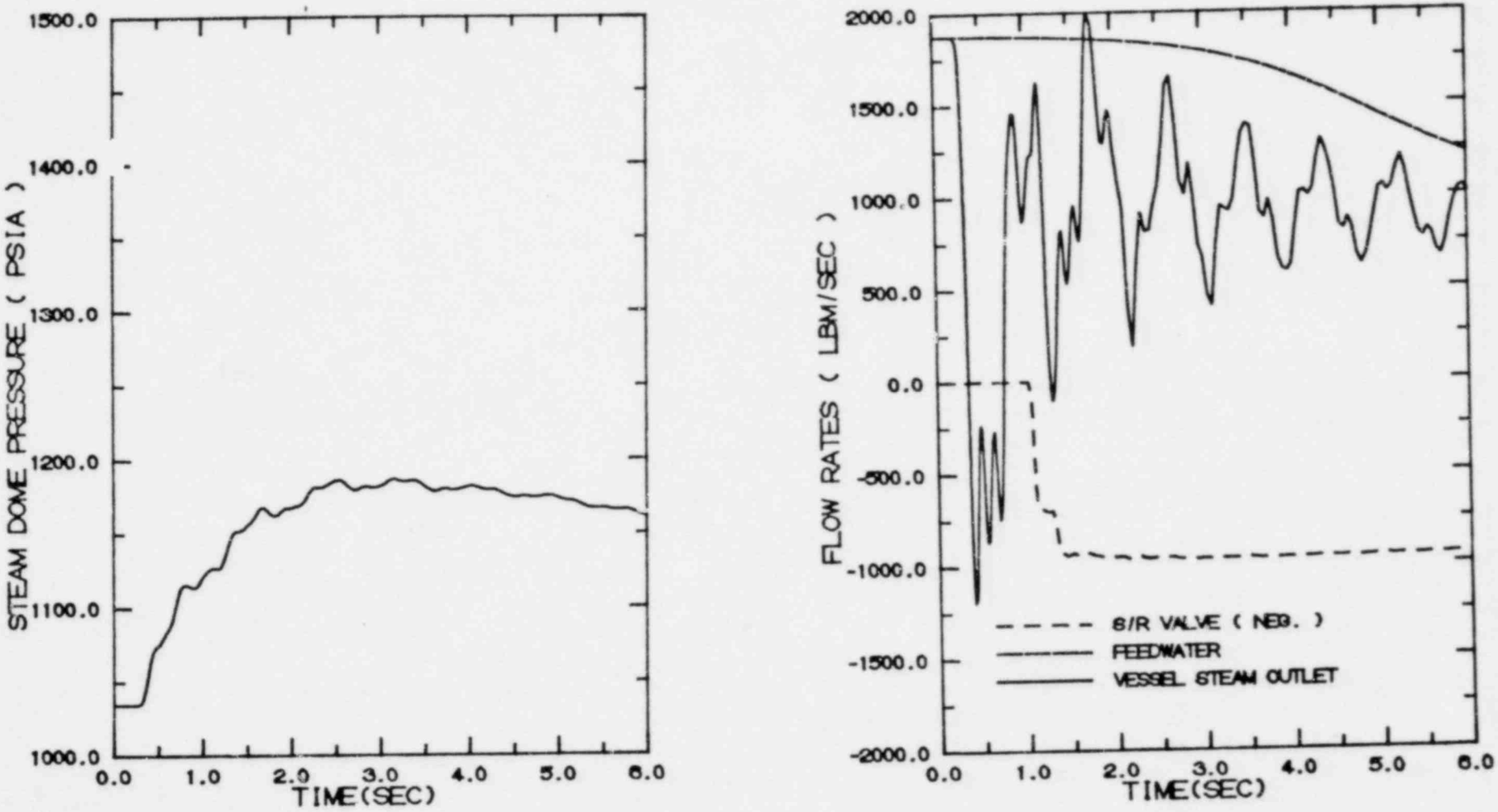

FIGURE 7.2.3-2

TURBINE TRIP WITHOUT BYPASS, EOC-2000 MWD/ST

"MEASURED" SCRAM TIME

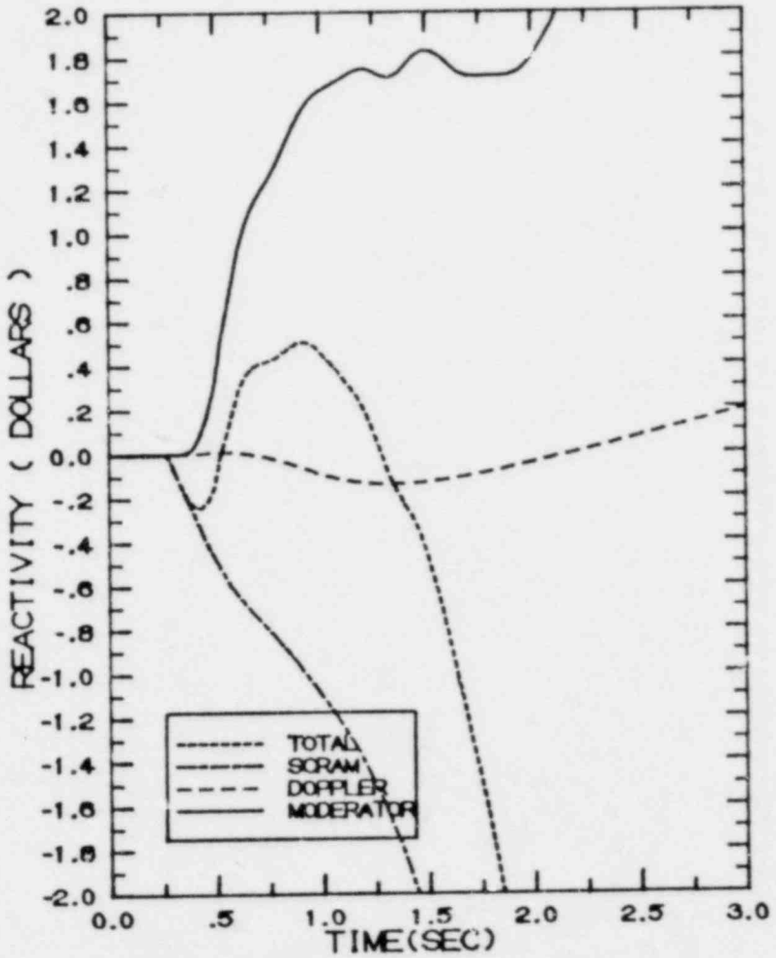

FIGURE 7.2.3-3

TURBINE TRIP WITHOUT BYPASS, EOC-2000 MWD/ST

"MEASURED" SCRAM TIME

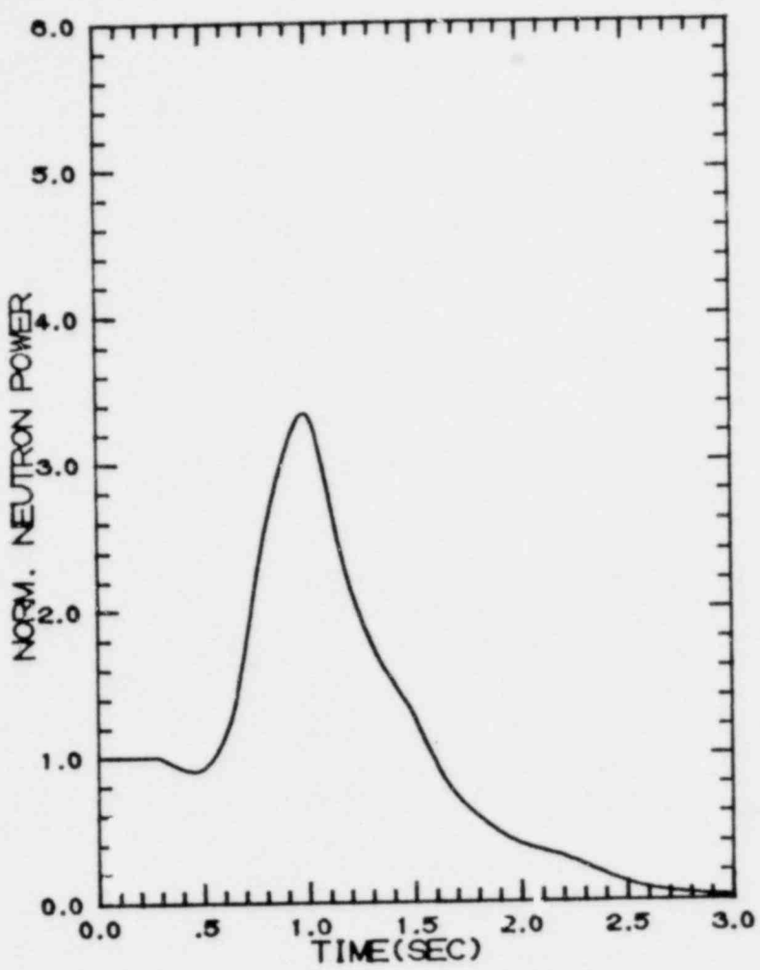

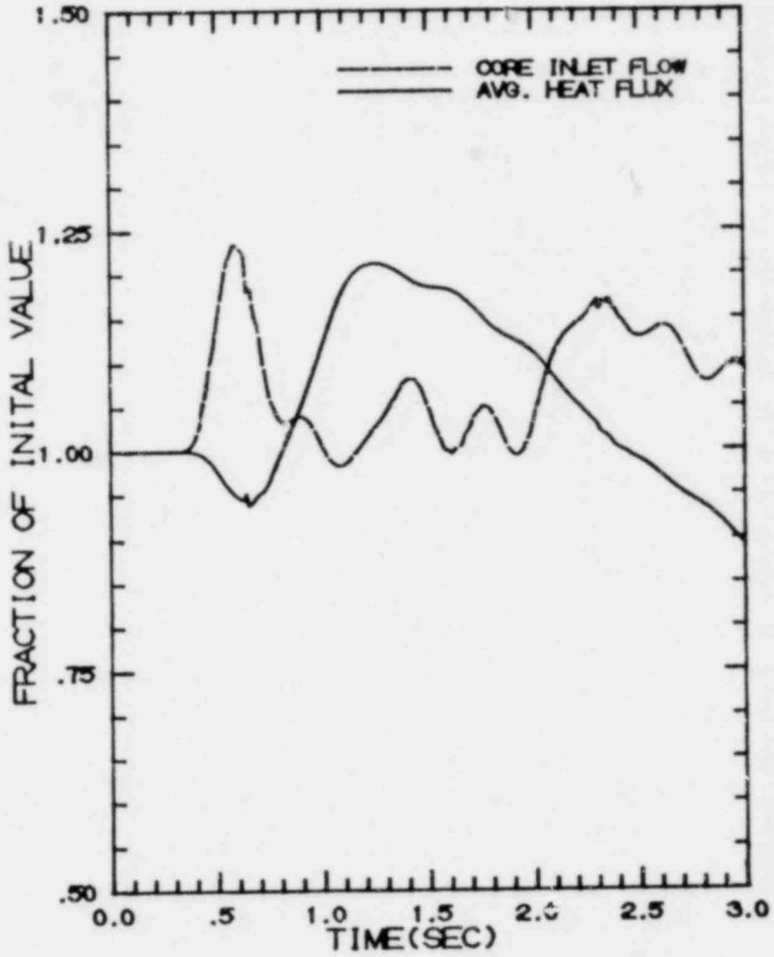

FIGURE 7.2.4-1

GENERATOR LOAD REJECTION WITHOUT BYPASS, EOC9

"MEASURED" SCRAM TIME

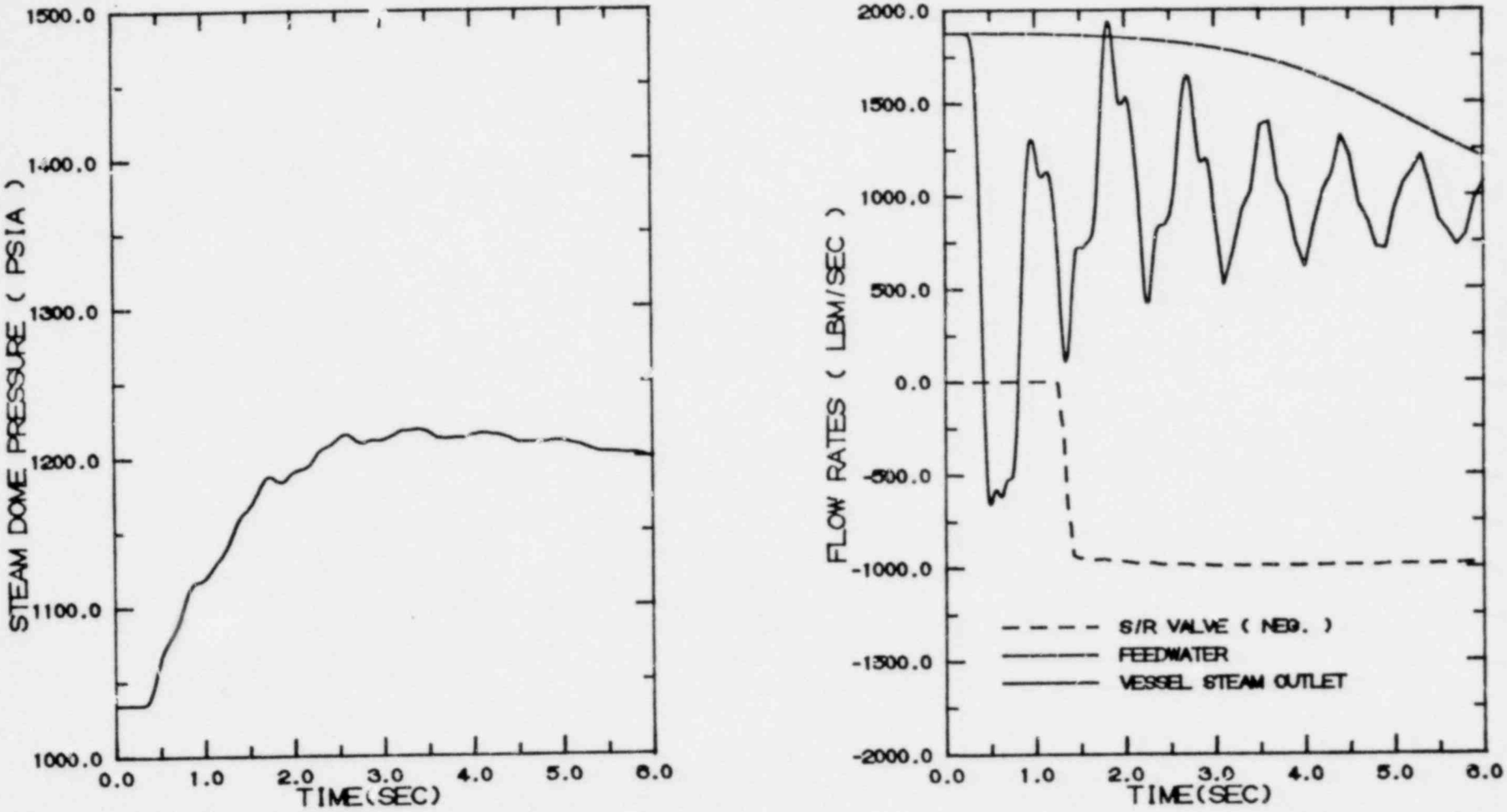

FIGURE 7.2.4-2

GENERATOR LOAD REJECTION WITHOUT BYPASS, EOC9

"MEASURED" SCRAM TIME

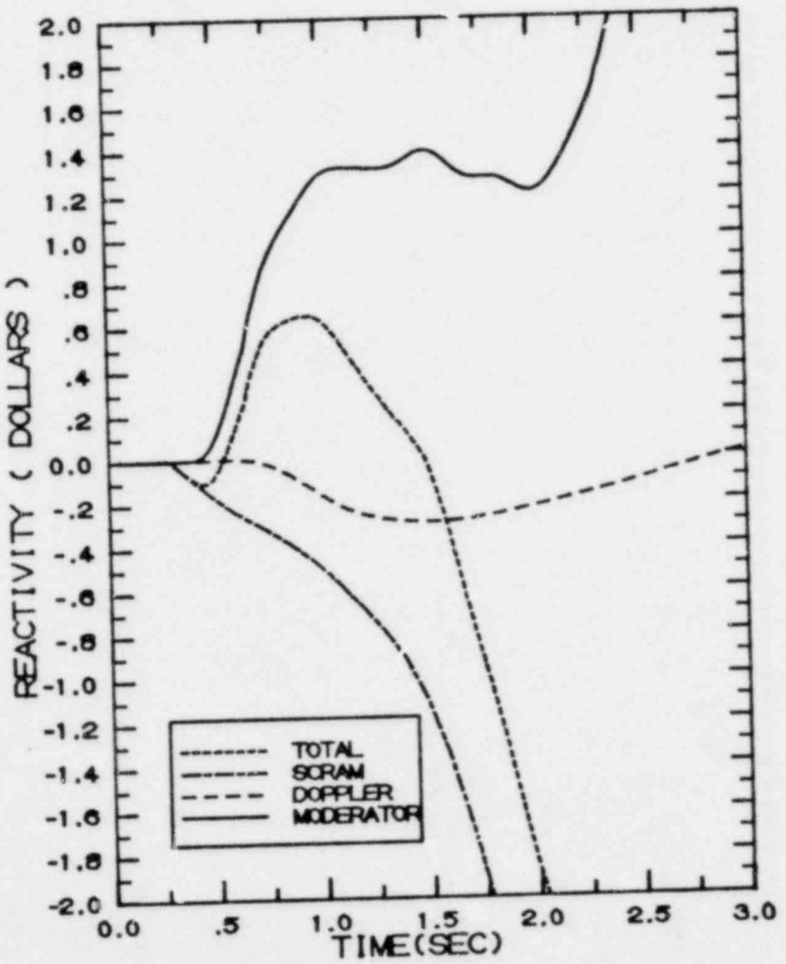

FIGURE 7.2.4-3

GENERATOR LOAD REJECTION WITHOUT BYPASS, EOC9

"MEASURED" SCRAM TIME

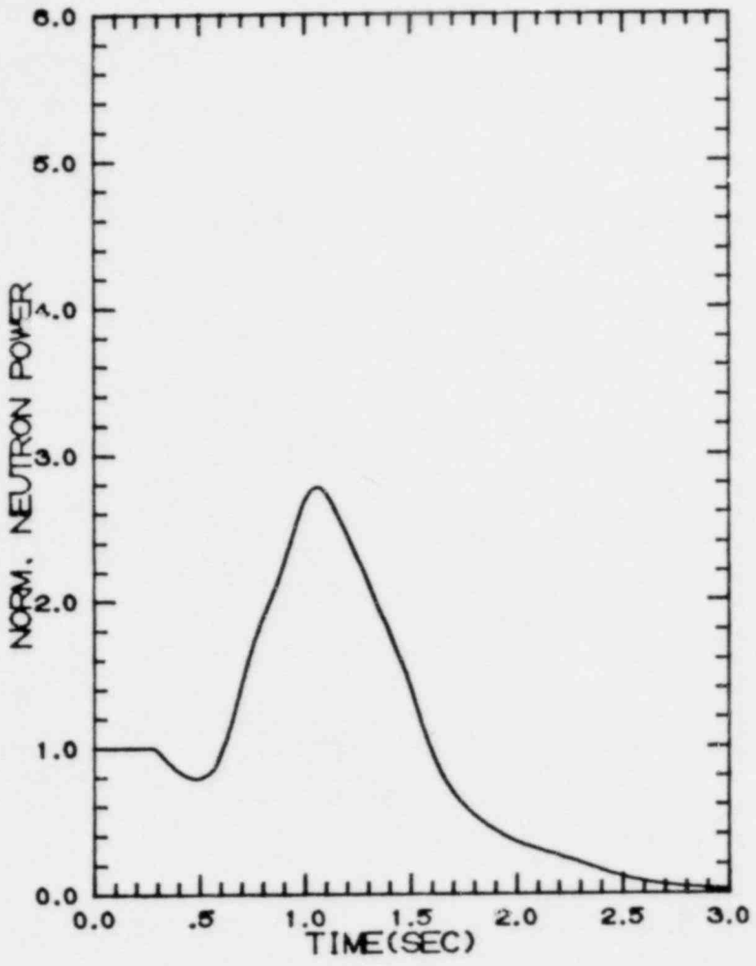

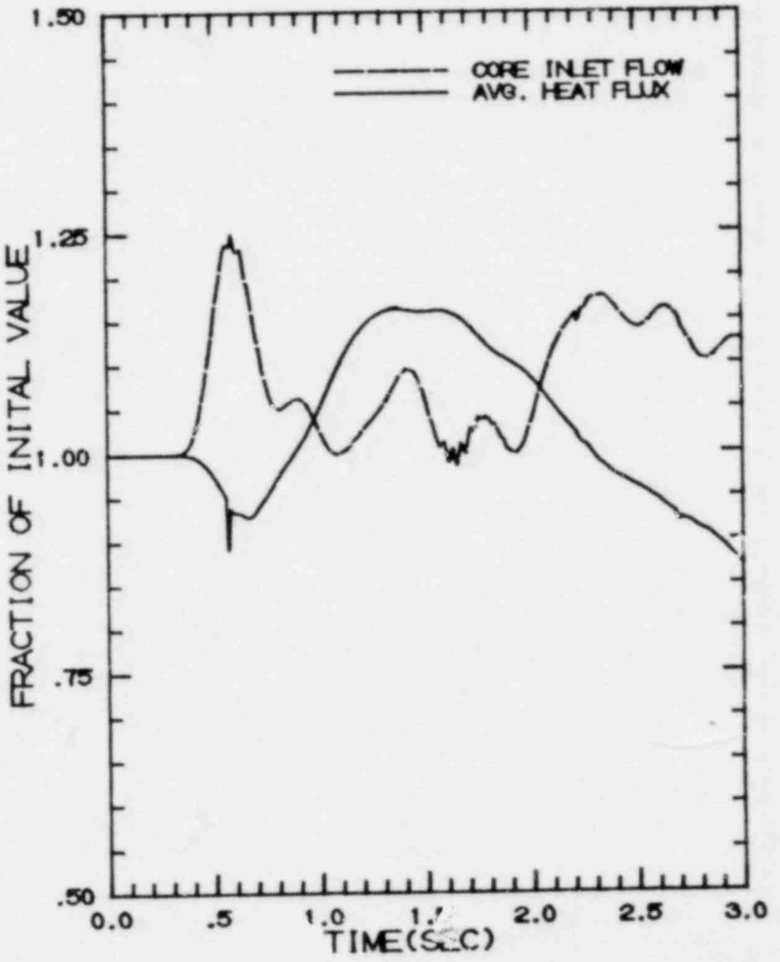

FIGURE 7.2.5-1

GENERATOR LOAD REJECTION WITHOUT BYPASS, EOC-1000 MWD/ST

"MEASURED" SCRAM TIME

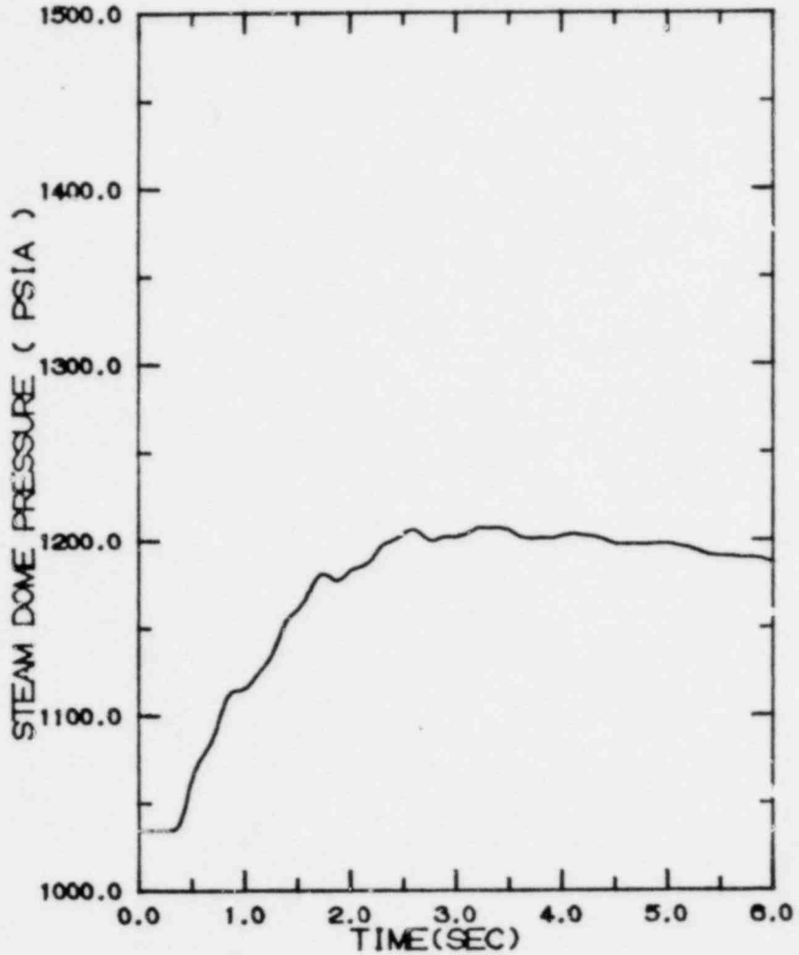

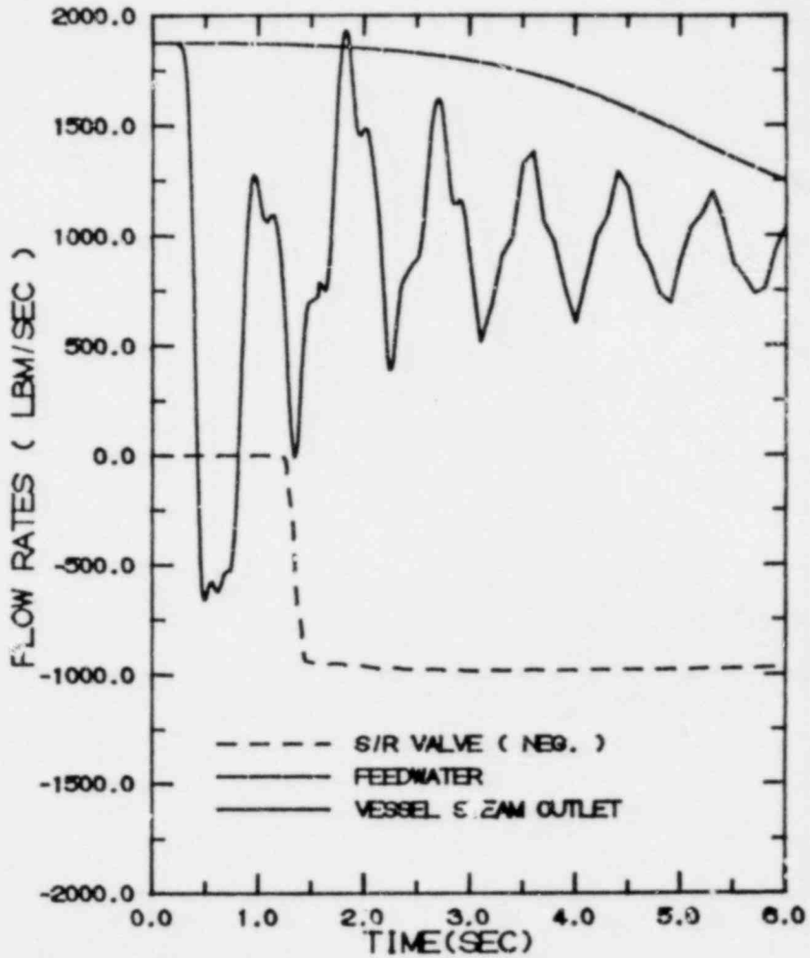

FIGURE 7.2.5-2

GENERATOR LOAD REJECTION WITHOUT BYPASS, EOC-1000 MWD/ST

"MEASURED" SCRAM TIME

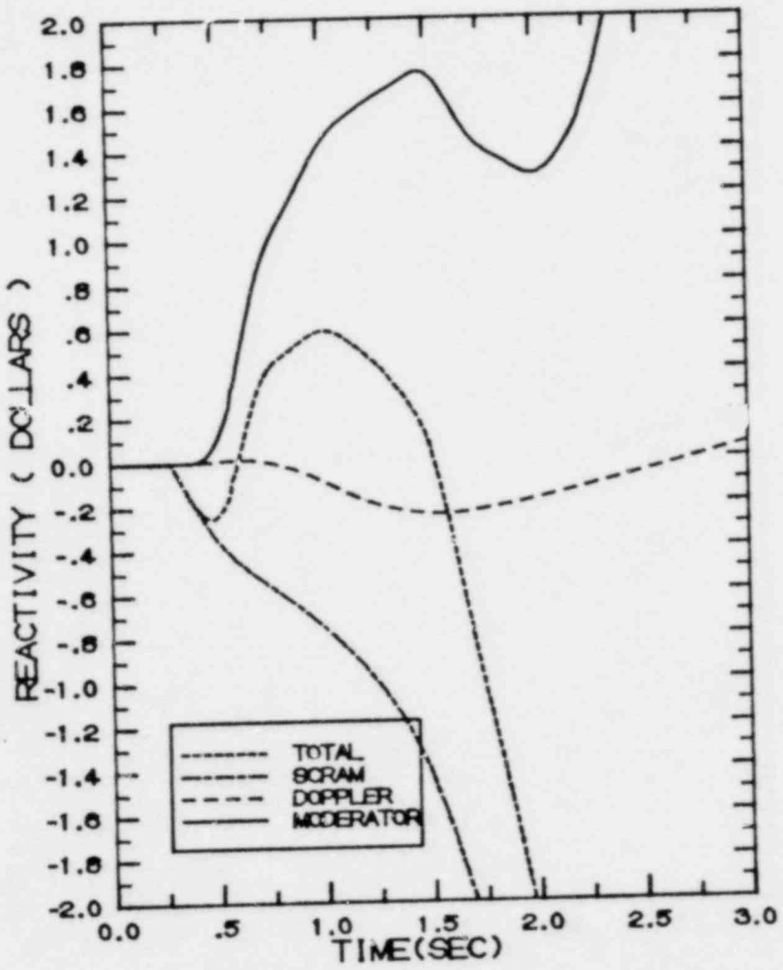

FIGURE 7.2.5-3

GENERATOR LOAD REJECTION WITHOUT BYPASS, EOC-1000 MWD/ST

"MEASURED" SCRAM TIME

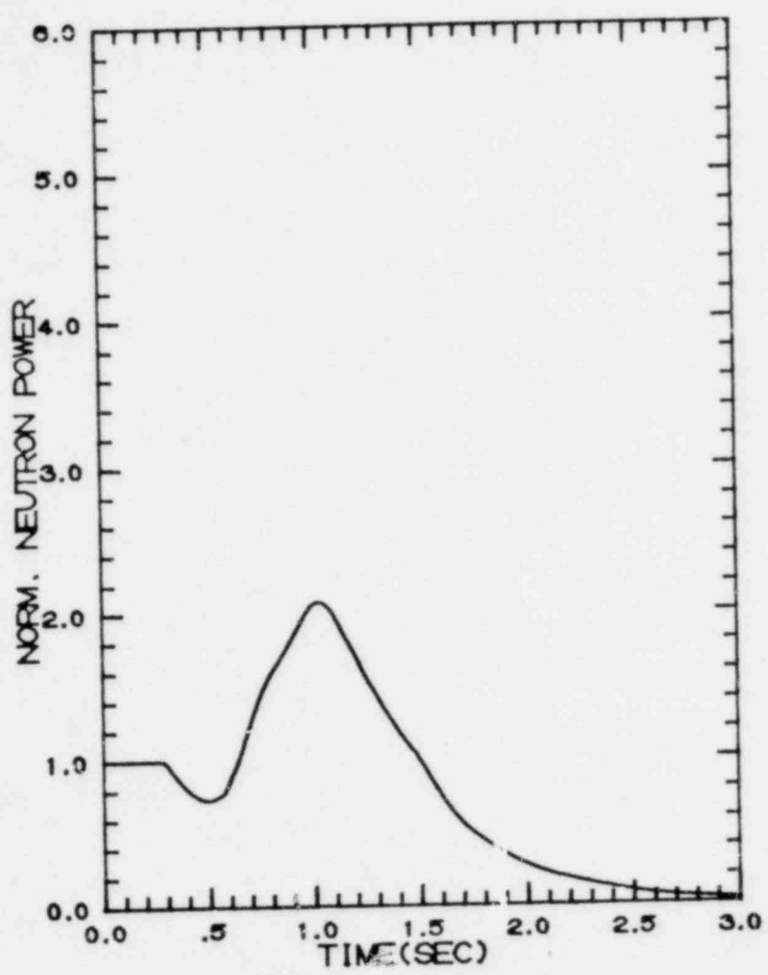

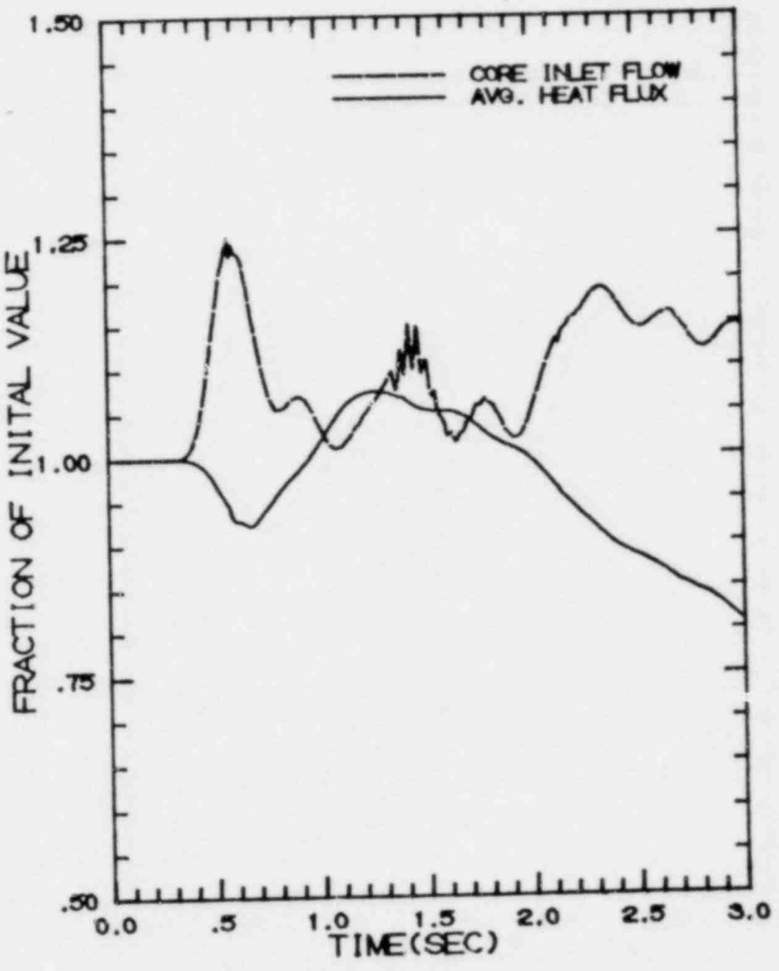

FIGURE 7.2.6-1

GENERATOR LOAD REJECTION WITHOUT BYPASS, EOC9-2000 MWD/ST

"MEASURED" SCRAM TIME

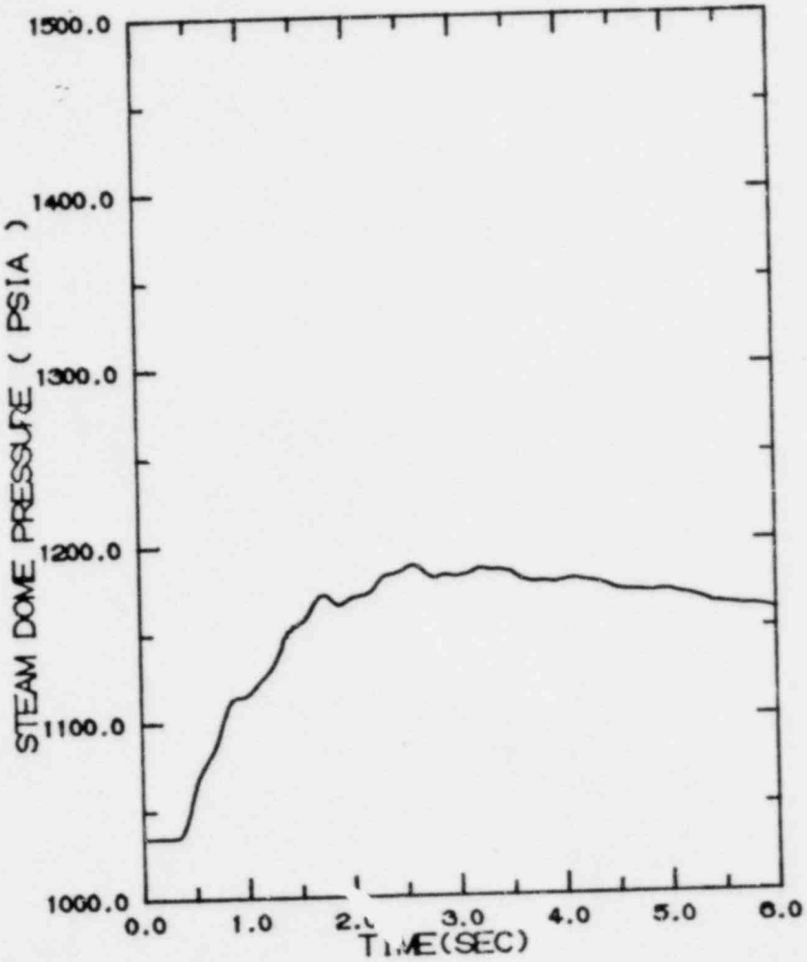

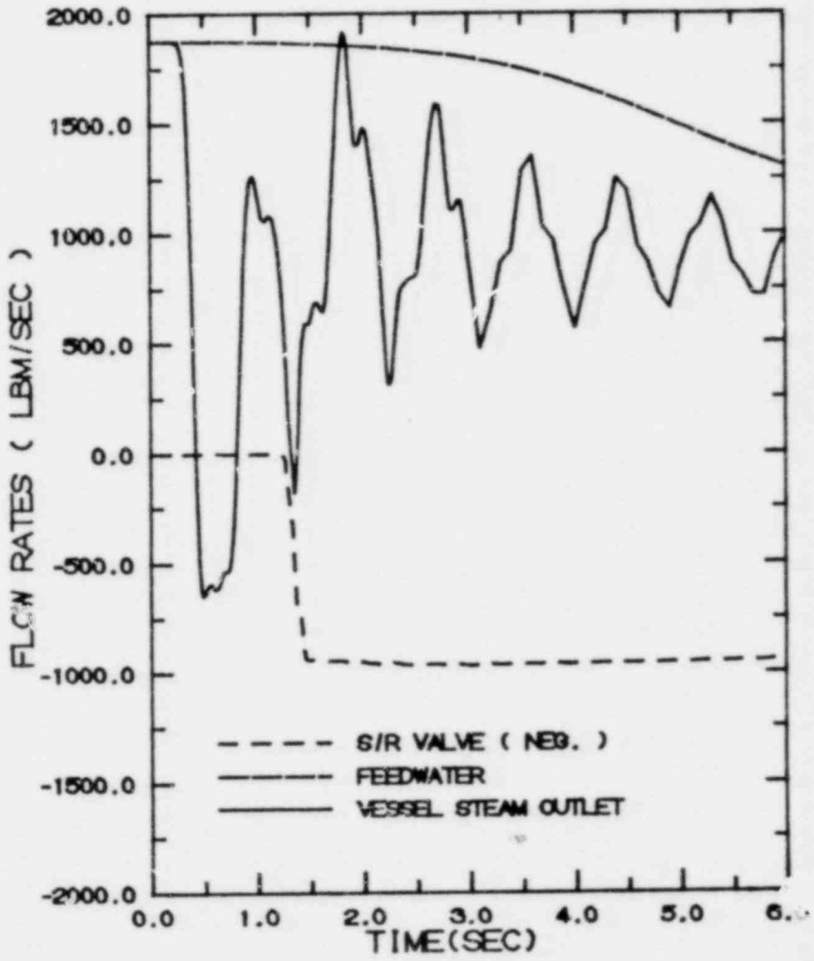

FIGURE 7.2.6-2

GENERATOR LOAD REJECTION WITHOUT BYPASS, EOC9-2000 MWD/ST

"MEASURED" SCRAM TIME

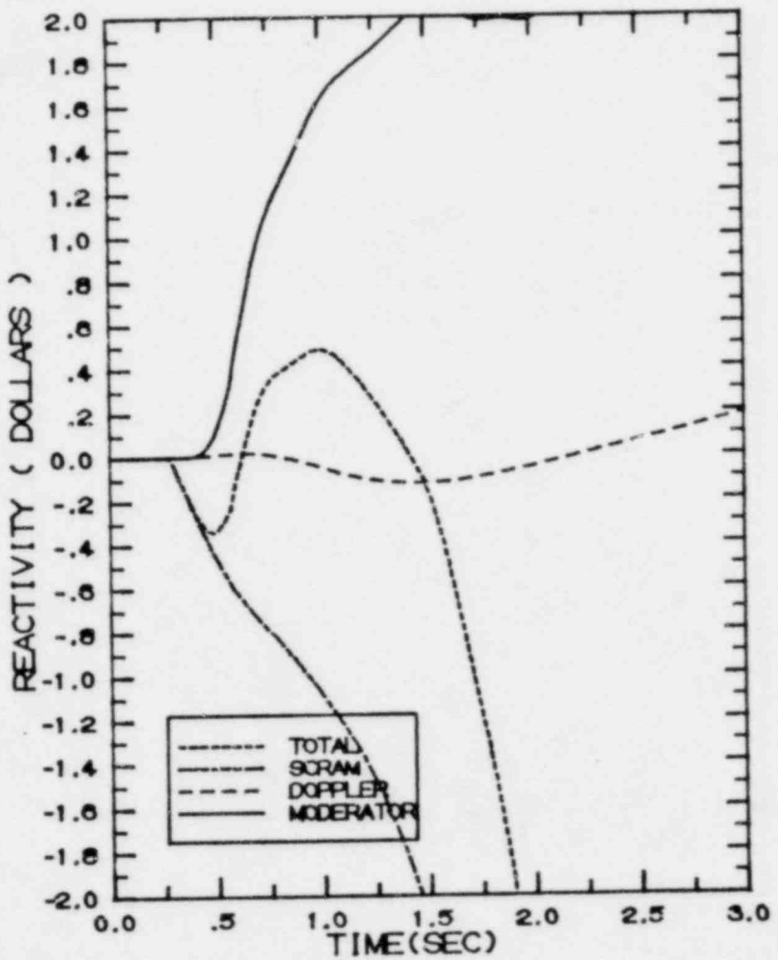

FIGURE 7.2.6-3

GENERATOR LOAD REJECTION WITHOUT BYPASS, EOC9-2000 MWD/ST

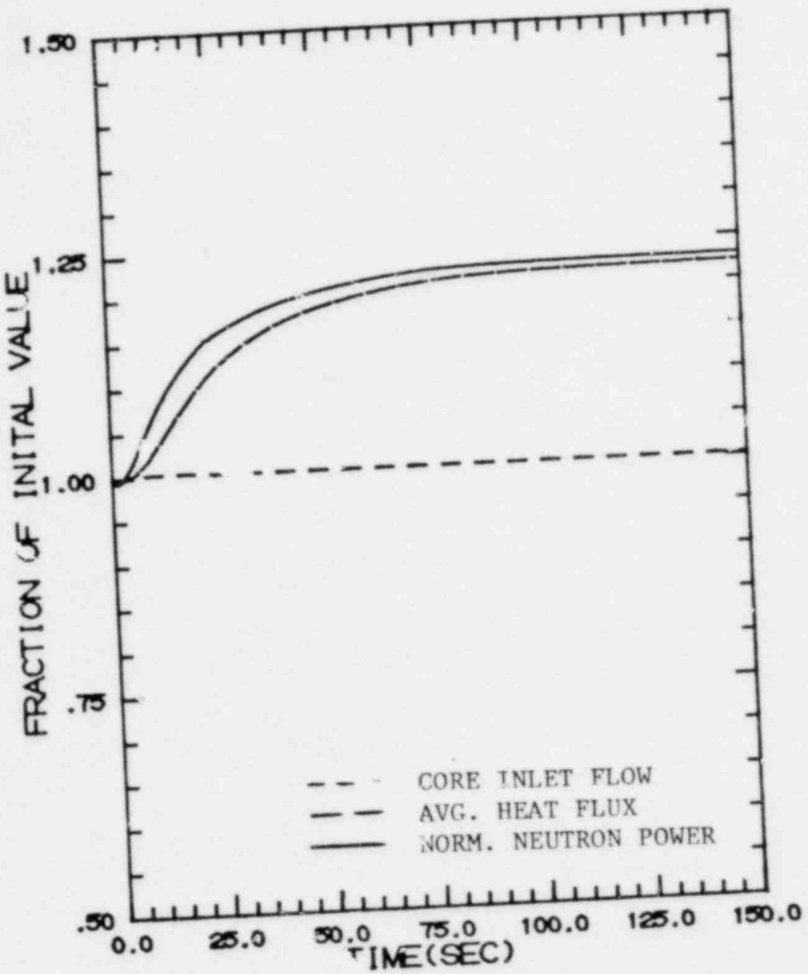

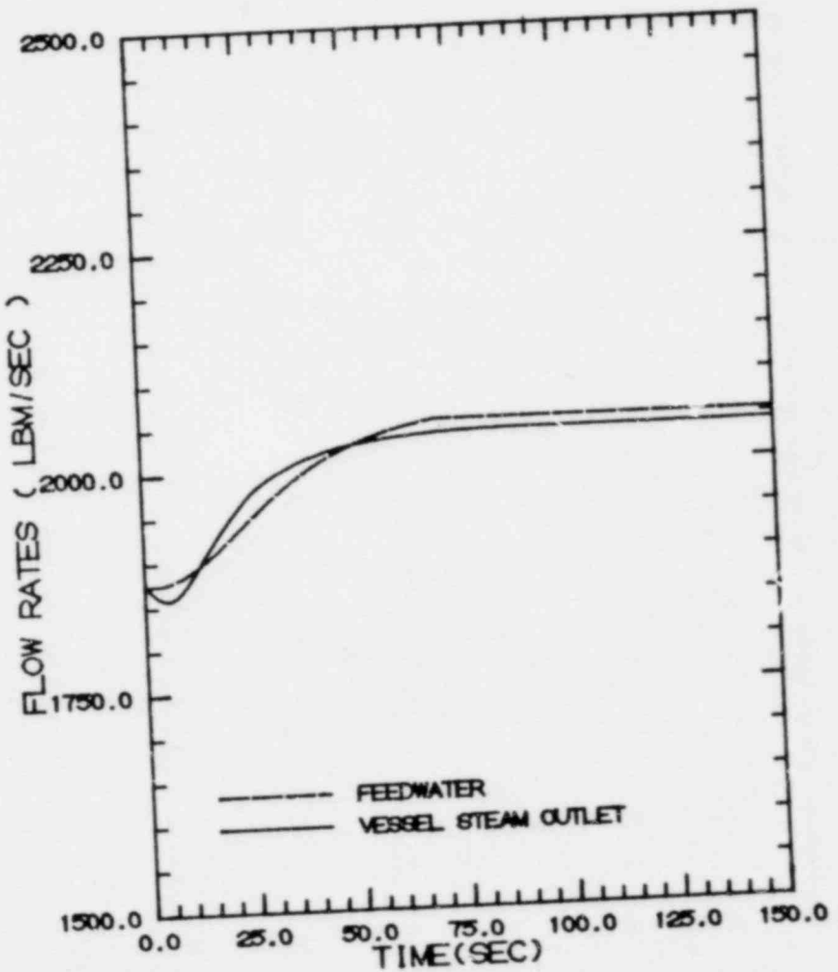

FIGURE 7.2.7-1

LOSS OF 100°F FEEDWATER HEATING, EOC9-2000 MWD/ST (LIMITING CASE)

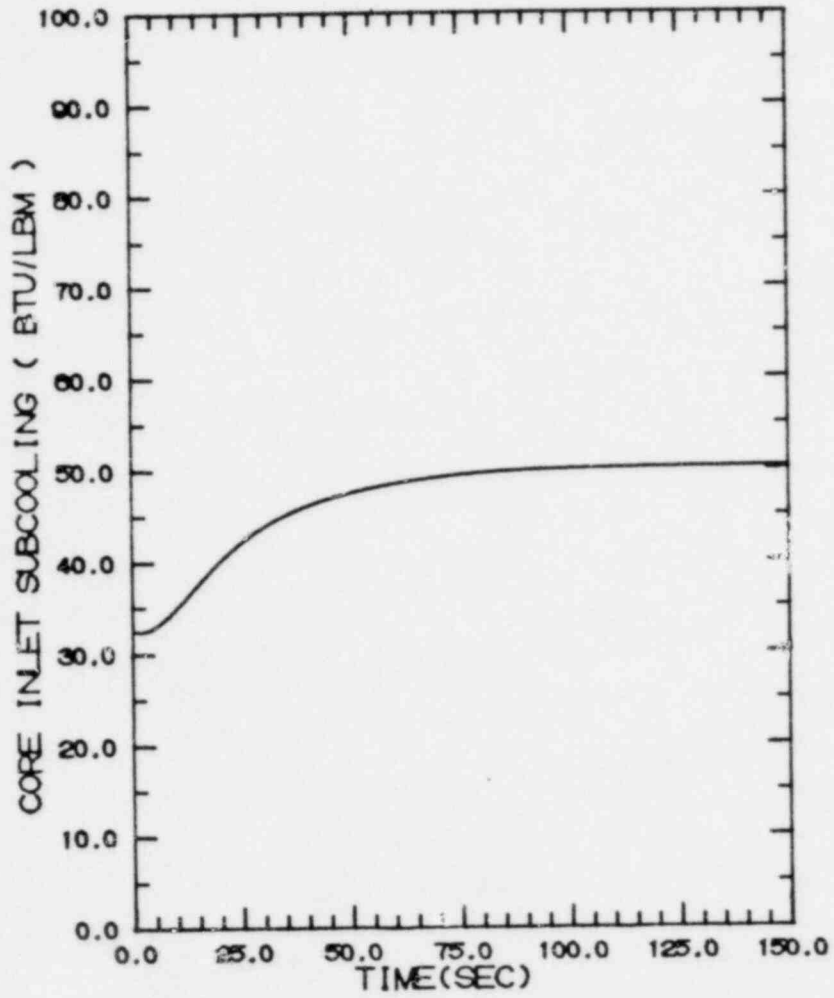

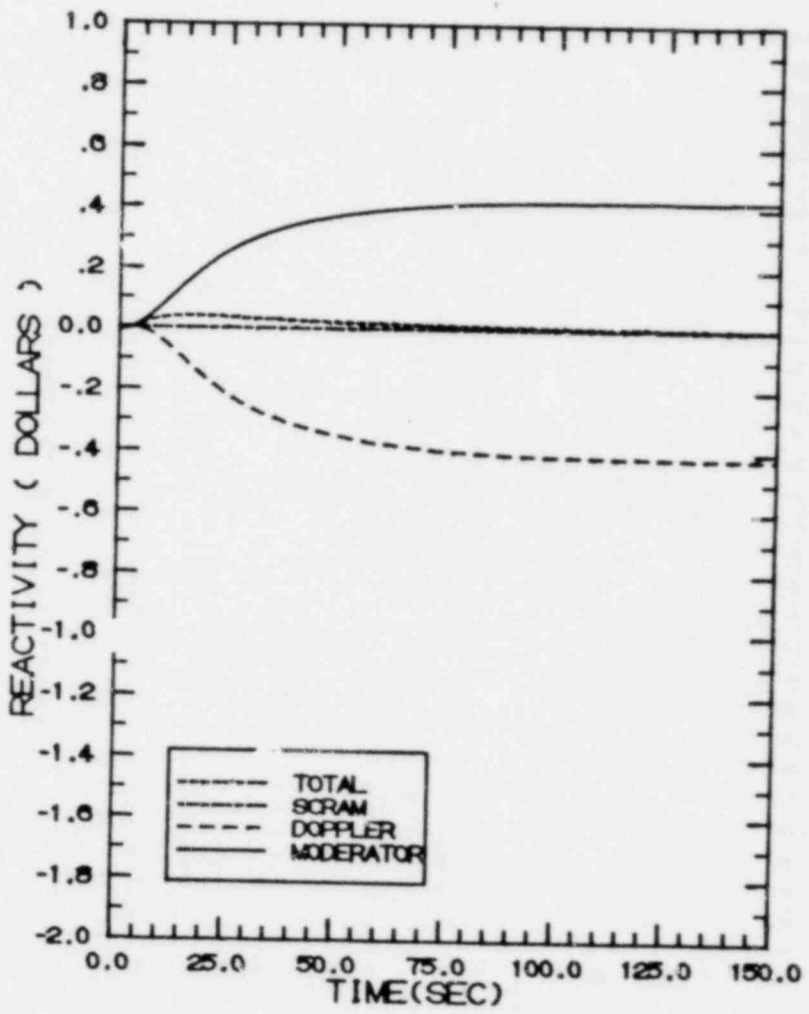

FIGURE 7.2.7-2

LOSS OF 100°F FEEDWATER HEATING, EOC9-2000 MWD/ST (LIMITING CASE)

"MEASURED" SCRAM TIME

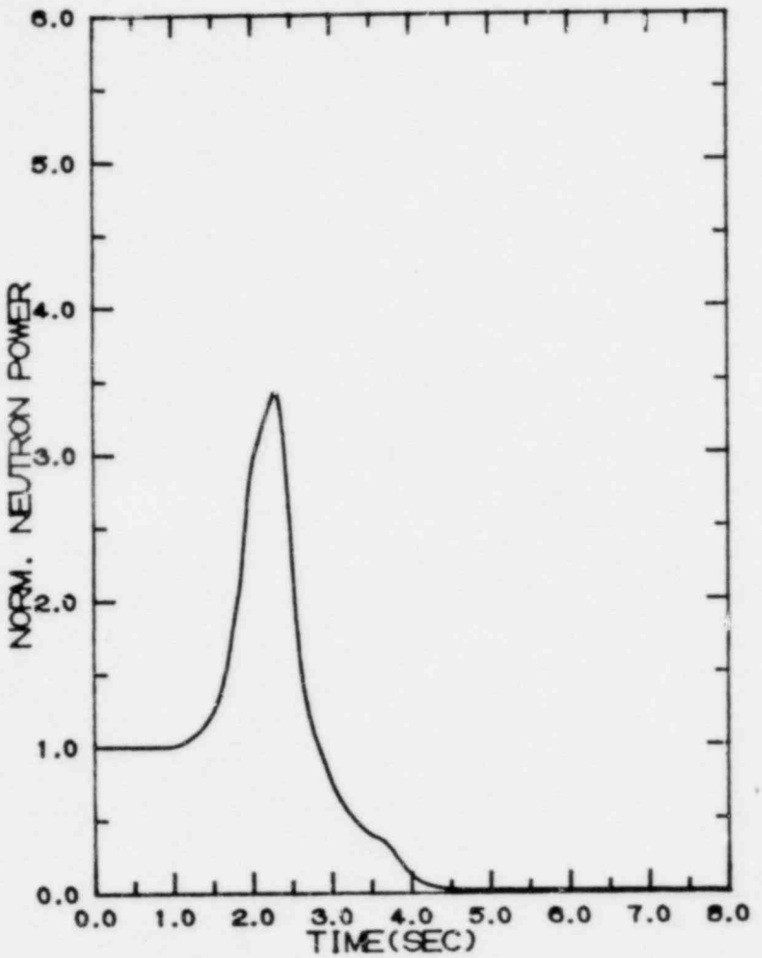

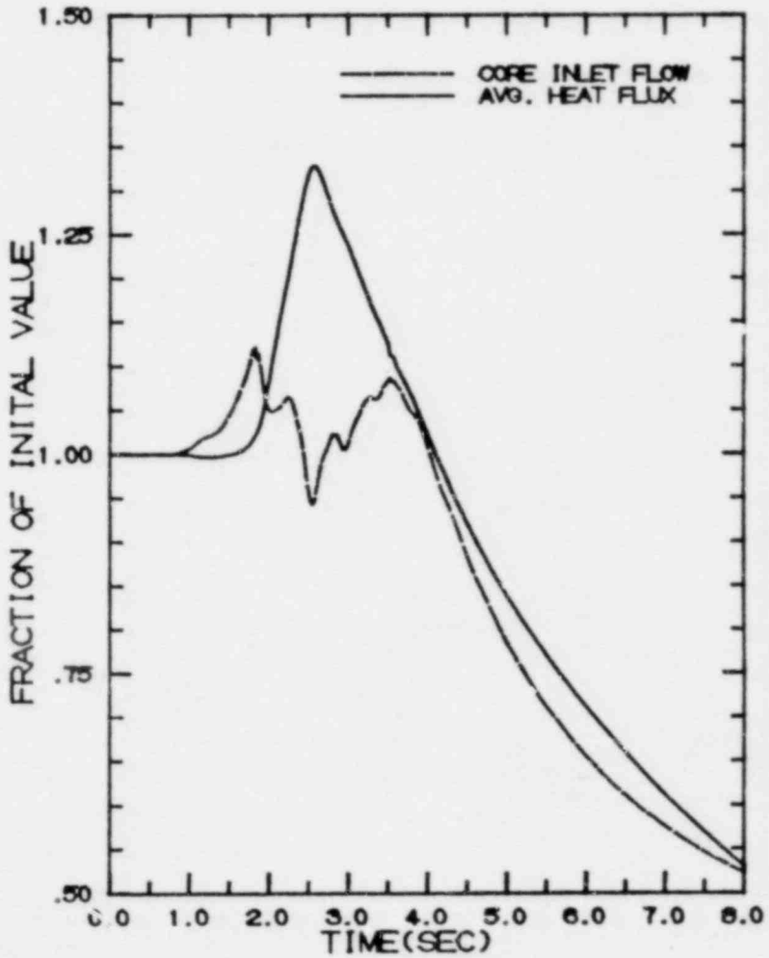

FIGURE 7.3.1-1

MSIV CLOSURE, FLUX SCRAM

"MEASURED" SCRAM TIME

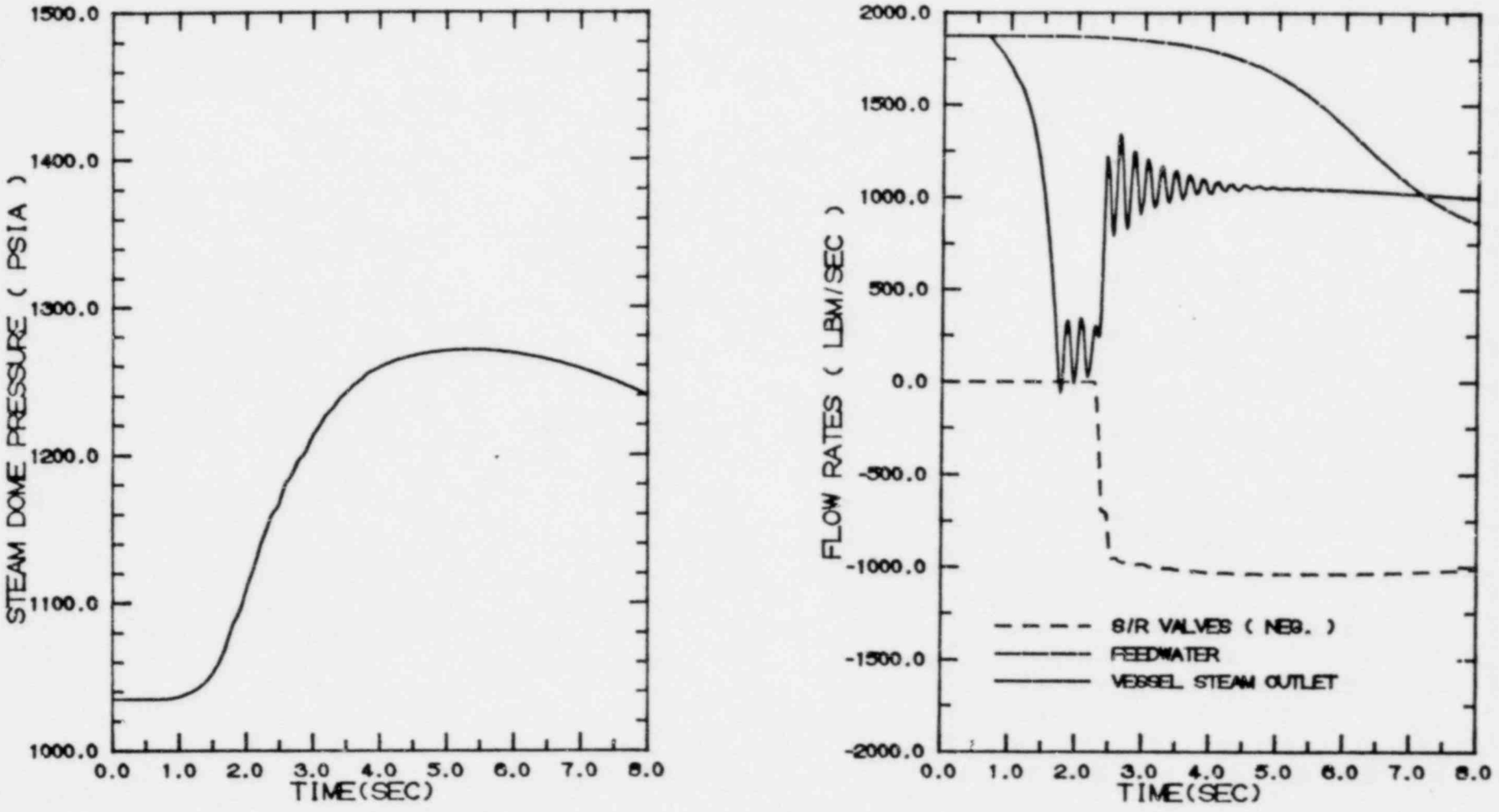

FIGURE 7.3.1-2

MSIV CLOSURE, FLUX SCRAM

"MEASURED" SCRAM TIME

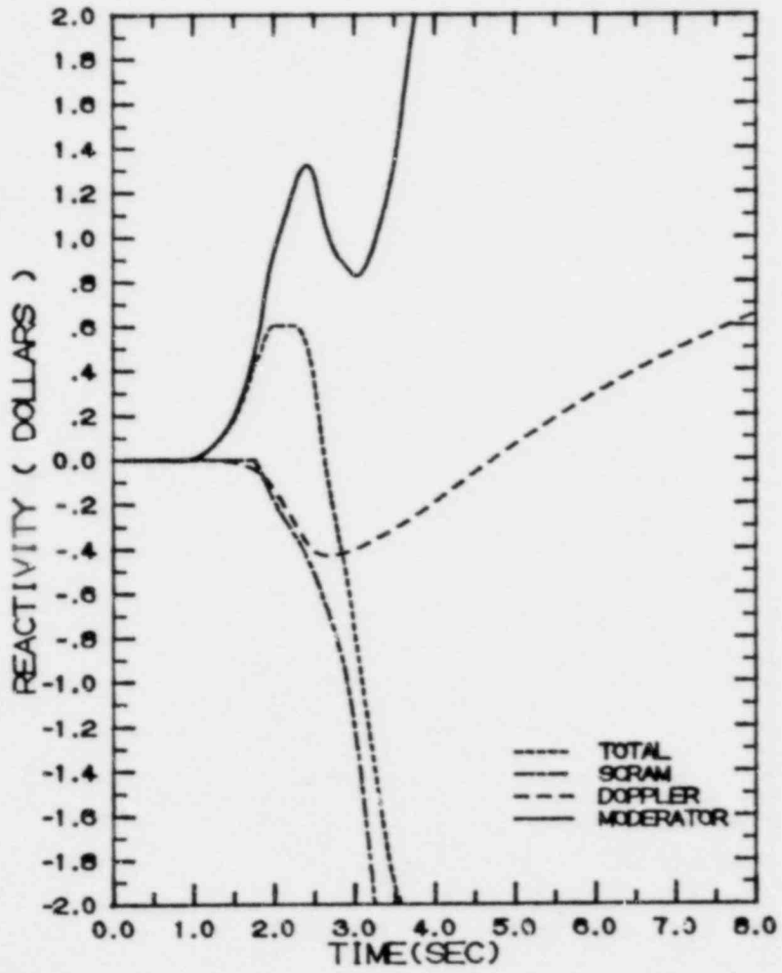

FIGURE 7.3.1-3

MSIV CLOSURE, FLUX SCRAM

CONTROL ROD PATTERN

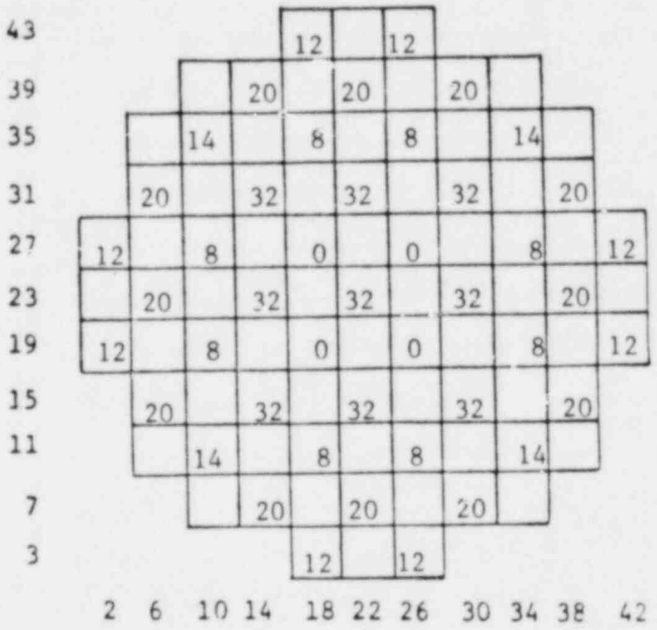

Numbers Indicate Number of Positions
Withdrawn Out of 48. Blank is a Withdrawn Rod.

Reactor Conditions:

Core Thermal Power	= 1664 Mwt
Core Flow	= 48 Mlb/hr
Cycle Exposure	= 4900 MWD/T
Xenon Free	
Initial MCPR	= 1.237
Initial LHGR	= 13.8 kw/ft

Case Description

- Operator attempts full withdrawal of the fully inserted rod at coordinates (26, 27).
- Bounding Case.

FIGURE 7.4.1

REACTOR INITIAL CONDITIONS FOR RWE CASE 1

CONTROL ROD PATTERN

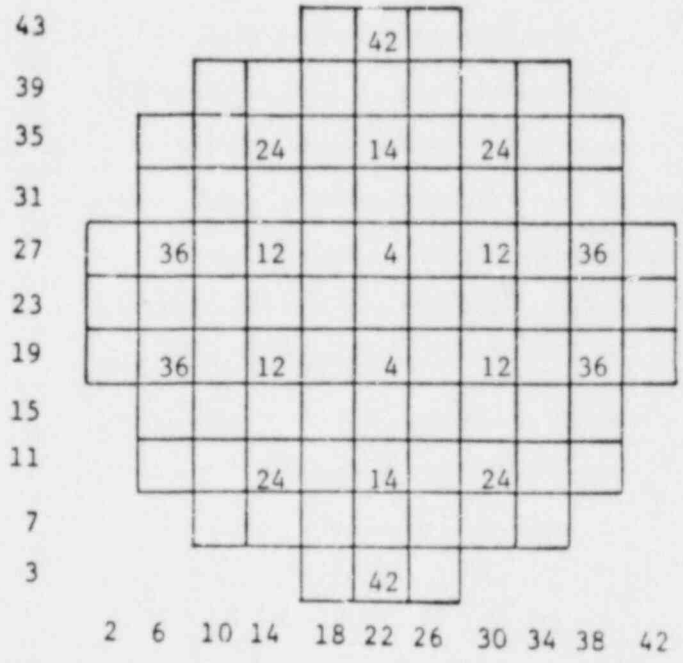

Numbers Indicate Number of Positions
Withdrawn Out of 48. Blank is a Withdrawn Rod.

Reactor Conditions:

Core Thermal Power	= 1664 Mwt
Core Flow	= 48 Mlb/hr
Cycle Exposure	= 4900 MWD/T
Equilibrium Xenon	
Initial MCPR	= 1.406
Initial LHGR	= 11.9 kw/ft

Case Description

- Operator attempts full withdrawal of the partially inserted rod at (30,27).
- Normal Xenon condition and control rod pattern.

FIGURE 7.4.2

REACTOR INITIAL CONDITIONS FOR RWE CASE 2

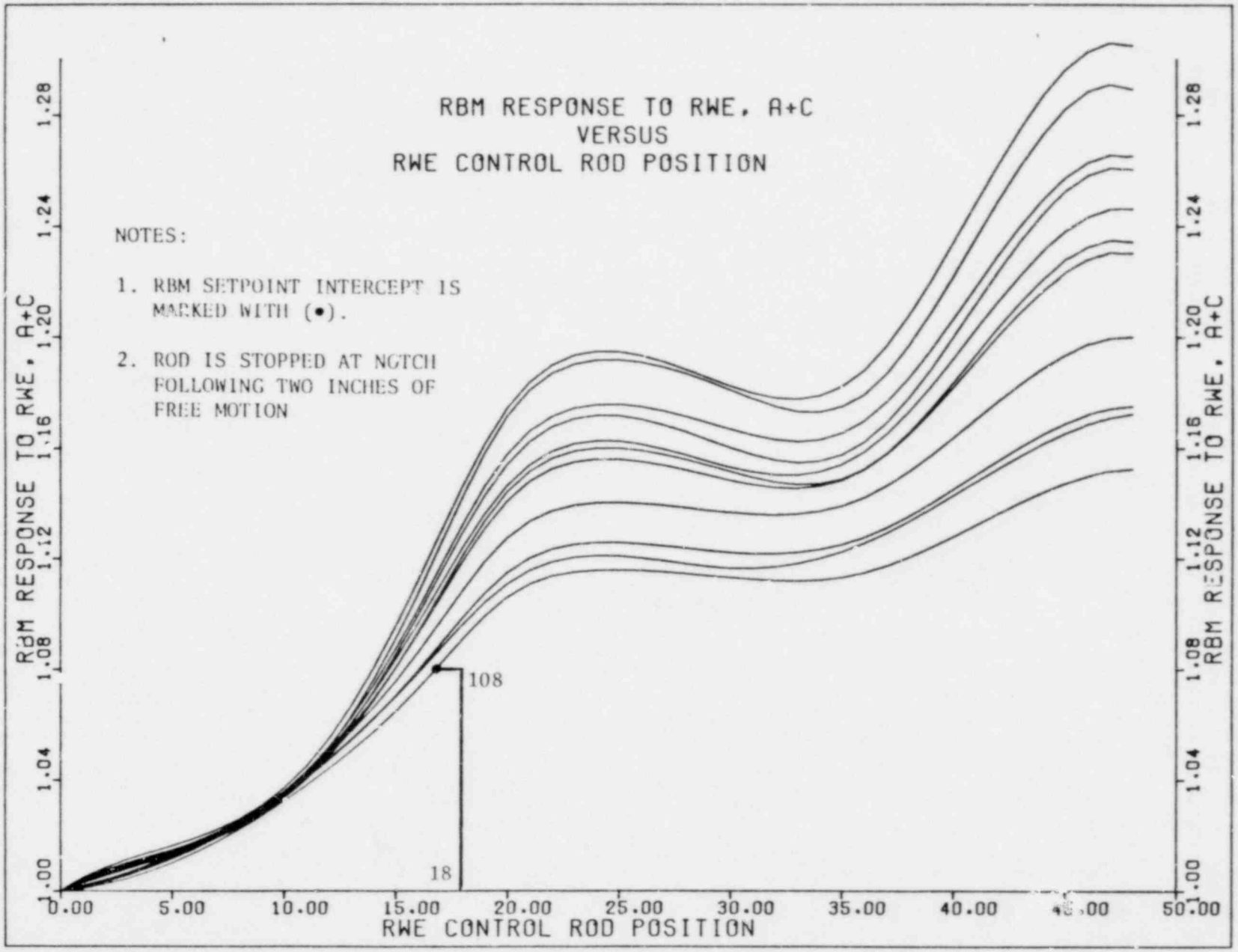

FIGURE 7.4.3

CASE 1 - SETPOINT INTERCEPTS DETERMINED BY THE A+C CHANNEL

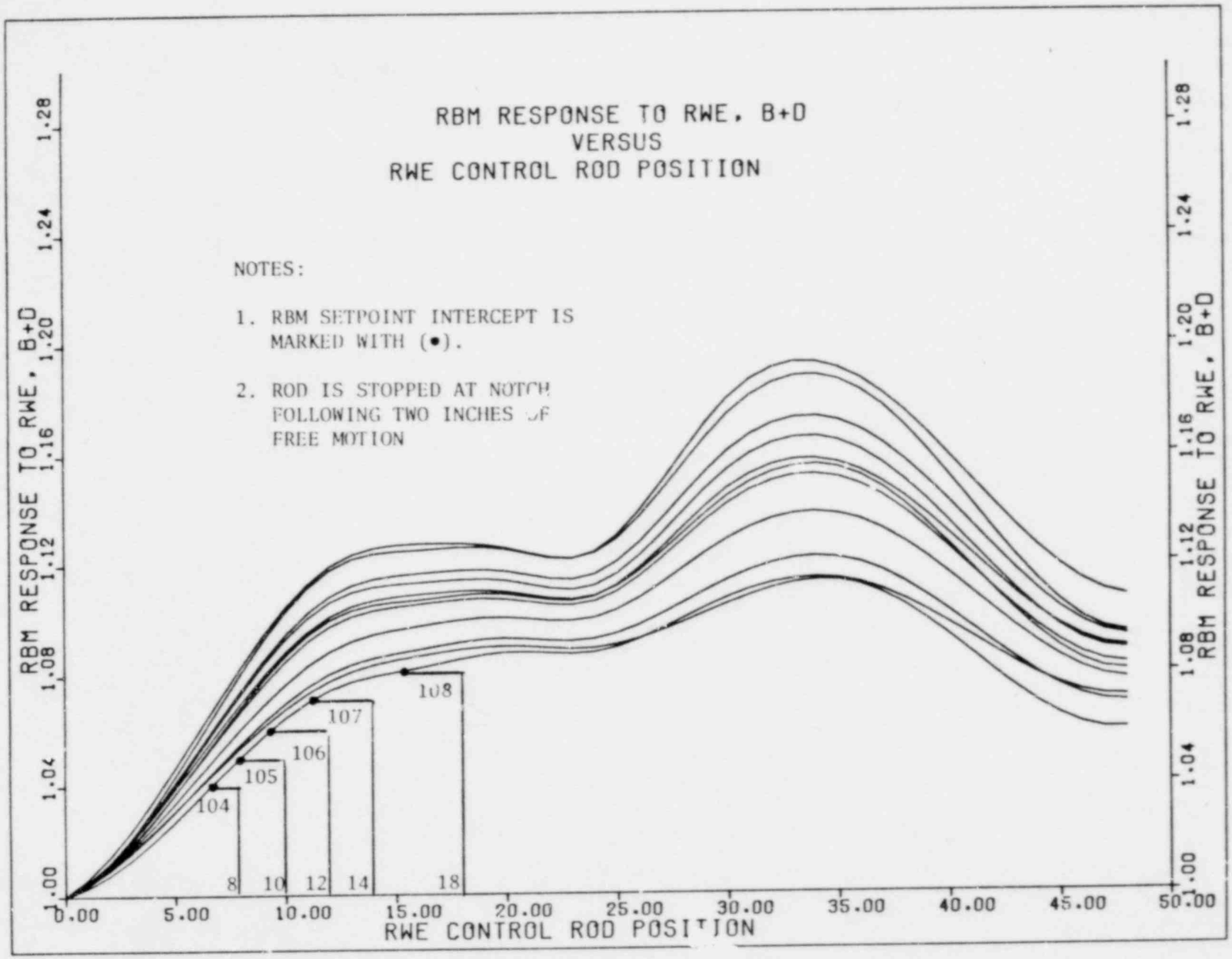

FIGURE 7.4.4

CASE 1 - SETPOINT INTERCEPTS DETERMINED BY THE B+D CHANNEL

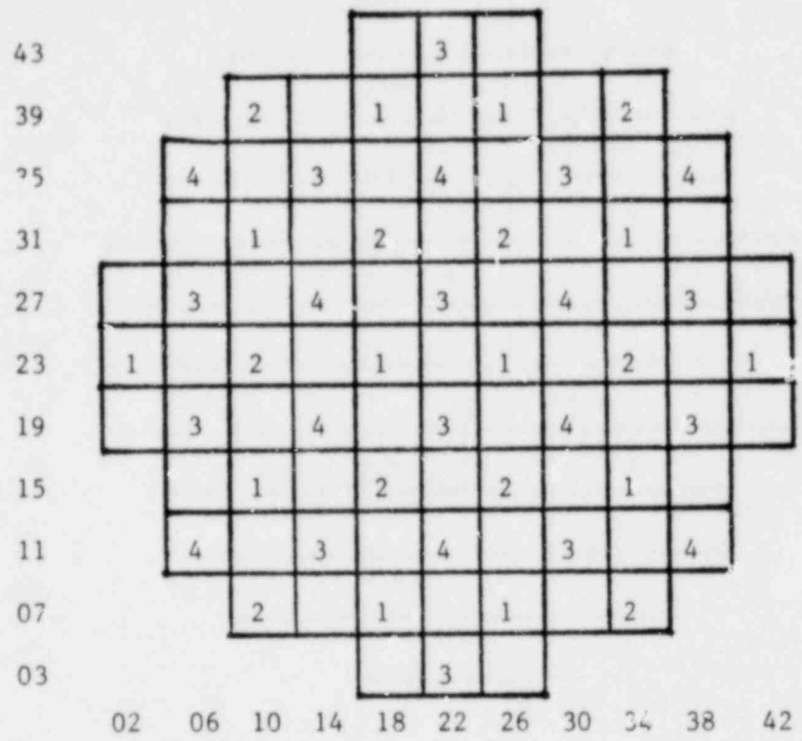

FIGURE 7.6.1 FIRST FOUR ROD ARRAYS PULLED IN THE A SEQUENCES

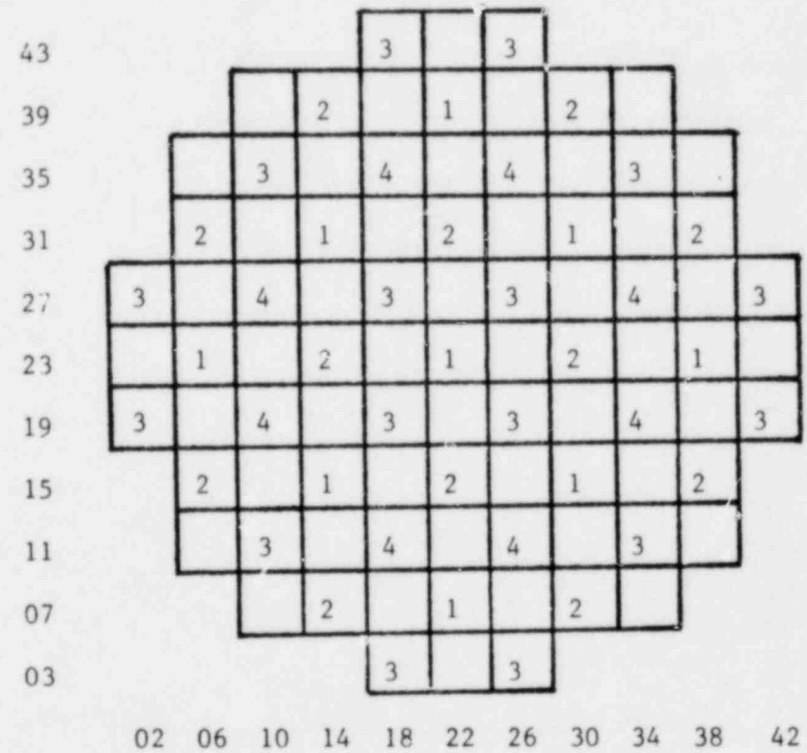

FIGURE 7.6.2 FIRST FOUR ROD ARRAYS PULLED IN THE B SEQUENCES

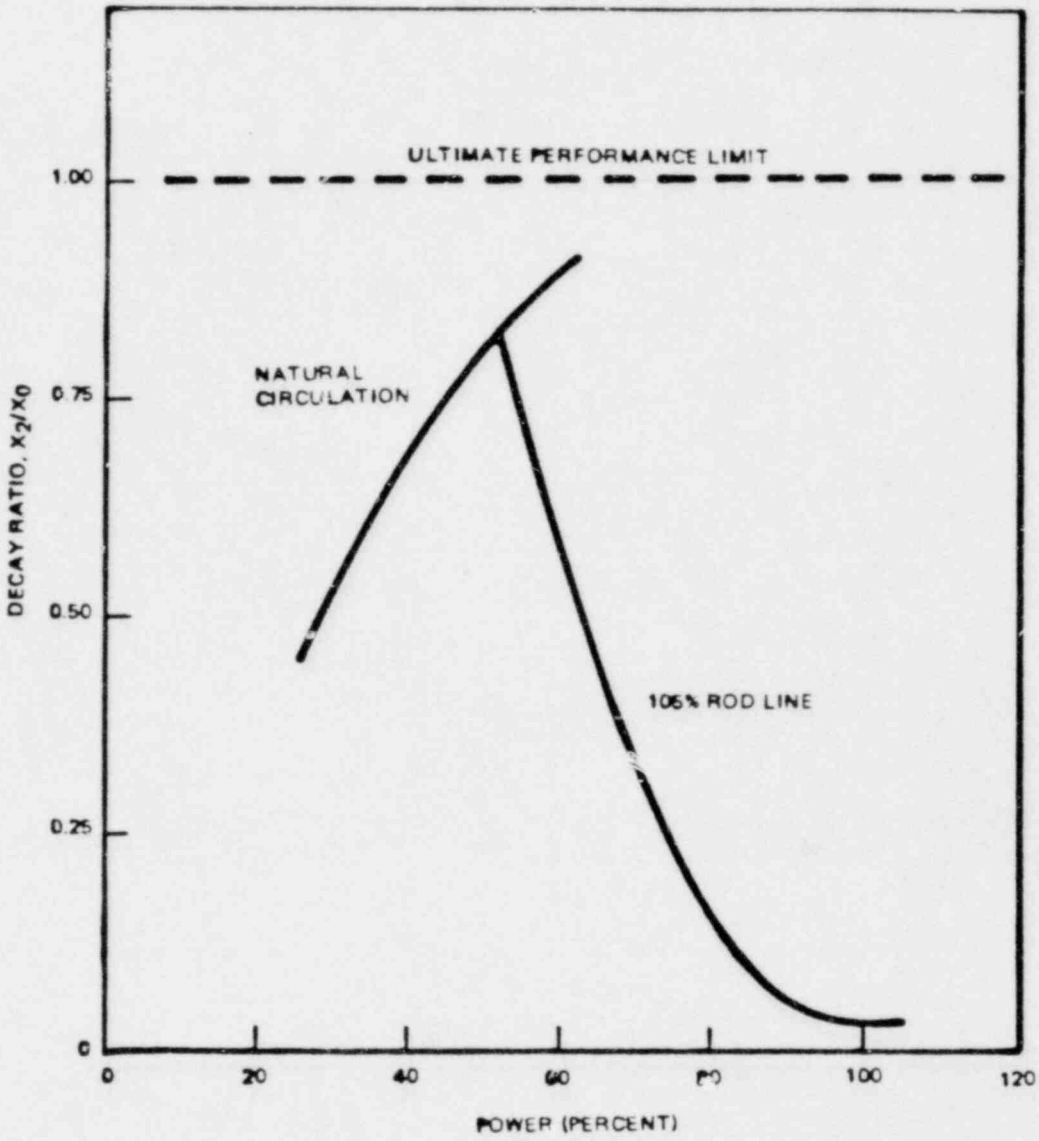

FIGURE 7.7.1

REACTOR CORE DECAY RATIO VERSUS POWER

8.0 STARTUP PROGRAM

Following refueling and prior to vessel reassembly, fuel assembly position and orientation will be verified by underwater television and videotaped.

The Vermont Yankee Startup Program will include process computer data checks, shutdown margin demonstration, in-sequence critical measurement, rod scram tests, power distribution comparisons, TIP reproducibility, and TIP symmetry checks. The content of the Startup Test Report [20] will be similar to that sent to the Office of Inspection and Enforcement subsequent to the start of Cycle 8.

9.0 LOSS-OF-COOLANT ACCIDENT ANALYSIS

The results of the complete evaluation of the loss-of-coolant accident for Vermont Yankee as documented in Reference 21 provide required support for the operation of Vermont Yankee Cycle 9. The MAPLHGR limits as a function of average planar exposure are provided for each fuel type in Table A.2 of Appendix A.

APPENDIX A

PLANT TECHNICAL SPECIFICATION CHANGES

The proposed operating limits changes to the Plant Technical Specifications for Vermont Yankee Cycle 9 operation are documented in the Appendix.

TABLE A.1
VERMONT YANKEE NUCLEAR POWER STATION
CYCLE 9 MCPR OPERATION LIMITS

Value of "N" in RBM Equation(1)	Average Control Rod Scram Time	Cycle Exposure Range	MCPR Operating Limit for Fuel Type(2) 8X8	8X8R	P8X8R
42%	Equal or better than L.C.O. 3.3 C.1.1	BOC to EOC-2 GWD/T	1.29	1.29	1.29
		EOC-2 GWD/T to EOC-1 GWD/T	1.29	1.29	1.29
		EOC-1 GWD/T to EOC	1.29	1.29	1.29
	Equal or better than L.C.O. 3.3 C.1.2	BOC to EOC-2 GWD/T	1.29	1.29	1.29
		EOC-2 GWD/T to EOC-1 GWD/T	1.30	1.30	1.30
		EOC-1 GWD/T to EOC	1.33	1.32	1.32
41%	Equal or better than L.C.O. 3.3 C.1.1	BOC to EOC-2 GWD/T	1.25	1.25	1.25
		EOC-2 GWD/T to EOC-1 GWD/T	1.25	1.25	1.25
		EOC-1 GWD/T to EOC	1.27	1.27	1.27
	Equal or better than L.C.O. 3.3 C.1.2	BOC to EOC-2 GWD/T	1.25	1.25	1.25
		EOC-2 GWD/T to EOC-1 GWD/T	1.30	1.30	1.30
		EOC-1 GWD/T to EOC	1.33	1.32	1.32
≤40%	Equal or better than L.C.O. 3.3 C.1.1	BOC to EOC-2 GWD/T	1.24	1.24	1.24
		EOC-2 GWD/T to EOC-1 GWD/T	1.24	1.23	1.23
		EOC-1 GWD/T to EOC	1.27	1.27	1.27
	Equal or better than L.C.O. 3.3 C.1.2	BOC to EOC-2 GWD/T	1.24	1.24	1.24
		EOC-2 GWD/T to EOC-1 GWD/T	1.30	1.30	1.30
		EOC-1 GWD/T to EOC	1.33	1.32	1.32
75%	Special Testing at Natural Circulation (Note 3, 4)		1.30	1.31	1.31

(1) The Rod Block Monitor (RBM) trip setpoints are determined by the equation shown in Table 3.2.5 of the Technical Specifications.

(2) The current analyses for MCPR Operating Limits do not include 7X7 fuel. On this basis further evaluation of MCPR operating limits is required before 7X7 fuel can be used in Reactor Power Operation.

(3) For the duration of pump trip and stability testing.

(4) K_f factors are not applied during the pump trip and stability testing.

TABLE A.2

VERMONT YANKEE MAPLHGR OPERATING LIMITS
VERSUS AVERAGE PLANAR EXPOSURE*

Average Planar Exposure (MWd/t)	MAPLHGR by Fuel Type (kw/ft)		
	8D219	8D274 (High Gd)	8DRB289 P8DRB289
200	11.4	11.1	11.2
1,000	11.5	11.1	11.2
5,000	11.9	11.6	11.8
10,000	12.1	12.1	12.0
15,000	12.3	12.2	12.1
20,000	12.1	12.1	11.8
25,000	11.3	11.6	11.3
30,000	10.2	10.6	11.1
35,000	9.6	10.0	10.4
40,000	-	9.4	9.8

* From Reference 21

REFERENCES

1. B. Buteau, "Stability and Recirculation Pump Trip Test, Special Test Procedure No. 81-01", Vermont Yankee Nuclear Power Corporation, February 1981.

2. General Electric Boiling Water Reactor Generic Reload Fuel Application, NEDE-24011-P- , GE Company Proprietary, July 1979.

3. D. M. VerPlanck, Methods for the Analysis of Boiling Water Reactors Steady State Core Physics, YAEC-1238, March 1981.

4. E. E. Pilat, Methods for the Analysis of Boiling Water Reactors Lattice Physics, YAEC-1232, December 1980.

5. S. P. Schultz and K. E. St.John, Methods for the Analysis of Oxide Fuel Rod Steady-State Thermal Effects (FROSSTEY) Code/Model Description Manual, YAEC-1249P, April 1981.

6. S. P. Schultz and K. E. St.John, Methods for the Analysis of Oxide Fuel Rod Steady-State Thermal Effects (FROSSTEY) Code Qualification and Application, YAEC-1265P, June 1981.

7. D. C. Albright, H2ODA: An Improved Water Properties Package, YAEC-1237, March 1981.

8. Appendix A to Operating License DPR-28 Technical Specifications and Bases for Vermont Yankee Nuclear Power Station, Docket No. 50-271.

9. A. A. F. Ansari, Methods for the Analysis of Boiling Water Reactors: Steady-State Core Flow Distribution Code (FIBWR), YAEC-1234, December 1980.

10. A. A. F. Ansari, R. R. Gay, and B. J. Gitnick, FIBWR: A Steady-State Core Flow Distribution Code for Boiling Water Reactors - Code Verification and Qualification Report, EPRI NP-1923, Project 1754-1 Final Report, July 1981.

11. General Electric Company, GEXL Correlation Application to BWR 2-6 Reactors, NEDE-25422, GE Company Proprietary, June 1981.

12. A. A. F. Ansari and J. T. Cronin, Methods for the Analysis of Boiling Water Reactors: A Systems Transient Analysis Model (RETRAN), YAEC-1233, April 1981.

13. EPRI, RETRAN - A Program for One-Dimensional Transient Thermal-Hydraulic Analysis of Complex Fluid Flow Systems, CCM-5, December 1978.

14. K. J. Burns, Methods for the Analysis of Boiling Water Reactors: Transient Thermal Margin Analysis Code (MAYU04-YAEC), YAEC-1235, December 1980.

15. J. M. Holzer, Methods for the Analysis of Boiling Water Reactors Transient Core Physics, YAEC-1239P, August 1981.

16. Vermont Yankee Nuclear Power Station Final Safety Analysis Report, Section 3.6.6

17. C. J. Paone, et.al., Rod Drop Accident Analysis for Large Boiling Water Reactors, NEDO-10527, March 1972.

18. C. J. Paone, Banked Position Withdrawal Sequence, NEDO-21231, January, 1977.

19. R. C. Stirn, et.al., Rod Drop Accident Analysis for Large Boiling Water Reactor Addendum No. 2 Exposed Cores, NEDO-10527, Supplement 2, January 1973.

20. Letter, FVY 81-52, dated March 31, 1981, R. L. Smith to Boyce H. Grier of USNRC Region I, "Cycle VIII Startup Test Report".

21. Loss-of-Coolant Accident Analysis for Vermont Yankee Nuclear Power Station, NEDO-21697, August 1977, as amended.